Universidad del País Vasco Euskal Herriko Unibertsitatea
BILBOKO INGENIARITZA ESKOLA
ESCUELA DE INGENIERÍA DE BILBAO

MÁSTER UNIVERSITARIO EN

CIENCIA Y TECNOLOGÍA ESPACIAL

TRABAJO FIN DE MÁSTER

VENUS CLIMATE DATABASE VALIDATION IN THE CLOUD REGION

Estudiante *del Val Munilla, Andrés*
Director/Directora *Garate López, Itziar*
Departamento *Física Aplicada*
Curso académico *2021-2022*

Bilbao, 18, septiembre, 2022

ABSTRACT

Venus's atmosphere is one of the most intriguing one within the Solar System with mysterious features such as the retrograde super-rotation, composition ambiguities or complex polar vortexes. To better understand and to enhance the research of the atmosphere, several Venusian Global Circulation Models (GCMs) have been developed. These represent a very powerful tool that may have a decisive role on the unveiling of the main enigmas in Venus's atmosphere and in future Venus's research. Nonetheless, these models present some main challenges that are being progressively addressed and some reasonably good simulations have already been developed.

One of these models is the one developed at the *Laboratoire de Météorologie Dynamique (LMD)* in Paris. In addition to the GCM, the LMD group has developed a database compiling the results of several simulations called *Venus Climate Database (VCD)*. The main aim of this thesis is to validate the VCD within the cloud region (~40-75km) by comparing the atmospheric simulation results with real observational datasets from several space missions to Venus. The main variables that are validated in this work are temperature, winds, number density and composition. In general terms, VCD results are very consistent with the studied observational data, especially at low to mid latitudes (below ~45°). The main focus is therefore set on the main biases found in the VCD output, which are the shift of the modelled cold collar to higher latitudes and the poleward drift of the VCD zonal jet streams, both compared to the observational data. Additional inconsistencies can be found in the simulation of the atmospheric composition, which seem to be the most difficult to replicate. The validation has revealed some of the main discrepancies between the VCD and the observations, so that these flaws can be addressed and both the LMD model and the VCD improved.

Keywords

Venus, planetary atmospheres, atmospheric dynamics, GCMs, VCD, validation, cloud region, super-rotation

RESUMEN

La atmósfera de Venus es una de las más interesantes del Sistema Solar, albergando características difíciles de explicar como su super-rotación, ambigüedades en su composición o los complejos vórtices polares. Para tratar de entender mejor esta atmósfera y para potenciar su estudio, varios Modelos de Circulación General (GCMs por sus siglas en inglés) han sido desarrollados. Estos pueden llegar a jugar un papel decisivo a la hora de esclarecer todos los misterios de la atmósfera venusiana y ser determinantes en la futura investigación del planeta. Sin embargo, los diferentes modelos se topan con algunos desafíos que progresivamente van siendo superados, hasta la consecución de simulaciones razonablemente buenas en la actualidad.

Uno de estos modelos es el elaborado en el parisino *Laboratoire de Météorologie Dynamique (LMD)*. Unido a este GCM, el grupo ha desarrollado una base de datos, llamada *Venus Climate Database (VCD)*, que compila los resultados de las diferentes simulaciones numéricas. El objetivo principal de este trabajo es validar la VCD en la región de las nubes (~40-75km), comparando los datos obtenidos por medio de la simulación de la atmósfera de Venus con datos obtenidos por medio de las observaciones llevadas a cabo por varias de las diferentes misiones espaciales al planeta. Las cuatro variables principales que han sido validadas en esta tesis son temperatura, vientos, densidad numérica y composición. En términos generales, los resultados de la VCD son muy consistentes con los datos observacionales, especialmente en las latitudes bajas y medias (por debajo de $\sim 45^{\circ}$). Siendo esto así, la validación se centrará en los principales sesgos encontrados en los resultados generados por la VCD: el desplazamiento en la simulación del *cold collar* a mayores latitudes y el deslizamiento de las corrientes en chorro del modelo hacia los polos, en comparación ambos con las observaciones. Algunas inconsistencias adicionales son detectadas en términos de composición atmosférica, que parece ser la parte más difícil de reproducir. La validación ha revelado algunas de las discrepancias más notorias entre la VCD y las observaciones, dando así pie a futuras mejoras en el modelo del LMD y por consiguiente en la VCD.

LABURPENA

Artizarraren atmosfera Eguzki Sistemako atmosferetatik interesgarrienetako bat da; ezaugarri misteriotsu ugari baititu. Hala nola supererrotazio atzerakoia, konposizio-anbiguotasunak edo bortize polar konplexuak. Atmosfera hori hobe ikertu eta ulertzeko, Zirkulazio Globalaren Ereduak (GCM ingeleseko terminotik) garatu dira. GCM-ak oso tresna ahaltsua dira, eta paper erabakigarria izan dezakete Artizarraren atmosferako enigma nagusiak argitzeko eta Artizarraren etorkizuneko ikerketaren nondik norakoak zehazteko. Hala ere, ereduek pixkanaka-pixkanaka lantzen ari diren erronka nagusi batzuk aurkezten dituzte, zorionez simulazio batzuk dagoeneko gainditu dituztenak. Hala ere, ereduek gainditu beharreko erronkak dituzte, pixkanaka-pixkanaka landuak izaten ari direnak eta simulazio batzuek dagoeneko gainditu dituztenak.

Eredu horietako bat Parisko Laboratoire de Météorologie Dynamique-n (LMD) garatutakoa da. GCMaz gain, LMDko taldeak Venus Climate Database (VCD) izeneko simulazioen emaitzak biltzen dituen datu-basea garatu du. Gradu Amaierako Lan honen helburu nagusia VCDa balioztatzea da, hodeien eskualdean (~40-75km) arreta jarriz. Horretarako, simulazioen emaitzak Artizarrera bidalitako zenbait misioek behatutako datu errealen multzoekin alderatu da. Lan honetan baliozkotutako aldagai nagusiak tenperatura, haizea, zenbaki-dentsitatea eta konposizioa dira. Oro har, VCDaren emaitzak oso bateragarriak dira aztertutako behaketa-datuekin, batez ere latitude baxuetatik ertainetara (~45°-tik behera). Arreta nagusia, beraz, VCDaren emaitzetan aurkitutako ezberdintasun nagusietan ipini da: behaketekin alderatuta *cold collar* deritzon egitura hotza modeloan latitude altuagoetan azaltzea eta VCDak lortzen duen abiadura zonalaren jeta simulazioetan polorantz desplazatzea. Beste kontraesanak ere aurkitu daitezke konposizio atmosferikoaren simulazioan, hori baita, antza, erreplikatzeko zailena. Balioztatzeak VCDaren eta behaketen arteko desadostasun batzuk erakutsi ditu, akats horiei aurre egin ahal izateko eta bai LMD eredua bai VCD eredua hobetzeko bide posibleak erakutsiz.

GENERAL INDEX

FIGURE INDEX

Appendix Figures

TABLE INDEX

1. INTRODUCTION

The Venus Climate Database (VCD) is a database of atmospheric statistics compiled from global circulation model (GCM) simulations of the Venusian atmosphere developed at the *Laboratoire de Météorologie Dynamique (LMD)* in Paris (*Lebonnois et al., 2021a*). Although explained in further detail in the following sections, GCMs are numerical models that simulate time-averaged planetary-scale atmospheric motions.

The main objective of this work is therefore to validate the Venus Climate Database (VCD) in the cloud region. Hence, it is to be assessed if the model accurately represents the long-term behaviour of the general circulation of Venus's atmosphere in that specific vertical extent. This main task will be carried out by determining if VCD model predictions are consistent with real observational datasets, mainly obtained from real space missions to Venus. This will lead to some conclusions about the reliability of the VCD output.

The importance of numerical models does not limit to a better understanding of the general circulation of an atmosphere, but also presents many other advantages. Once a model has been satisfactorily validated, it turns into an incredibly valued tool. For example, in the case of Venus, if we have a reliable model, this will result on a great resource for the space community. With the help of GCMs, scientists and engineers could achieve more prolific scientific and technical results by fine-tuning future Venus's mission concepts and proposals and by optimising spacecraft and instrument design, with improved longer-lasting missions and at optimised costs. Therefore, model validation is critical as there could not be a good and reliable model without proper validation.

As just mentioned, the aim of this thesis is limited only to the cloud region, as it poses as a good complement and continuation to the validation accomplished so far (*Lebonnois et al., 2021b*), which mainly covers the aerobraking region in the upper atmosphere (above 80km including upper mesosphere, thermosphere, and exosphere). This cloud region will be described and defined in the first part of the work, after general review of the whole Venusian atmosphere.

To better understand the observational data used in this thesis for the validation purposes, a general overview of Venus's missions will be presented as well. The closing of this first section will include an ample explanation of Global Circulation Models (GCMs), Venus's modelling and its challenges, and a presentation of the Venus Climate Database (VCD).

In the second part of this thesis methodology will be described and, finally, in the third section validation results will be shown, being this the central part of the work. Main conclusions about the VCD validation will be presented at the end of the work.

1.1 VENUS CHARACTERISTICS AND ATMOSPHERE

Named after the ancient Roman goddess of beauty, Venus is known for its exceptional brightness in the night sky. It is one of the four terrestrial planets we can find on our Solar System and the second planet from the Sun, being also the closest from the Earth. Probably due to this proximity, Venus was the first target for planetary research back in the early sixties.

In this first section of the report, the key characteristics of Venus will be presented such as orbital parameters, geology, composition, or atmospheric dynamics. Great emphasis will be set on describing the Venusian atmosphere as it is the cornerstone of the thesis.

Venus and Earth are very similar and very different at the same time. Venus is frequently referred as our twin planet, although this may be accurate only when thinking about the origin and formation of both planets. Today we can find striking differences between them, meaning that they have followed totally different evolutive paths.

In *Table 1* we can see that in mass and dimensions Venus is quite like Earth. They are also at similar distances from the Sun. However, the first great difference is Venus's axial tilt of 177.3° versus the Earth's one of 23.44°. This great axis inclination means that Venusian rotation is retrograde, which in astronomy means that it spins in the opposite direction to its orbit. It is the only terrestrial planet with this feature in the Solar System. In addition, the rotation of Venus around its axis is so slow that one day in Venus lasts longer than one year. It takes Venus 225 Earth days to make one trip around the Sun while one day – one spin around its axis – lasts 243 Earth days. This axial tilt also makes Venus not to have any seasons.

	Venus	*Earth*	*Ratio (Venus/Earth)*
Sun Distance (km)	108.21 x10^6	149.60 x10^6	0.72
Mean Radius (km)	6051.8	6371.0	0.95
Mass (kg)	4.87 x10^{24}	5.97 x10^{24}	0.82
Mean Density (kg/m^3)	5243	5513	0.95
Surface Gravity (m/s^2)	8.87	9.80	0.91
Axial Tilt (°)	177	23.44	-
Orbital Period (Earth days)	225	365	0.62
Rotation Period (Earth days)	243	1	243
Seasons	No	Yes	-

***Table 1**: Venus vs. Earth General and Orbital Facts. Source: NASA*

From a geological point of view, Venus internal structure is differentiated, so as the Earth is: it has an iron core, a hot mantle, and a solid rocky exterior crust. Nonetheless, Venus does not have the global system of plate tectonics we can find on Earth (*Solomon et al., 1992; Nimmo et al., 1998*). It is also particularly astonishing the youthful surface that Venus has, partially confirmed by being the terrestrial planet with the fewest impact craters. Scientist firmly believe that the surface is younger than one million years, and probably much younger, about 250,000 years or even less (*Smrekar et al., 2010*). There is a big debate between those who think that the resurfacing of Venus is gradual and those who think it was catastrophic. What it is quite firmly confirmed is that Venus presents a vigorous volcanic activity, much greater to the one on the Earth, having thousands of volcanoes (*Titov et al., 2009; Svedhem et al., 2009; Smrekar et al., 2010*).

Topography is also important on the planet, having several mountainous ranges (*Bruegge et al., 1991*). The greatest in extent is Aphrodite Terra, which has the size of Africa. The tallest top is Maxwell Montes, a volcano reaching 11km height (much taller than Mount Everest) and located in another highland region called Ishtar Terra.

Although Venus and Earth have a similar internal structure and composition, the first does not contain its own internally generated magnetic field (*Nimmo, 2002*). Instead, it has a weak induced magnetic field created by the interaction of the Sun's magnetic field and Venus's outer ionosphere (*Zhang et al., 2008*). We will see later on what implications this will have to its atmospheric composition.

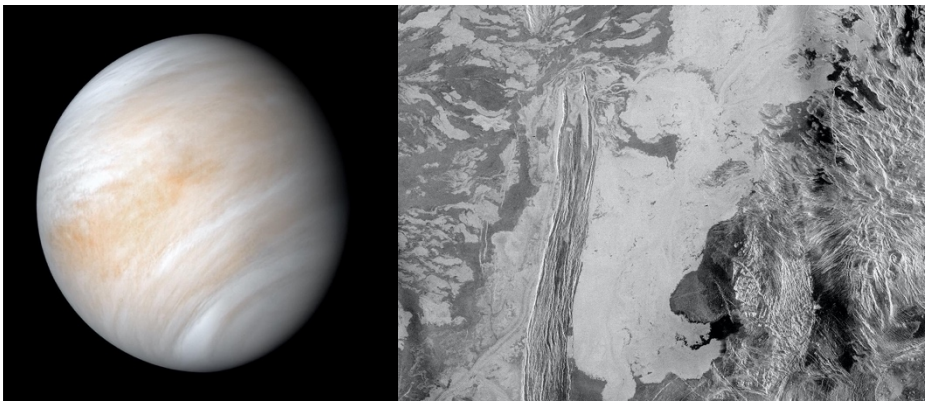

***Figure 1**: processed Marineer 10 image of Venus (left), Magellan radar image of Lada region surface (right), Source: NASA.*

The greatest differences between Venus and the Earth are found on their atmospheres. Venus's one is extremely thick and toxic. Pressure at its surface reaches 92 bars (*see Table 2*), thus being 90 to 91 times the one of the Earth (*Basilevsky et al., 2003*). This is the pressure we can find at one kilometre depth in the ocean.

Venus's atmosphere is divided into three regions based on its composition, chemistry, and clouds: the upper atmosphere, above ~ 110 km, has low densities and overlaps with the ionosphere so that photodissociation, ion-neutral, and ion-ion reactions are increasingly dominant as one goes to higher altitudes; the middle atmosphere, ~60-110 km, that receives sufficiently intense ultraviolet (UV) radiation from the sun that its chemistry is dominated by photon-driven processes, termed "photochemistry"; and the lower atmosphere, below ~ 60 km, receives little UV radiation from the sun and, due to the high atmospheric temperatures, the chemistry is controlled increasingly by thermal processes, known as "thermochemistry", as one goes lower in the atmosphere (*Mills et al., 2013*).

	Venus	*Earth*	*Ratio (Venus/Earth)*
Surface Average Pressure (bar)	92	~1	~ 90
Surface Average Temperature (℃)	464	15	~ 31
Surface Density (kg/m^3)	65	1.22	~ 53
Scale Height (km)	15.9	8.5	~ 2

***Table 2**: Venus vs. Earth Surface Atmospheric Variables. Source: NASA*

Venus is also the hottest planet in the Solar System with surface average temperatures as high as 460-480°C. Interestingly, in the lower and middle atmosphere, temperature is almost constant at every local time despite its slow rotation. The main reason of this thermal structure is a runaway greenhouse effect due to the extremely dense atmosphere that traps the heat and develops on an enormous thermal inertia.

Regarding the atmospheric composition (*see Table 3*), the 96.5% of the atmosphere is Carbon Dioxide (CO_2), one of the major greenhouse gases. The second most abundant gas is Nitrogen (N_2), with a 3.5%. Though Venus's and Earth's abundancies may look very different at a first glance, the net amount of some of these compounds might be very similar on both planets. We could think that there is much more CO_2 on Venus that on the Earth but, in fact, similar quantities are present on both planets, but in different states (*Gierasch et al., 2003*). On Earth, carbonaceous compounds are mainly in the crust, in the form of carbonate minerals while in Venus it is encountered in gaseous form.

In terms of Nitrogen, it results that the 3.5% portion existing on the massive Venus's atmosphere corresponds to approximately the same net Nitrogen quantity that supposes a 78% on Earth's one (*Gierasch et al., 2003*).

	Venus	*Earth*	*Ratio (Venus/Earth)*
Carbon Dioxide (CO_2)	96.5%	0.04%	~ 2500
Nitrogen (N_2)	3.5%	78%	~ 0.050
Oxygen (O_2)	0.0010%	21%	~ 0.00005
Water Vapour (H_2O)	0.004%	1%	~ 0.004

***Table 3**: Venus vs. Earth Atmospheric Composition. Source: NASA*

Water and oxygen seem to diverge from this behaviour. Nonetheless, some hypotheses affirm that there were big amounts of H_2O on Venus, even oceans (*Grinspoon, 2013*). However, due to the greenhouse effect caused by the great quantities of gaseous carbon dioxide, water evaporated and reached the upper atmosphere. Up there and due to the action of Sun's ultraviolet radiation – in the absence of a magnetosphere as advanced before – it got dissociated. Hydrogen escaped to space and oxygen chemically combined with crustal materials, vanishing from the gaseous atmosphere (*Kasting et al., 1983*). Although this has not been demonstrated, what we really know is that nowadays there is very little water in any form or gaseous oxygen in Venus as compared to the Earth.

There can therefore be a high probability that quite similar compounds inventories were present at both Venus and Earth formation, supporting the twin planet theory. Nevertheless, due to their different evolutional fates we now face two opposite situations: the Earth, an oasis for every kind of life possibilities and Venus, a toxic, high-pressure hot inferno. Some support that maybe millions of years ago, if oceans once existed on Venus, life could have had flourished in many forms (*Way et al., 2016*). In spite of the considerable debate among the scientific community, some affirm that even nowadays there may be some microbial life on Venus's atmosphere (*Schulze-Makuch et al., 2004; Limaye et al., 2018*).

Venus is also completely covered by a continuous vertically thick cloud layer (*see Fig. 1*) (*Esposito et al., 1983; Titov et al., 2018*). The principal component of this cloud is Sulfuric Acid (H_2SO_4) droplets (*Zahn et al., 1983; Esposito et al., 1997; Mills et al., 2007*). In addition to its obvious impact on climate, these clouds also have important effect on atmospheric chemistry (*Zhang et*

al., 2012). Hence, it is in the upper cloud where we can find the photochemical sulphuric acid production from SO_2 and H_2O (*Zhang et al., 2012; Marcq et al., 2017; Titov et al., 2018*). Obviously, this implies a great difference with Earth's cloud structure and especially composition. Further details will be given about these clouds on the next section.

There is also an unknown UV absorber in this cloud layer with an absorption band in the near-UV, roughly from 0.28µm to 0.5µm (*Pollack et al., 1980*). There are some hypotheses about what it could be, but it is not clear yet. This mysterious compound is temporally, vertically, and spatially inhomogeneously distributed (*Molaverdikhani et al., 2012*) creating those well-known arbitrary patterns we can see on many Venus's photographs (*see Fig. 2*). Fortunately, it helps with cloud morphology and atmospheric dynamic studies.

Sulphur Dioxide (SO_2), Carbon Monoxide (CO), Chlorohydric Acid (HCl), Argon (Ar), Helium (He) or Neon (Ne) traces can be also found on Venus (*Bezard et al., 1990; Pollack et al., 1993; Marcq et al., 2017*).

To conclude with this first overview, Venus's atmospheric general circulation will be discussed. The 40% of the total atmospheric mass of Venus is found between the surface and 10km height. In this part, winds are very light and constant, and the temperature is very high (*Sánchez-Lavega et al., 2017*). As we increase in height from this point, wind intensity commences to increase until the point at which the planet dynamics are totally dominated by strong zonal winds (*Schubert et al., 1983; Gierasch et al., 1997; Hueso et al., 2015; Sánchez-Lavega et al., 2017; Horinouchi et al., 2018*). These strong winds predominate in the lower and middle atmosphere (up to ~100km), with peak speeds at around 70-75km height, coinciding with the top of the clouds. These reach wind speeds beyond 100m/s (*Hueso et al., 2015; Sánchez-Lavega et al., 2017*), which are three times faster to what we consider hurricane winds here on Earth.

Strong winds imply a fast rotation of the atmosphere, with a rotational period around Venus of four days. This means that the atmosphere rotates 60 times faster than the solid planet (*Sánchez-Lavega et al., 2017*). This is known as zonal Retrograde Super-Rotation (RSR). As Venus's spin is also retrograde, the zonal winds are prograde relative to the surface. In other words, the wind flow is in the same direction as the surface rotation (*Schubert et al., 1983*). Above 75km winds again decrease as the atmosphere also becomes thinner and thinner. On the upper atmosphere above 100km height the dynamics change, and we will find a solar anti-solar circulation (*Lellouch et al., 1997; Widemann et al., 2007*).

The strong zonal winds are therefore the main principal feature of the general circulation of Venus's atmosphere and one of the most complex brainteasers in atmospheric dynamics to be clarified. Conservation of angular momentum and some other mysteries about this pattern are to be explained. Meridional winds are very weak in comparison (*Counselman et al., 1980*).

Lower Venus's atmosphere is mainly stable and stratified. There is only a weak-stable region at the middle cloud at about 50km height where we can find some vertical convection and some gravity waves may form (*Imamura et al., 2014*). Gravity waves can be created by orographic lifting close to the surface too (*Bertaux et al., 2016*). Some planetary-scale waves can be also found (*Covey et al., 1982; Schubert et al., 1983*). Probably the most famous one is the 'Y' shaped one. It travels at similar speeds to cloud tops, and it is thought to follow the Kelvin Wave theoretical frame (*Smith et al., 1993*) although its structure and the nature of its excitation are still not clear. Some Rossby waves can also be observed at mid latitudes (*Covey et al., 1982; Imamura, 2006*).

Polar Vortex, swirls of wind and temperature, are the one final characteristic of Venus's atmosphere. There are two of them, one at each pole. Although they are permanent features, they present strong and chaotic variability on their shape and dynamics (*Garate-López et al., 2013*). This yet needs further study so that it can be explained. These regions are delimited by what is known as the cold/circumpolar collar starting at 60-70° latitude.

1.2 VENUS'S CLOUD REGION

We have so far reviewed a general view of our neighbour planet Venus, but we now need to deepen into the scope of this work. As the validation is to be carried out within the cloud region, this must be better described and defined. Lower and an upper cloud limit must be established. Nonetheless, this is not as easy as it could seem.

As seen before, Venus is completely enveloped by a huge cloud structure (*Esposito et al., 1983; Titov et al., 2018*). This conforms by far the largest aerosol system among the terrestrial planets on the Solar System. Clouds reflect the 70% of the light it receives, being this what makes Venus so bright during the night. This complex system can be subdivided in three main layers according to particle population and size (*see Table 4*): lower, middle, and upper cloud layers (*Esposito et al., 1983*). In addition to the clouds, we can also find a thin haze layer close to the surface, some lower haze below the cloud base and an upper haze above the top of the clouds (*Golovin et al., 1982; Esposito et al., 1997; Satoh et al., 2009*).

The separation of the lower and middle clouds is not very clear as the border is usually not well defined. Upper and middle clouds are often separated by a 2km gap with reduced extinction coefficient, situated at approximately 56km height (*Titov et al., 2018*). Sulphuric acid is the mayor aerosol constituent among all cloud layers (*Zahn et al., 1983; Esposito et al., 1997; Mills et al., 2007*). Besides, in the middle and lower cloud we can also find significant elemental abundances of chlorine and phosphorous (*Krasnopolsky, 1985; Bézard et al., 2007*). Episodes of sulphuric acid virga and rain are common in Venus (*Meadows et al., 2014*).

Region	*Altitude Range (km)*	*Optical depth (at 0.63 μm)*	*Mean diameter (μm)*	*Number Density (N cm^{-3})*
Upper Haze	70-90	0.2-1.0	0.4	500
Upper Cloud	56.5-70	6.0-8.0	0.4-2.0	1500
Middle Cloud	50.5-56.5	8.0-10.0	0.3-7.0	350
Lower Cloud	47.5-50.5	6.0-12.0	0.4-8.0	1300
Lowe Haze	30-47.5	0.5-3.0	0.1-0.3	500

***Table 4**: different cloud and haze regions between 30 and 90 km altitude. Optical depth and particle size information from Esposito et al., 1983, aerosol population from Knollenberg et al., 1980, and lower haze parameters from Satoh et l., 2009.*

A first approach to the vertical extent of the cloud region is depicted on Fig. 3. It shows the general averaged vertical distribution of the cloud structure. It establishes a cloud base at 45-48km height and the cloud top at 70-73km height. Nonetheless, this figure does not consider latitudinal and temporal variability of cloud limits.

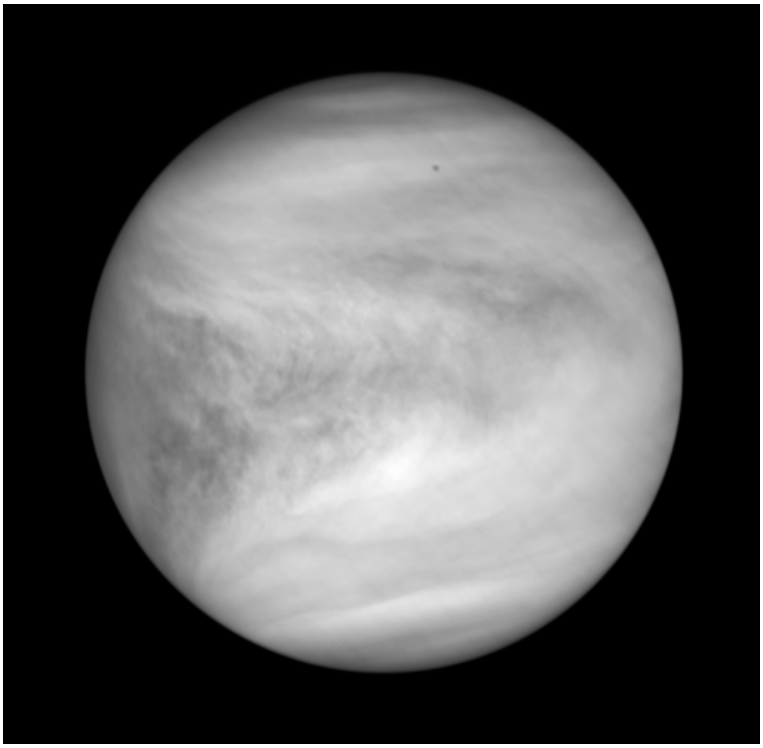

***Figure 2**: unknown UV absorber traces on cloud region captured by Akatsuki UVI instrument. Source: JAXA*

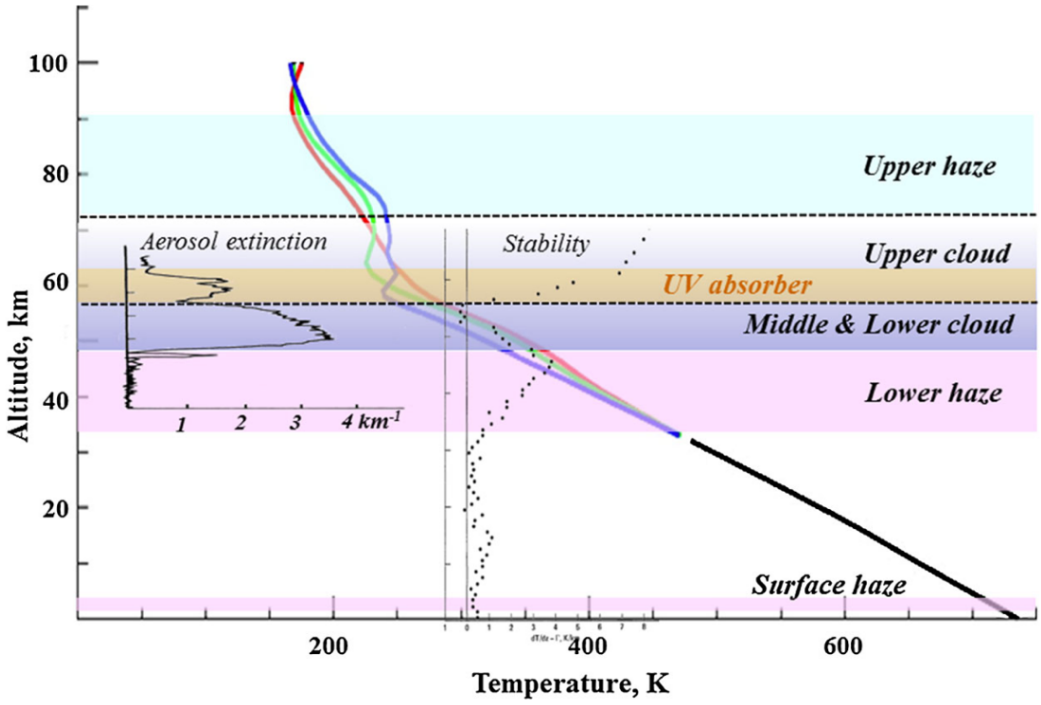

***Figure 3**: vertical structure of Venus's clouds as derived by Venera and Pioneer Venus descent probes. The colour lines show mean temperature profiles at low (red), middle (blue) and high (green) latitudes with a single black line representing the temperature structure below 30 km. The typical vertical profile of aerosol extinction (Ragent et al., 1985) is shown on the left. The static stability profile from the VIRA model (Seiff et al., 1985) is shown in the middle. Figure from Titov et al., 2018.*

At 60° latitude there is a vast polar depression on the cloud structure, and cloud tops height progressively lowers between 4-8km (*Ignatev et al., 2009; Grassi et al., 2014; Haus et al., 2014; Titov et al., 2018; Sato et al., 2020*) (*see Fig. 4*). This area coincides with the cold collar region (*Lee et al., 2012; Haus et al., 2014; Titov et al., 2018; Sato et al., 2020*). Temporal variation of cloud's tops is not that clear or shows any logical pattern (*Lee et al., 2012; Titov et al., 2018*). This is not essential for the scope of this work as validation is based on averaged long-term conditions. We can then encounter a cloud top altitude varying from 65-73km height according to latitudinal aspects. It is also important to remark that cloud top altitude is symmetric with respect to equator (*Ignatev et al., 2009; Grassi et al., 2014; Haus et al., 2014; Titov et al., 2018; Sato et al., 2020*). Although cloud's top shrink vertically towards the pole, there is not a significant change in middle cloud structure (*Titov et al., 2018*).

Cloud base does not present that evident latitudinal variation, although it slightly follows the same behaviour at that same 60° latitude. It decreases in height no more than 2-5km (*Barstow et al., 2012; Tellmann et al., 2009*). This supposes that cloud base reaches down to 45km in polar regions. On the other hand, it is firmly believed that there is much stronger temporal variability in the deep cloud structure related to optical thickness in comparison with middle and upper clouds (*Titov et al., 2018*). Lower hazes consist of very small particles and comprise between 30-40km height and cloud base (*Satoh et al., 2009*). Upper haze extends from cloud top up to 90km height, what means that they cover a vertical extension of about 20km (*Esposito et al., 1983*).

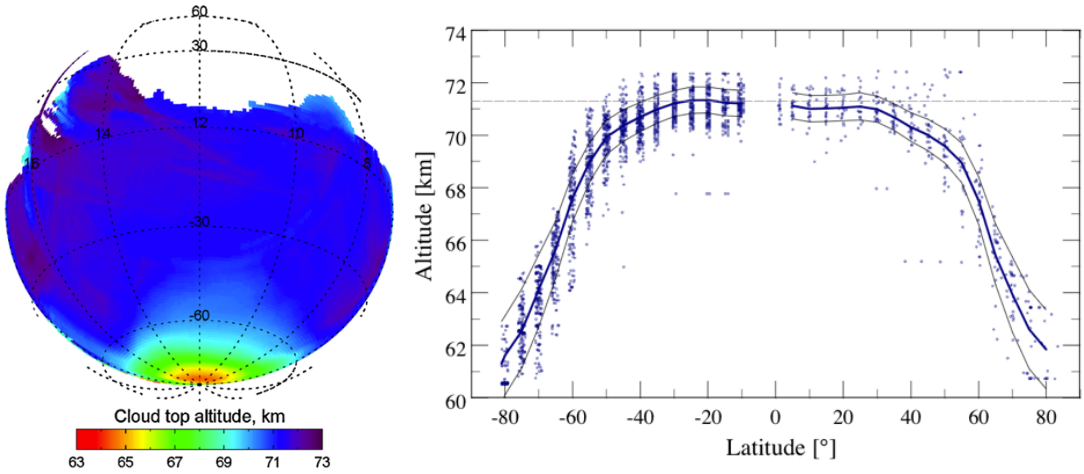

Figure 4*: cloud's top altitude. Left: mean cloud to altitude as a function local time in the south hemisphere (figure from Ignatiev et al., 2009). Right: zonal average cloud top altitude at 1 μm as a function of latitude on both hemispheres. Thin solid lines show retrieval error range boundaries referred to the mean curve (figure from Haus et al., 2014).*

It is now clear that latitudinal and temporal variability, optical thickness variations, and upper and lower hazes make it difficult to clearly establish a cloud lower and upper limit, which is the main objective of this section. By putting together the values given by the many sources it has been decided to cover from 40km up to 75km height for the validation purposes. This is probably slightly beyond the cloud region, but it will let a more ample and comprehensive study and will be more tolerant to measurement errors and some possible temporal variability.

In addition, when studying composition, the inferior limit will be lowered down to 35km as there is a much larger amount of actual data.

1.3 THE EXPLORATION OF VENUS

Planetary studies have been carried out for centuries and, due to its proximity, Venus has always been one main target within the Solar System. From the initial ground based telescopic observations and findings carried out by Galileo Galilei in the XVII century (*Palmieri 2001*) Venus's research has evolved to modern robotic exploration based on fly-bys, orbiters, and landers.

The first spacecraft observations of Venus took place in the early sixties and, from then on, several space missions have been conducted in the last decades. Soviet ones have predominated, constituting about the 75% of the total (*Bonnet et al., 2013*). After some failed soviet attempts, the first successful Venus flyby was performed by the NASA *Mariner 2* in 1962, confirming the radioastronomy observations of a dense carbon dioxide atmosphere and extremely high surface temperatures (*Sonett, 1963*).

In the following years, the URSS *Venera* programme finally bloomed, entailing some crucial interplanetary milestones. *Venera 3* crash-landed on the Venusian surface, being the first human-made object to impact another planet's surface while *Venera 4* was the first human mission to perform in situ atmospheric measurements on another planet. *Venera 4 to 6* probes allowed some atmospheric measurements including pressure, temperature, composition, and density and confirmed some early evidence of Venus's atmospheric dynamics including the strong zonal wind super-rotation (*Marov 1972*).

Then, *Venera 7 to 14* were mainly landers equipped with a wide variety of instruments for surface studying including cameras, microphones, surface samplers or seismometers, among others. *Venera 9* returned the first picture of the surface of another planet (*see Fig. 5*). Finally, *Venera 15 and 16* orbiters replaced the entry probes of previous missions with imaging radars allowing global coverage and providing the first tectonic study data (*Basilevsky et al., 1986*). This data was later surpassed by the American *Magellan* radar mapping dedicated mission in 1990 with a much greater resolution of about 100m (*see Fig. 1*) (*Johnson, 1991*).

Venera programme was therefore continuously succeeding for more than two decades (1961-1983), pioneering and boosting Venus and other planetary research. It settled the basis for Venus's exploration and founded our nearest planet as the principal objective in the early years of the space age (*Taylor 2014*). Coinciding with the latter *Venera* missions, NASA launched the *Pioneer Venus* project in 1978. It consisted of the *Pioneer Venus Orbiter* and the *Pioneer Venus Multiprobe*. The first was used to map the surface, characterise the upper atmosphere and ionosphere, and study the solar wind impact on Venus; while the second involved four in situ probes to measure mainly winds, composition and temperature (*Colin et al., 1977*). The data provided by the mission was tremendously valuable and together with the latest *Venera* missions they provided the necessary legacy to the modern understanding of the Venus's atmosphere (*Kasprzak, 1990*).

Motivated by Venera design, *Vega 1 and 2* missions (1984) involved two identical aerobots designed to drift on the Venusian atmosphere at an altitude of about 55km to undertake in situ measurements. The balloons continuously operated during two Earth's days. They allowed for better comprehension of Venus's atmospheric dynamics, especially concerning the strong zonal winds (*Blamont et al., 1986*). The mission was the result of the cooperation between the URSS and several European countries.

The mentioned missions ended by the late 80s and early 90s. From then there was a more than fifteen-year period without any further spacecraft research on Venus (except from *Galileo*, *Cassini-Huygens*, and *MESSENGER* fly-bys). It was not until 2005 that the ESA launched its first dedicated mission to the planet, known as *Venus Express (VEx)*.

Figure 5: on the upper figure we can see Venera 9 first image of the Venusian and other any planetary surface. Lower figure shows posterior Venera 10 image of the Venus's surface.

VEx orbited on a highly elliptic polar orbit for about nine years (2006-2015) providing highly valued data and it is of vital importance for this thesis. The great technological improvement in in space research from *Venera* and *Pioneer Venus* era permitted more complete and advanced instruments and techniques. This and the outstanding results make *Venus Express* the principal and most valuable source of data for this work as it allows a very extensive study of the atmosphere including winds, temperature, density and even composition (*Tsang et al., 2008; Haus et al., 2014; Grassi et al., 2014; Parkinson et al., 2015; Hueso et al., 2015; Vandaele et a., 2015; Limaye et al., 2017*). Furthermore, observations were carried out with unprecedented spatial and temporal detail of cloud morphology and patterns enhancing the study of complex atmospheric dynamics such as waves, super-rotation or polar vortex (*Markiewicz et al., 2007; Dmitrij et al., 2012; Hueso et al., 2012; Picalli et al., 2014; Garate-López et al., 2013; Patsaeva et al., 2015; Machado et al., 2022*).

The main VEx experiments related to the extent of this work are explained on *Limaye et al., 2017*:

- Solar Occultation in the Infra-Red (SOIR): the solar occultation method retrieves vertical profiles of carbon dioxide abundance and atmospheric temperature from CO_2 number density as well as molecular rotational temperatures from CO_2 spectral structure (*Bertaux et al., 2007*) at the morning and evening terminators at occulted latitudes.

- Spectroscopy for Investigation of Characteristics of the Atmosphere of Venus (SPICAV): stellar occultations allow the determination of vertical profiles of CO_2 abundances and derive the temperature from the CO_2 number density (*Bertaux et al., 2007*).
- Venus Express Radio Science (VeRa) instrument: radio occultations allow the derivation of vertical profiles of temperature, pressure and total neutral number density between 40 km and 100 km altitude (*Häusler et al., 2006, 2007*).
- Visible and Infra-Red Thermal Imaging Spectrometer (VIRTIS) instrument: VIRTIS observations provide thermal maps at medium spectral resolution and profiles from nadir and limb locations at high spectral resolution (*Piccioni et al., 2007*). This instrument also let the study of zonal winds and has been very successful on its tasks.

VEx mission also had some other instruments but has not been used for this validation. The last mission on Venus was launched on 2010 by the Japanese JAXA. It is known as *Akatsuki, Venus Climate Orbiter (VCO) or Planet-C*. Due to a failed orbital insertion on that year the first data collected was in 2015 and after various mission extensions it is still working in 2022. *Akatsuki's* orbit (highly elliptical but not polar) is complementary to that of *VEx* and therefore supposes a great continuation to *Venus Express* on atmospheric research. *Akatsuki* orbiter has several instruments including an Ultraviolet Imager (UVI), two infrared cameras, and some other instruments for Venus's observation.

The review of the historical Venus's space missions allows us to understand the data used for the validation. Two different periods on Venus's research can therefore be differentiated, with a long interval between them without any dedicated mission launched to Venus. Although *Venus Express* constitutes the main source of data due to its technological advantages, the *Venera* missions*, Pioneer Venus* and *Vega* balloons results have been also used in this validation because of the in-situ measurements, vital on importance and not repeated in the recent years of space exploration. These last are especially necessary when studying the atmospheric composition and they also complement the most recent remote data.

Referring to Akatsuki, although some data from this mission have been used in this work (especially for wind validation), the focus has been on VEx results and scientific papers, as they were more numerous. In the short future, as more and more Akatsuki results will be published, this validation could be completed with the last Akatsuki results. As a conclusion, data from very different decades (and thus technologies) has therefore been used for the VCD validation in this thesis, but each have their unique properties that make the VCD validation more complete.

The future of Venus's Exploration

History shows that Venus was the protagonist of planetary exploration during the first two decades of modern space research but only *Venus Express* (2005) and *Akatsuki* (2010) missions have been launched recently. One main reason is that Mars took most of the efforts and resources of planetary exploration within the Solar System in the recent years, in the pursuit of past or present life on the planet.

Nonetheless, the tendency is now reversing, and Venus has retaken the interest it had. NASA announced two missions that will reach the planet in the late 20s, thirty years after the last American mission to the planet. Roscosmos will also continue with the *Venera* saga, half a century later, and European ESA and Indian ISRO are working on new missions too. The main aim of the next missions is to try to reveal the divergence on the Earth's and Venus's evolution paths and to study the complex atmospheric properties and dynamics (*Bonnet et al., 2013*).

Mission Name	*Agency*	*Planned Launch Date*	*Spacecraft Characteristics*
Shukrayaan-1	ISRO	2024	Orbiter and Atmospheric Balloon
VERITAS	NASA	2028	Orbiter
DAVINCI	NASA	2029	Atmospheric Probe
Venera-D	Roscosmos	2029	Orbiter and Lander
En-Vision	ESA	2031	Orbiter

Table 5: summary of the announced future missions to Venus.

Future research must rely on advanced mission architecture, involving multiple orbiters, landers, rovers, balloons, and atmospheric probes (*Bullock et al., 2009*). This means that atmospheric modelling efforts are essential and should to be increased for two main reasons:

1. It is vital to predict the atmospheric conditions the probes will encounter for in-situ science so that we can optimise spacecraft design and instrument characteristics and specifications. This is traduced on cost-adjusted, longer-living and more prolific missions.
2. There is a continuous inter-connection between observational data and models, as observations would permit better modelling capabilities and finest results while modelling may boost the value of the observations value as these can be better interpreted and understood if we are able to reproduce them on numerical models. Models might also fill in the blanks of the observational data that could not been measured.

This remarks the importance of atmospheric modelling for planetary research. It is obvious that only accurate and correct models can be relied on. Therefore, their validation process is as critical as the model itself. Consequently, the importance of VCD and VCD validation for Venus's future research is hereby shown and justifies the main purpose of this thesis.

1.4 GENERAL CIRCULATION MODELS (GCMs) AND VENUS MODELLING

General Circulation Models (GCMs) are numerical models that simulate the evolution, maintenance, and variations of the time-averaged planetary-scale atmospheric motion (*Mechoso et al. 2003*). They will therefore represent the long-term behaviour of the general circulation of a planetary atmosphere.

GCMs were developed after Numerical Weather Prediction (NWP) models that proposed a mathematical approach to weather forecasting. All these ideas advocated in the early twentieth century, but it was not until the electronic computer era when they have tremendously flourished (*Edwards 2007*). The simple idea behind GCMs fundamentals is the representation of atmospheric processes by a set of governing equations to be repeatedly solved by the use of powerful supercomputers (*Lynch 2007*).

The first GCMs were conceived for Earth atmospheric modelling. The today's main applications are weather and climate prediction and investigations aimed for an enhanced understanding of the climate system (*Mechoso et al. 2014*). Another important application is the study of climate change and mankind's impact on climate variability. You can run the simulation of the atmosphere's circulation for any intended time lapse so that you can anticipate the future conditions and the evolution of climate (*Lynch 2007*). With all these advantages, big efforts are set towards the continuous refinement of advanced models and the increase in their sophistication.

Being Earth's GCMs such a useful tool, it will come as no surprise that GCMs have also been developed for planetary science. Modelling of other atmospheres such as Venus's, Mars's or Titan's provides us with a better understanding of the atmosphere's general circulation and dynamics. In the case of Venus, GCMs will help us studying its thermal structure, balance of angular momentum, planetary-scale waves or thermal tides, among many others. In addition, it progressively helps on revealing the mysterious mechanisms behind the origin of the atmospheric super-rotation (*Mendonça et al., 2016*).

Nonetheless, Venus's GCMs are quite different from Earth's ones. Probably, the most obvious dissimilarity is that the quasi-geostrophic balance models developed for the Earth do not fit Venus's characteristics, due to its slow rotation. Here we can see the main challenges that may be present on Venus's modelling (*Lewis et al., 2013; Sanchez-Lavega et al., 2017*):

- For realistic simulations, the development of full radiative transfer is needed. Simplified temperature forcing does not provide fully satisfactory results. Radiative transfer calculations are usually complex in Venus because of the very opaque cloud layer and dense CO_2 atmosphere, with very high temperatures and pressures below clouds.
- Features tend to be very difficult to reproduce. Super-rotation is easily lost without proper computation of opacities and albedo. These are determined by the cloud structure and properties, the gas composition of the atmosphere, and the spectral properties of the different gas constituents.
- The dense and optically thick atmosphere results in very long radiative relaxation times, so models must be run for many tens of Venusian years to approach equilibrium. This supposes higher computational costs.
- Great sensitivity to model parameters. As an example, zonal wind fields are normally extremely sensitive to many of them such as topography.
- Extreme sensitivity to angular momentum budget. Some examples might be found when establishing the impact of mesoscale gravity waves on Venus atmospheric circulation as they transport angular momentum with their propagation, possibly playing a role in the acceleration of the circulation. Atmospheric interactions with terrain could also be problematic as exchanges of angular momentum with the surface are hard to parametrize.
- The representation of the polar vortexes in the GCMs may also be an issue. Though some GCM simulations exhibit a plausible polar vortex structure, the modelling of the cold collar region generally needs improvement.

As we can see, the main challenges are mostly related to radiative transfer and angular momentum budget. Therefore, a proper design of the governing equations and parameters tend to be defiant and at the same time crucial for satisfactory modelling of Venus atmosphere. Different model inter-comparisons have been made with very different results, even when most parametrizations are chosen to be identical (*Lebonnois et al., 2013*). The dispersion of the results is therefore quite surprising in some of the cases. These intercomparisons remain important for model improvement and some of the principal challenges have already been overcame in certain recent models. Venus GCM simulations are now realistic enough to start data assimilation projects (*Sánchez-Lavega 2017*).

It is important to remark that we are focusing on Venus's modelling from surface to 100km altitude, where dynamics are governed by super-rotation. As stated on the introduction, above 100km non-LTE radiative processes become dominant and control both the thermal structure and the solar-antisolar circulation. This implies a completely different approach outside of the scope of this work.

1.5 VENUS CLIMATE DATABASE (VCD) AND ITS WEB INTERFACE

The Venus Climate Database (VCD) is a database of atmospheric statistics compiled from state-of-the art GCM simulations of the Venusian atmosphere (*Lebonnois et al., 2021a*). It aims at providing scientists, engineers, and enthusiasts with a realistic and reliable modelisation of the Venusian atmospheric and climatological system. This GCM is developed and maintained by the planetary science group at *Laboratoire de Météorologie Dynamique* in Paris and was one of the first GCM simulations that implemented a full radiative model and solar heating through the gaseous atmosphere. Many of the other challenges previously mentioned are also being addressed and gradually overcame, except that it seems to be very difficult to consider the variability of opacities on these radiative transfer models.

Several simulations were carried out for more complete VCD possibilities by modifying and creating different scenarios. All these are saved on the VCD database, and you can access one or another by a fine tuning of your data enquiry. The duration of each simulation comprises between 250-350 Venusian days (*Lebonnois et al., 2013a*).

Simulations were run for two main differentiated regions: the lower atmosphere and the thermosphere. The boundary between both is at 150km altitude. Therefore, VCD provides information about both super-rotation dynamics in the lower atmosphere and subsolar anti-solar circulation in the upper part, governed by non-LTE processes (*Lebonnois et al., 2021a*).

Some of the main features considered in VCD simulation are presented here (*Lebonnois et al., 2013*):

- Convection in the boundary layer
- Non orographic and orographic gravity waves
- Diurnal cycle
- Topography
- Dependence of specific heat capacity on temperature
- Latitudinal variability of the cloud top
- Thermosphere Extreme UV heating from look-up tables that depend on solar zenith angle, provided by *Crisp, 1986*
- Conduction and molecular diffusion in the thermosphere
- Photochemistry that controls atmospheric composition in upper thermosphere

Variables were obtained and stored on the database on a spherical grid with a resolution of 96x96 longitude x latitude. This supposes steps of 3.75° in longitude and 1.875° in latitude. Vertically, the database extends over 90 levels. The first 50 comprise the lower previously mentioned region up to 150km altitude and the other 40 the thermosphere region between 150-350km. The temporal structure is stored along one full Venus's day, that lasts 10087200s. 24 data points are stored for a day, that is, one data point per local hour or 1/24 of a Venusian day (*Lebonnois et al., 2021a*).

The VCD software can be completely installed on a PC or server and called using some of the most popular programming languages such as Python or IDL (*Lebonnois et al., 2021a*). This is not used in this work, but the web version instead. The VCD Web interface is a free and user-friendly online tool that allows the user to easily extract the desired data from the database. It is more limited that the software but allows plenty of options.

The VCD Web interface is divided in three main categories (*see Fig. 6*): main settings, advanced settings and one-click pre-sets. It is in the main settings section where you can select the spatial coordinates and variables to be plotted (up to four), the altitude, the latitude, the longitude, or the local time.

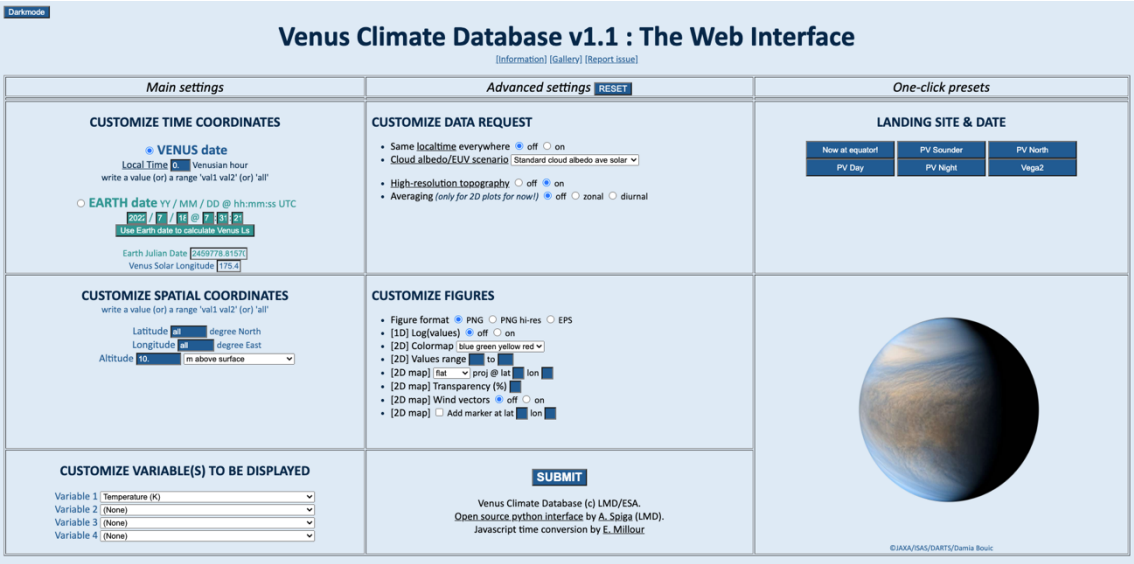

***Figure 6**: screenshot of the Venus Climate Database Web Interface v1.1. Note that few days before the publication of this thesis version v2.0 was launched. Functionalities are maintained identical; it is only the design of the web that has changed (http://www-venus.lmd.jussieu.fr/vcd_python/)*

The advanced settings require some more comprehension as combinations of solar and cloud albedo scenarios are provided. EUV scenarios permit average solar, maximum solar and minimum solar based on the Sun 11-year cycle. Albedo scenarios can be chosen between standard cloud albedo (*Haus et al., 2014*), low cloud albedo (*Lee et al., 2019*) and high cloud albedo. Therefore, in the VCD Web Interface we can find the following combinations:

- Standard Cloud Albedo average solar
- Standard Cloud Albedo minimum solar
- Standard Cloud Albedo maximum solar
- Low Cloud Albedo average solar
- High Cloud Albedo average solar
- EUV deduced from Earth date
- EUV specified

To the extent of this work, EUV input will have no impact for the results as it only has effect on the thermosphere. Therefore, only the albedo option needs to be taken into consideration. As we are looking for averaged long-term conditions for the validation, the standard albedo option is chosen for all the presented results. This means that all the VCD results presented on this thesis are run in the Standard Cloud Albedo average solar configuration.

Another feature of the advanced settings is High Resolution Topography. VCD is compiled from a GCM in which topography used but it is very smoothed because of its low resolution. The “high resolution mode” includes 23pixels/degree topography measured with Magellan radar altimeter combined with a few topography measurements from Pioneer Venus to fill in the gaps

(*Lebonnois et al., 2021a*). This computes surface pressure as accurately as possible and redefines some values of atmospheric variables such as temperature and density.

Although the High Resolution Topography option has been selected to ON in all cases in this VCD validation, this will have no effect on the results of this work for two reasons: the validation cloud region begins higher in the atmosphere and is not therefore affected by this feature and, more importantly, we are mainly working with altitudes above Venus's reference sphere where topography has no implication.

Finally, the zonal or diurnal average options in the advanced settings are another useful tool that the Web Interface includes. Figure customization is not of great use in our thesis as we just extract the VCD data to craft our own representations (see next section). The online click pre-sets can be used to tune the exact locations and Venus dates at which the given missions operated.

2. METHODOLOGY

In this section the validation process carried out in this work will be reviewed. Mainly, the way the validation is executed is by visually comparing the Venus Climate Database output with results obtained from measurements and observations taken by several space missions and published in scientific papers. This process comprises three main stages:

1. **Documentary Research**

After some familiarization with the VCD Web Interface – so that you are aware of the available data that it can provide – the first step is to collect and read different bibliographical sources (mainly articles and reviews published in scientific journals). Then, from the literature you extract the most valuable and appropriate real observational results to work with. The four main variables taken from the papers are number density, temperature, winds, and chemical composition because of their main relevance within the VCD output options. At the same time, in this stage the study references are widen so that a more rich and complete literature is achieved to expand the information variety and sources.

2. **Data acquisition and presentation**

Once we have compiled the proper observational data from the literature it is time to extract the same variables from the VCD database. This will be made by using the VCD Web Interface. Special attention is needed so that the correct data enquiry is carried out by appropriately parametrizing the main and advanced settings on the VCD interface.

Now we have both the observational and the simulated data to be validated but in a format that is not be the best. It is desired to present the data properly so that it can be validated easily. At this point, we can differentiate between two main dataset layouts: profile plots and 2D maps.

The best way to set up profile plots is by overlapping them one on top of the other(s). In other words, it is desired to plot both VCD data and Venus observational data on a single plot. This will allow rapid and intuitive comparison, immediately identifying the similarities and differences between them. To be able to do this, computerised plots are made with programming tools in the *Spyder* environment using *Python* language.

One of the difficulties is that, for doing this, you need the actual observational dataset so that the software can plot it. In the case of the VCD data this is not a problem because you can download the ASCII file containing data directly from the Web Interface as a *.txt* file. On the flip side, the only piece of information you can obtain from most of the literature is the illustrated plot. Therefore, if you want to re-plot the dataset for the validation purposes the only way to do this it is by extracting the (x, y) values and export them onto a new text file. Initially it was made manually but the inaccuracies are considerable; besides, it is prone to slip errors and lapses and tremendously time-consuming.

For this reason, an automated web-based tool has been used. It is called *WebPlotDigitizer*. With it you can screenshot the graph and after loading it into the software, you start by calibrating the axes. Then you select the data to be retrieved. To do this, several functions are available – manual, automatic or a combination – being possible to use the one that fits better for a particular plot. Once the points are selected, the software will automatically extract the (x, y)

coordinates. Now it is possible to plot the VCD and the literature Venus data on the same graph in with the use of the *Spyder* software.

With the 2D maps, the best strategy is to arrange the VCD 2D maps next to the real maps picked from the different papers. Therefore, data presentation could be almost direct. Nevertheless, VCD and maps from the literature are in most cases totally different in appearance to those generated by the VCD, even when the results are quite similar. Although from the scientific point of view this is not problematic, again for easier and more visual validation VCD maps have been modified to get closer to the design used on the bibliographical source.

At this point, validation results can be analysed and presented, and validation conclusions are extracted. All the results are presented in the next section.

To conclude this methodology section, the main difficulties found in the validation are described here. First, it is important to mention the personal struggles I encountered in the use of programming language, as I had never programmed before. That entailed an initial learning process in close collaboration with my thesis tutor, from some basics to more advanced commands, until I acquired the enough knowledge and familiarity with the programming language so that I could produce elaborated plots.

Secondly, it is important to mention some of the hurdles found related with the VCD Web Interface version. Although this is not directly related with the validation of the numerical model simulation itself, it may be positive feedback so that the software/interface can also be improved:

- For night-time data acquisition, if you want to cover a time range that passes through midnight, the VCD Web Interface output is exactly the opposite one. For example, if your desired enquiry ranges from 20:00LT to 04:00LT, the interface will generate a plot/map from 04:00LT to 20:00LT. There is no way to parametrize the interface correctly. Therefore, when this kind of data was needed, two different data calls had to be made, one between 20:00LT to 23:00LT and another from 00:00LT to 04:00LT. Then data was put all together on a same text file.

- Another software flaw was found when generating the ASCII file of colour maps. Several slightly different values of the dependant variable are given to the independent one. Imagine that a temperature colour map on a height (y-axis) versus latitude (x-axis) grid is represented. When exporting the ASCII file, this will contain each latitude value repeated several times (*see Fig. 7*). Moreover, for each fixed height value the same repeated latitude will have slightly different temperatures value (on the third decimal). This will create colour/contour maps distortion. Therefore, repeated values are supressed for the representations in this validation. It should be made clear that this does not only happen with latitude but with any feature set as the independent variable (i.e., longitude or local time).

- The final issue that should be corrected on the VCD Web Interface is the one associated with the zonal or diurnal averaging. If you select one of those two functions but you inadvertently leave a local time value in the time coordinates box (for example 10), results will be shown for that particular local time (10LT in this example) instead of the zonal or diurnal mean results you were expecting to retrieve. This entails a software flaw but would

not be that problematic if at least you can realise afterwards (so that a new correct enquiry could be made). However, the following software fault is even more alarming as the plot and the ASCII will show the "*Zonal mean over al longitudes*" or "*Diurnal mean over all local times*" extract phrases on their titles, without the user being able to realise that the enquiry that was made is not corresponding with the VCD Web Interface output. Even if you are aware that you have a certain local time value on the VCD settings and you run any of the averaging options you may wrongly think that zonal or diurnal mean has priority over the local time selection setting.

```
################################################################################################
### VCD_v1.1 with Standard cloud albedo scenario, average solar EUV conditions. Longitude
### ------------------------------------------------------------------------------------------
### Column 1 is North latitude (degrees)
### Columns 2+ are Temperature (K)
### Line 1 is altitude above Venus ref sphere (m)
### ------------------------------------------------------------------------------------------
### Retrieved on:
### Venus Climate Database (c) LMD/ESA
################################################################################################
---- ||    4.00000e+04    4.10294e+04    4.20588e+04    4.30882e+04    4.41176e+04    4.5
-----------------------------------
+030 ||    4.17221e+02    4.09708e+02    4.02317e+02    3.96145e+02    3.89973e+02    3.8
+030 ||    4.17202e+02    4.09683e+02    4.02288e+02    3.96114e+02    3.89941e+02    3.8
+030 ||    4.17186e+02    4.09661e+02    4.02260e+02    3.96085e+02    3.89910e+02    3.8
+030 ||    4.17170e+02    4.09638e+02    4.02233e+02    3.96056e+02    3.89880e+02    3.8
+031 ||    4.17153e+02    4.09615e+02    4.02205e+02    3.96027e+02    3.89849e+02    3.8
+031 ||    4.17136e+02    4.09592e+02    4.02177e+02    3.95998e+02    3.89818e+02    3.8
+031 ||    4.17120e+02    4.09570e+02    4.02150e+02    3.95969e+02    3.89787e+02    3.8
+032 ||    4.17100e+02    4.09544e+02    4.02120e+02    3.95936e+02    3.89752e+02    3.8
+032 ||    4.17081e+02    4.09519e+02    4.02090e+02    3.95903e+02    3.89716e+02    3.8
+032 ||    4.17061e+02    4.09494e+02    4.02061e+02    3.95871e+02    3.89681e+02    3.8
+033 ||    4.17042e+02    4.09469e+02    4.02032e+02    3.95839e+02    3.89646e+02    3.8
+033 ||    4.17023e+02    4.09445e+02    4.02003e+02    3.95807e+02    3.89611e+02    3.8
+033 ||    4.17004e+02    4.09420e+02    4.01973e+02    3.95775e+02    3.89576e+02    3.8
+034 ||    4.16982e+02    4.09393e+02    4.01942e+02    3.95741e+02    3.89539e+02    3.8
+034 ||    4.16960e+02    4.09366e+02    4.01910e+02    3.95706e+02    3.89502e+02    3.8
+034 ||    4.16938e+02    4.09338e+02    4.01878e+02    3.95671e+02    3.89465e+02    3.8
+035 ||    4.16916e+02    4.09311e+02    4.01847e+02    3.95637e+02    3.89428e+02    3.8
+035 ||    4.16894e+02    4.09283e+02    4.01815e+02    3.95603e+02    3.89390e+02    3.8
+035 ||    4.16873e+02    4.09256e+02    4.01784e+02    3.95569e+02    3.89354e+02    3.8
```

***Figure 7**: screenshot of the ASCII file. It can be seen on Column 1 how latitudes are repeated and the slightly different temperature values (rest of the columns) for a given latitude-altitude parameter.*

3. RESULTS

This is the main section of this thesis, at which the validation of Venus's cloud region will be presented, analysed, and interpreted, and where the main conclusions will be reached. Temperature, winds, number density, and composition results will be shown.

3.1 TEMPERATURE

Temperature validation will be accomplished by separately studying nightside, dayside, and terminator temperatures. VCD night temperatures are primarily compared with VIRTIS instrument results on Venus Express (VEx). Due to its eccentric polar orbit, VEx's trajectory was slower and further from Venus when overflying the south hemisphere allowing for better and more global observations, as compared to the northern hemisphere. Therefore, part of the validation focuses on the southern hemisphere as there is a considerably greater amount of observational data with more reliable results. Nonetheless, hemispheric symmetry is expected at the atmospheric levels (~40-75km), so conclusions can be extrapolated from south to north hemisphere.

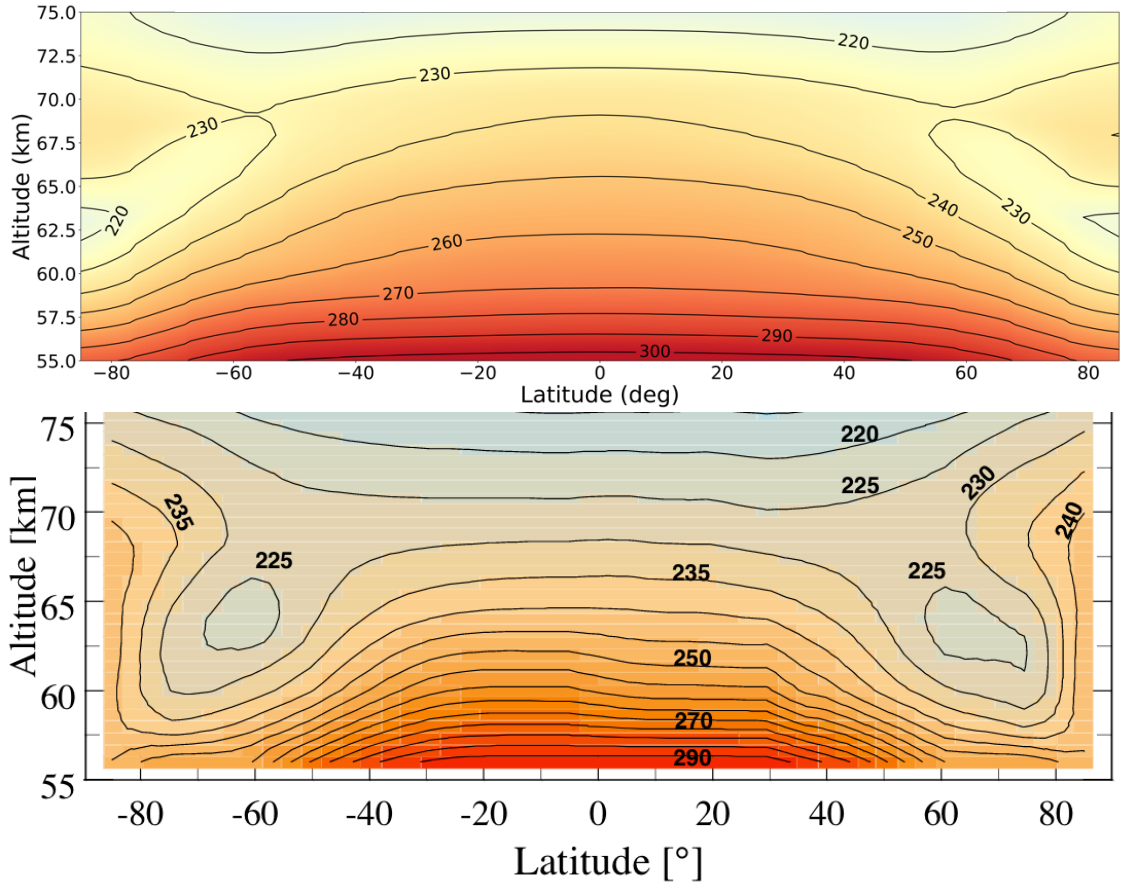

***Figure 8**: zonally averaged night-time (19:00LT and 05:00LT) mean temperature field (units: Kelvin) as a function of latitude and altitude. The lower map shows data measured by VEx's VIRTIS-M-IR instrument (reconstructed from Haus et al., 2013, northern hemisphere, and Haus et al., 2014, southern hemisphere). The upper map shows the temperature field retrieved from VCD, where altitudes are taken above a reference sphere of radius 6052km.*

A first global nightside temperature distribution is shown in Fig. 8. VCD nightside temperature results from Equator to mid-latitudes (up to 45°-50°) are quite consistent with VIRTIS observations. However, above those latitudinal values some divergences arise. Cold collar is clearly shifted to higher latitudes on VCD when compared to observations. The maximum temperature deviation is found on the cold collar's core, representing a divergence between model and VIRTIS measurements of about 15 to 20 degrees in latitude. Additionally, the cold collar on the VCD appears 2 to 4 kilometres higher in altitude as compared to VIRTIS results. Both modelled and observed temperature fields show a similar and clear hemispheric symmetry.

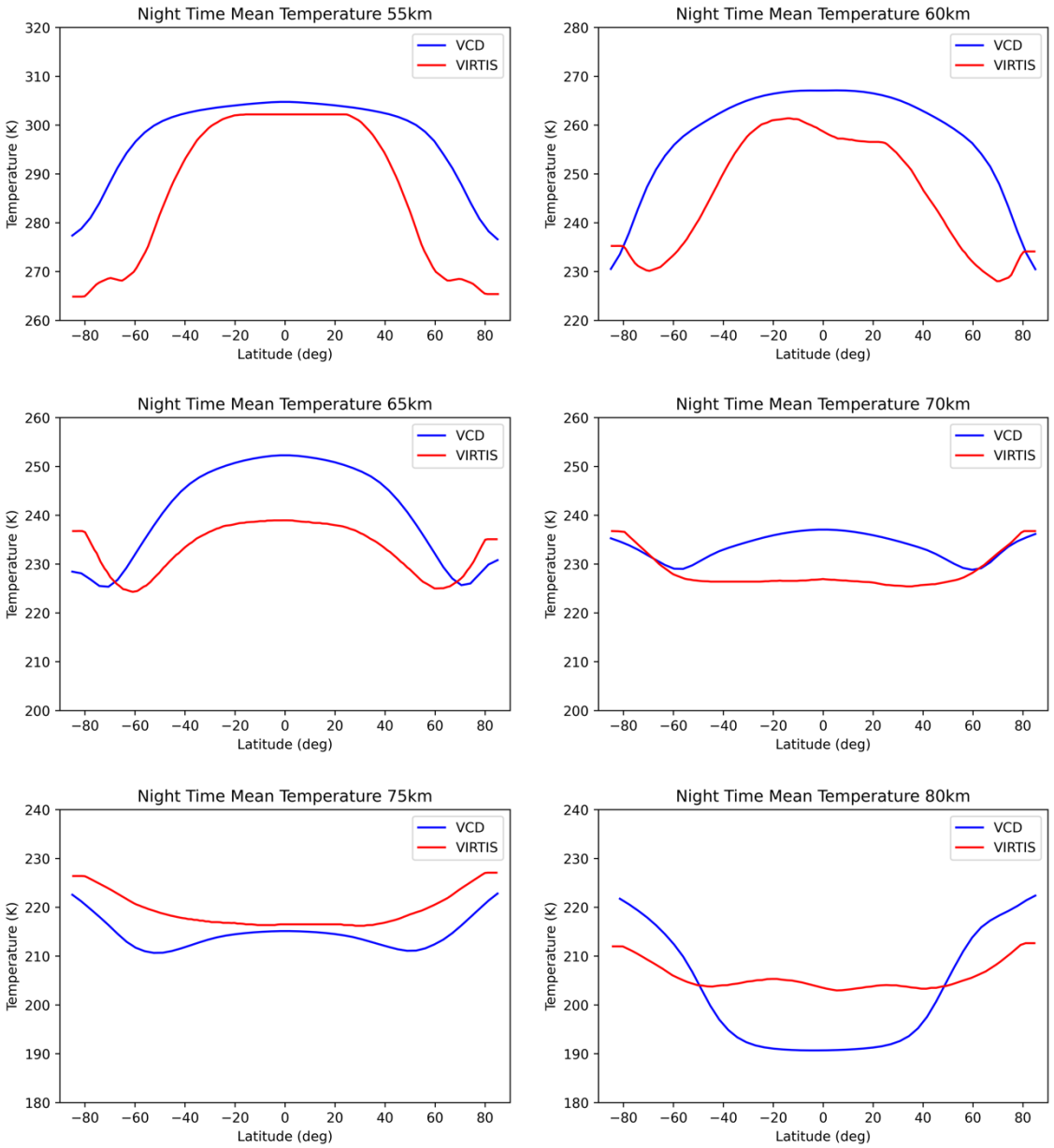

***Figure 9**: latitudinal mean temperature profiles at night-time (19:00LT - 05:00LT) for different altitudes. Red lines are zonal averages of night temperatures measured by VEx's VIRTIS-M-IR instrument by Haus et al., 2014. Blue lines are VCD data output at those altitudes above a reference sphere of radius 6052km, retrieved at each single night hour between 19:00LT and 05:00LT and then mathematically averaged.*

Nighttime latitudinal temperature profiles in Fig. 9 also show the VCD cold collar latitudinal shift to higher latitudes and its displacement to slightly higher altitudes as compared to observational data. At 60km height, VIRTIS results depict the appearance of the cold collar at about 65° latitude while VCD output does not until 65km altitude. Moreover, this temperature pattern appears again 8 to 10 degrees higher in latitude on the model as compared to observational results. VIRTIS show a progressive diminishing of the cold collar pattern at 70 to 75km altitude while VCD's profile still describes a clear curve, characteristic of the cold collar.

Fig. 9 is also a good complement to Fig. 8 as it allows for further deductions not so easily noticeable in the nocturnal temperature field map. From 55 to 75km, overall VCD night temperatures are warmer than observational ones for about 5 to 10K. This temperature difference has different behaviour depending on altitude. For middle cloud (55km altitude), modelled and observed temperatures are quite similar at low latitudes, starting to diverge at latitudes above 40 degrees. Inversely, at upper cloud and at the top of the clouds (60 to 70km altitude) the greatest difference in temperature takes place at low latitudes. Exceptionally, VCD temperatures get colder than VIRTIS's at 75km altitude, just above cloud top.

Vertical profiles on Fig. 10 top panels depict hemispheric night temperature averages and show consistency with previous conclusions: VCD temperatures are warmer as compared to VIRTIS up to ~72km altitude, where VCD turns colder than observations.

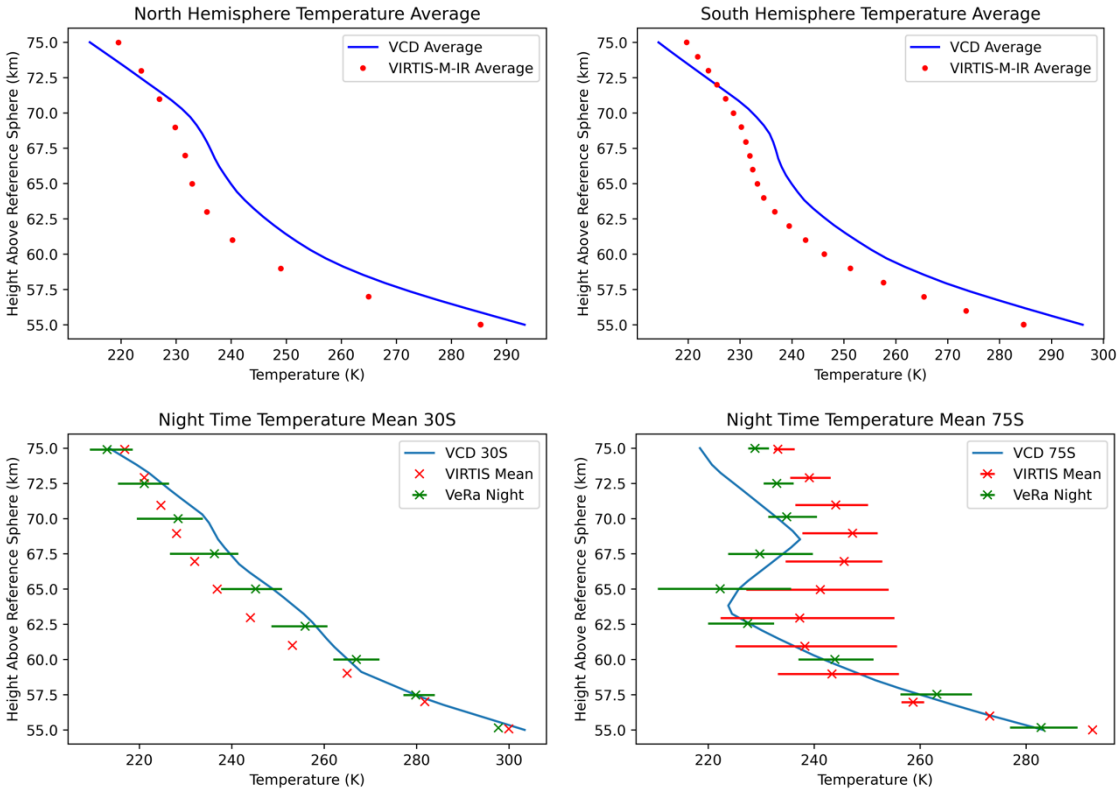

***Figure 10**: vertical temperature profiles in the night side (19:00LT - 05:00LT). Upper figures: red marks are for south (left) and north (right) hemisphere average temperatures measured by Haus et al., 2014, from VEx's VIRTIS-M-IR data. Blue lines are for south (left) and north (right) hemisphere average temperatures as given by VCD. Lower figures: red marks are the observations from VEx's VIRTIS-M-IR instrument by Haus et al., 2014 at 30 °S (left) and 75 °S latitude (right). According to authors, error at 30 °S is negligible. Green marks are VEx VeRa results from Limaye et al., 2017. Blue lines are VCD data output at those latitudes retrieved at each single hour between 19:00LT and 05:00LT and then mathematically averaged.*

These model and observational profiles follow a very similar temperature decreasing trend with altitude from 55km up to ~70km, the point at which VCD thermal vertical gradient changes more abruptly than observational data. This traduces on colder VCD temperatures at high altitudes as compared with observational temperature values. Interestingly, those ~70km altitude coincide with the top of the clouds. Hemispheric comparison can be analyzed on Appendix Fig. 23. Both hemispheres present almost identical values consistent with VIRTIS results, being the south hemisphere slightly warmer than the north one. Nevertheless, this VCD hemispheric temperature difference is too large between 55 and 60km (between middle and upper cloud) and too small above 60km (upper cloud) when compared with observational data.

The lower panels on Fig. 10 represent vertical temperature profiles at low and high latitudes. At latitude 30S, the profile is comparable to the total hemispheric average situation, whereas at 75S latitude a great temperature inversion is observed. This confirms the cold collar structure in both VCD and observational data. VeRa results are added to VIRTIS, reinforcing, and confirming the validation conclusions with a different observational instrument. VCD results are very consistent with VeRa ones too, even more than with VIRTIS, although both VeRa and VIRTIS temperature values coincide within their error range.

Fig. 10 lower panels show again that VCD results are a few Kelvins warmer than VIRTIS observational data at low latitude. Such is not so much the case at 75S latitude and above 62.5km altitude, where VCD is colder than VIRTIS (although mostly within VIRTIS measurement error) and the cold collar pattern appear a bit more acute in its shape. This could be linked and reaffirm the VCD vertical displacement of the cold collar structure when compared with VIRTIS.

At high latitude (65S), temperature local time dependance observations (first panel on Fig. 11) show that the cold collar is not very pronounced during the first half of the night and then it starts developing as the atmosphere keeps cooling down at after midnight and along late night. Nonetheless, the cold collar appears a bit weak on VCD as compared to VIRTIS. This may be associated with the VCD cold collar poleward shift.

Fig. 11 panels for latitude 75S rise the suspicion that VCD nighttime cooling may occur a bit deferred with the associated late intensification of the VCD cold collar. This conclusion can be confirmed and more intuitively reached if we refer to the bottom panels of Fig. 11, which represent VIRTIS and VCD local time dependance at ~65km altitude (corresponding with the observational core of the cold collar). It is observed that in VIRTIS observations the cold collar intensifies at midnight and reaches the coldest temperature at 03LT. In the VCD, however, the cold collar starts strengthening at around 02LT, reaching the coldest temperatures at 04-05LT, which means about 1-2 hours later. VCD's cold collar southerly shift can clearly be observed too on the bottom panels of Fig. 11. Appendix Fig. 26 depict the same VIRTIS-VCD comparison at 65km altitude, showing very similar results, with VIRTIS results by *Grassi et al., 2014*.

In relation with nightside temperatures local time dependance at low latitudes (see Appendix Fig. 24), below ~60km altitude there is no significant temperature variability either on VCD or VIRTIS results. Above that altitude up to the top of the clouds, observations show a slight temperature drop during nighttime, being this variability satisfactorily reproduced on the VCD.

After an exhaustive VCD nighttime temperature validation based on VEx's VIRTIS instrument, VCD dayside and terminators temperature validation is performed with VeRa and SOIR results (see Fig. 12). Due to the similarity of the temperature profiles, several have been supressed from the main text. The complete validation is shown in Appendix Figs. 28, 29 and 30.

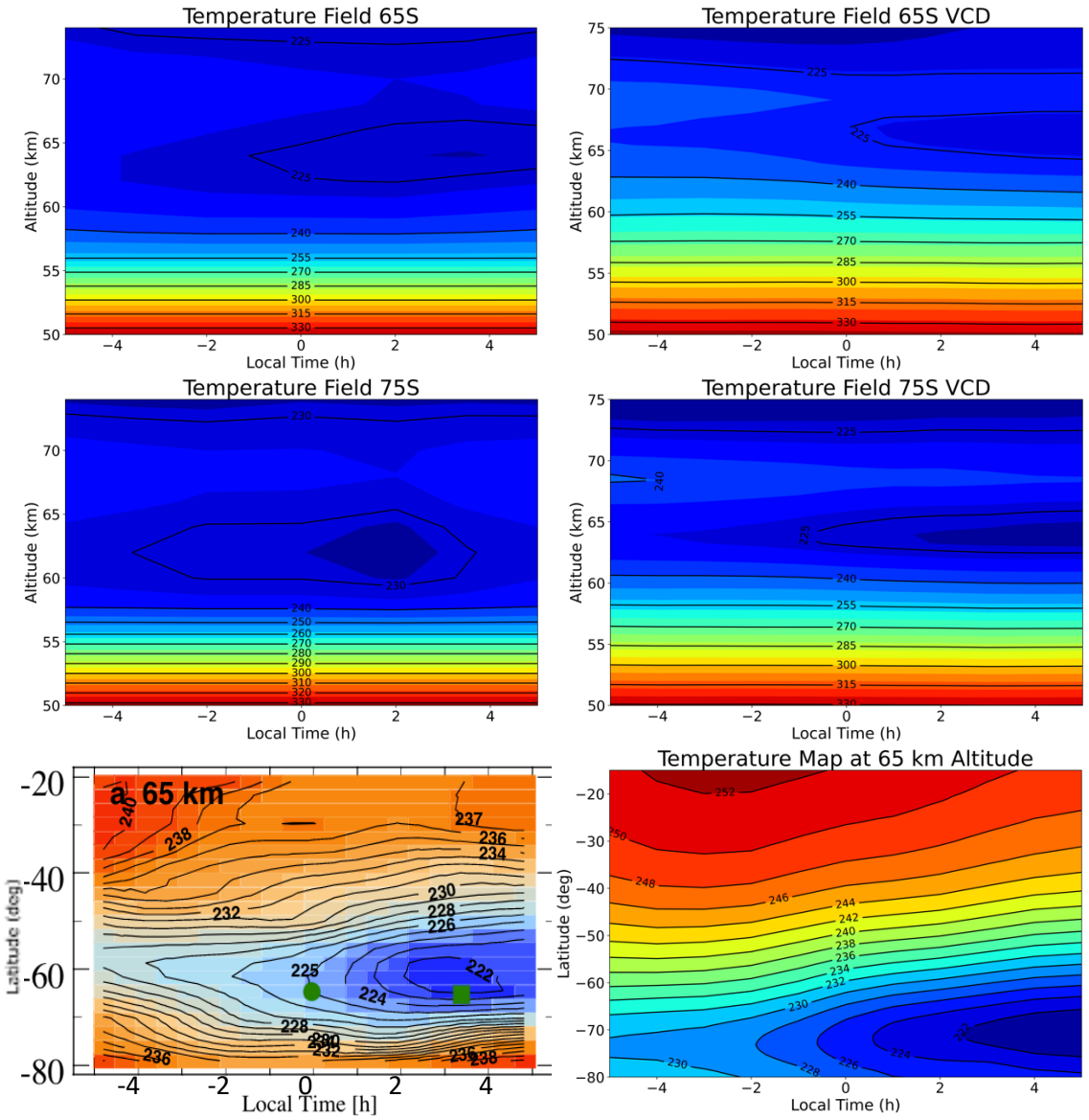

***Figure 11**: mean temperature fields (units: Kelvin) as function of local time (-05:00LT - 05:00LT). Upper two rows: on the left, self-crafted contour maps at latitudes 65° S and 75° S from VIRTIS-M-IR data at the Appendix of Haus et al., 2014. On the right, contour maps from VCD data. Lower row: on the left, contour map from Haus et al., 2014 measured by VEx's VIRTIS-M-IR at 65km altitude. On the right, VCD output at 65km. All VCD altitudes are above a reference sphere of radius 6052km.*

The temperature validation conclusions that can be obtained from Fig. 12 are consistent with previous VIRTIS nightside ones: firstly, VCD temperatures are slightly warmer than observational results (especially from mid to high latitudes). Additionally, Venus's cold collar manifestation is evident at 50-70° latitude according to VeRa and SOIR observations, while at this latitude band it is just slightly incipient in VCD results. It is not until 75° latitude that there is an evident cold collar temperature pattern on VCD output, due to the VCD poleward shift of the cold collar. Secondly, VCD cold collar again appears vaguely displaced to higher altitudes (by 2 to 3km) when compared with VeRa and SOIR; in good agreement with the value obtained when compared to VIRTIS. There is a small local VCD temperature anomaly, patent at latitude 65N (see Fig. 12). Further VCD analysis has shown that this manifests just in the north hemisphere and between latitudes 62-70°N, in which the VCD cold collar's morphology appears a bit wavy and more vertically extended. This irregularity has no diurnal dependence, appearing at any local times.

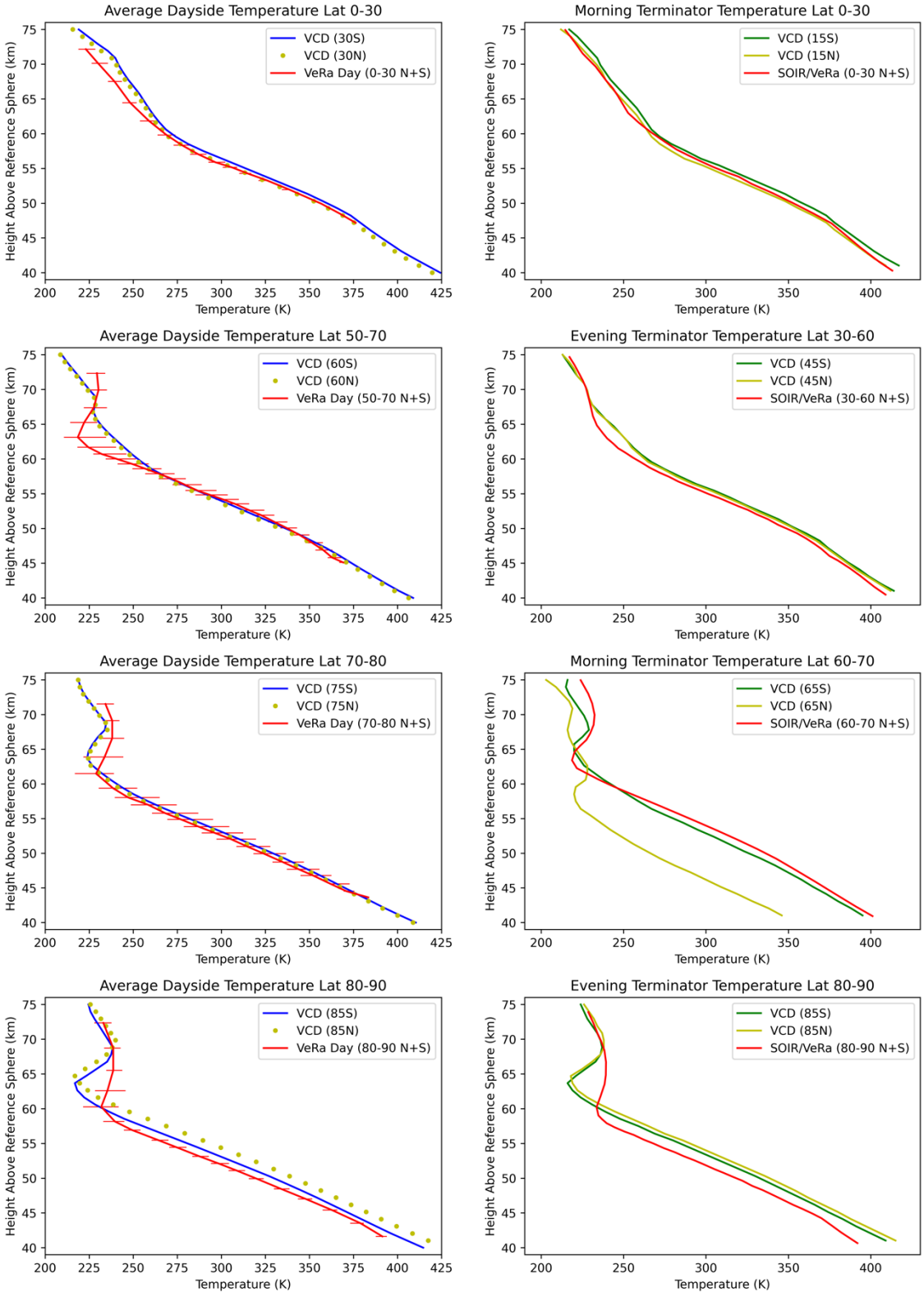

***Figure 12**: vertical profiles of dayside and terminator temperatures at different latitudes. Red lines represent VEx's VeRa dayside mean temperatures between 07:00LT and 17:00LT (left) and VEx's SOIR/VeRa terminator (05:00-07:00LT or 17:00-19:00LT) mean temperatures (right) as presented on Limaye et al., 2017 for the different latitude bands. Left: blue lines (for south hemisphere) and yellow marks (for north hemisphere) represent VCD dayside temperature at 12:00LT at latitudes 15°, 60°, 75°, 85° N and S. Right: green lines (for south hemisphere) and light green lights (for north hemisphere) represent VCD morning/evening terminator temperatures at 06:00LT/18:00LT at latitudes 15°, 45°, 75°, 85° N or S.*

3.2 WINDS

Zonal and meridional wind validation will be accomplished on upper, middle, and lower cloud. Observational instruments for the uppermost part of the clouds are VEx's VIRTIS in three different wavelengths (UV, VIS and NIR), and Akatsuki UVI instrument in UV wavelengths. These measurements are made during daytime because of the nature of the observations. For deep cloud analysis, Akatsuki IR2 instrument is used during nighttime. As on the temperature section, whenever VIRTIS is used for the validation, the study extensively focuses on the southern hemisphere. In the case of Akatsuki, as it has an equatorial orbit, the datasets of low to mid latitudes are more abundant and reliable. These two spacecraft observations therefore complement each other.

Fig. 13 constitutes a very complete representation, allowing a straightforward validation of mean zonal winds at different cloud regions. VCD zonal wind intensity at the top of the clouds (67-75km altitude) is in good accordance with VIRTIS and Akatsuki results (see top-left panel on Fig. 13), showing that the retrograde super-rotation is patent within the simulations. In addition, VCD zonal wind latitudinal distribution at cloud top is consistent with observations at low to mid latitudes (below ∼45° latitude). Nonetheless, VCD zonal wind jet is shifted 10-20° to higher latitudes than observed by Venus Express and Akatsuki, what supposes an important bias for the modelled atmospheric dynamics. This is probably related with the temperature issues previously seen, being the cold collar closer to the pole than observed.

The same happens at the base of the upper cloud (57-63km altitude, top-right panel), with strong zonal winds reaching very high latitudes. In addition to this south drift of the wind distribution, at this cloud layer the VCD jet stream is much more pronounced that it should be according to observations, with a marked mean zonal wind peak well above VIRTIS measurements (10-20m/s).

At the lower clouds (50-53km, bottom panels), during nighttime, VCD mid latitude jet stream only diverges by 5° latitude and it seems slightly weaker than observations (although it is mostly within the measurement error). Nonetheless, in this cloud layer we can find the greatest discrepancy between model and observational zonal winds at low latitudes, where Akatsuki measurements are more reliable. VCD zonal wind is considerably weaker (by 20-25m/s), barely reaching 50m/s at 50-53km altitude, while observations show winds up to 70m/s. This again traduces on excessively marked jet streams on VCD model, this time at deep cloud.

VCD dayside zonal winds local time dependance at cloud top as studied in upper Fig. 14 suits correctly with observational results. Observations present a progressive decay of zonal winds in the morning and a subsequent increase between noon and 14-16LT, perhaps a little more violently than in the model. Same behavior takes place on VCD, thus showing a good local time variability. However, this wind variability takes place a bit in advance (1-3h), being the VCD wind valley at ∼10LT as compared to the Akatsuki measurements at ∼12LT. Just remember that this 1 to 3 hour offset was also present in the temperature local time dependance validation.

This VCD untimed zonal wind temporal variation is also present at 75km altitude (see lower-left panel of Fig. 14) as VCD zonal winds are slightly stronger at 12LT than at 09LT in disagreement with Akatsuki results. The VCD trend is more consistent at 70km as observable in the lower right panel of the same figure. At the same time, lower Fig. 14 clearly shows VCD zonal jets drifting to higher latitudes with local time and their increasingly marked shape as compared with Akatsuki: VCD-Akatsuki wind peak difference is stronger at afternoon hours, reaching an almost 20m/s greater intensity at 15LT for VCD.

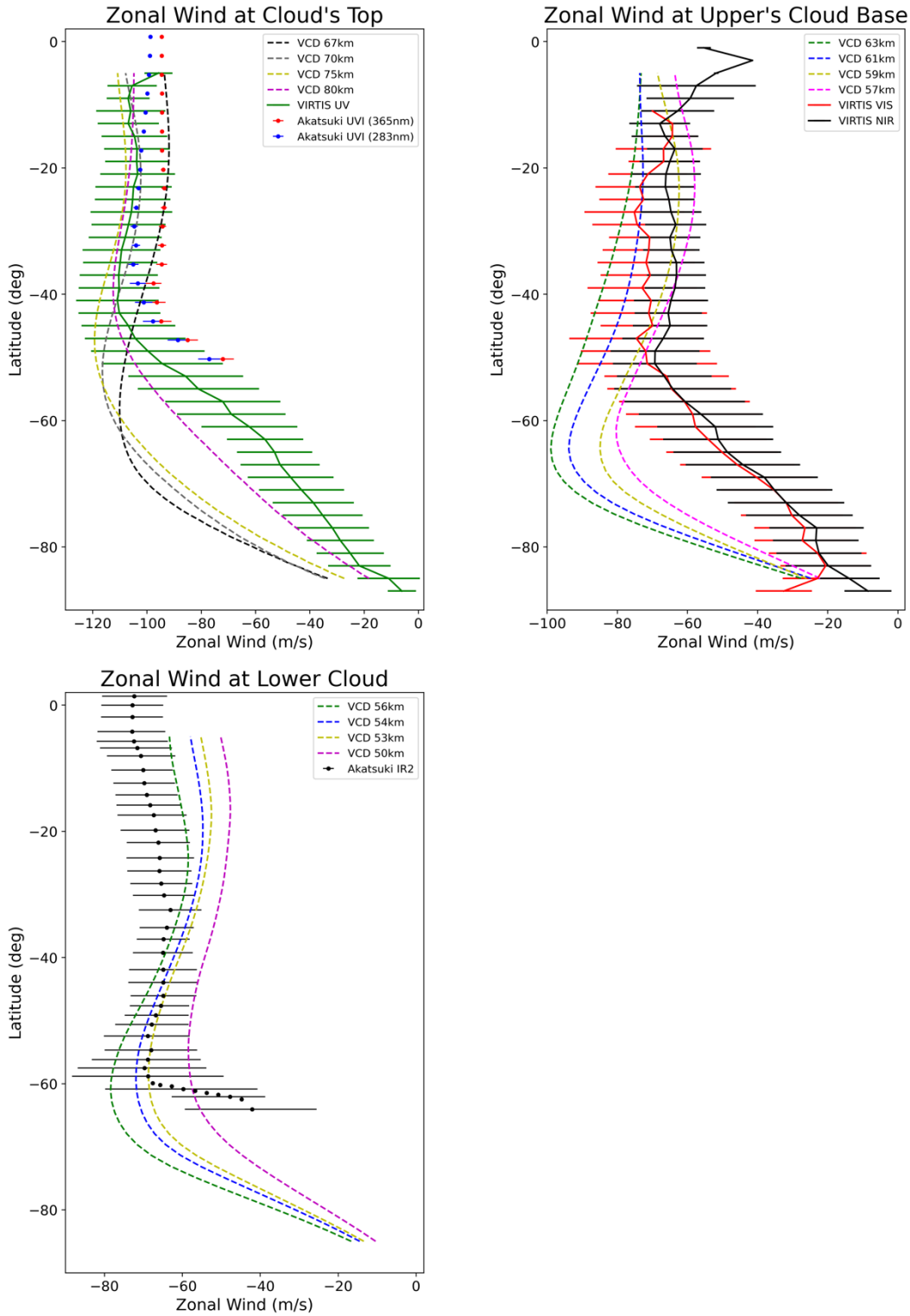

***Figure 13**: zonal wind profiles at different cloud regions as a function of latitude. Several VCD altitudes have been considered in order to find the best fit. Values are taken above Venus's reference sphere of radius 6052km. Upper left: VEx's VIRTIS UV at 360-400 nm dayside mean zonal winds from Hueso et al., 2014 corresponding to 67-70km altitude (green), and Akatsuki UVI at 365 nm (70km) (dotted red) and 283nm (75km) (dotted blue) zonal winds at noon (12LT) from Horinouchi et al., 2018. VCD zonal winds are dayside mean values between 07LT and 17LT (dashed). Upper right: VEx VIRTIS VIS (red) at 570-680 nm and NIR (black) at 900-955 nm from Hueso et al., 2014 corresponding to ~62km and ~58km altitude, respectively, are shown. VCD data is the dayside mean values between 07LT and 17LT (dashed). Lower left: Akatsuki IR2 at 2.26 μm (50km) (dotted black) from Peralta et al., 2018. VCD data is retrieved at 00LT.*

In contrast to Fig. 13, Fig. 14 shows the zonal wind behavior in both hemispheres, revealing the same jet stream poleward drift bias on both north and south latitudes. This zonal wind hemispheric symmetry is consistent with the discussed thermal one.

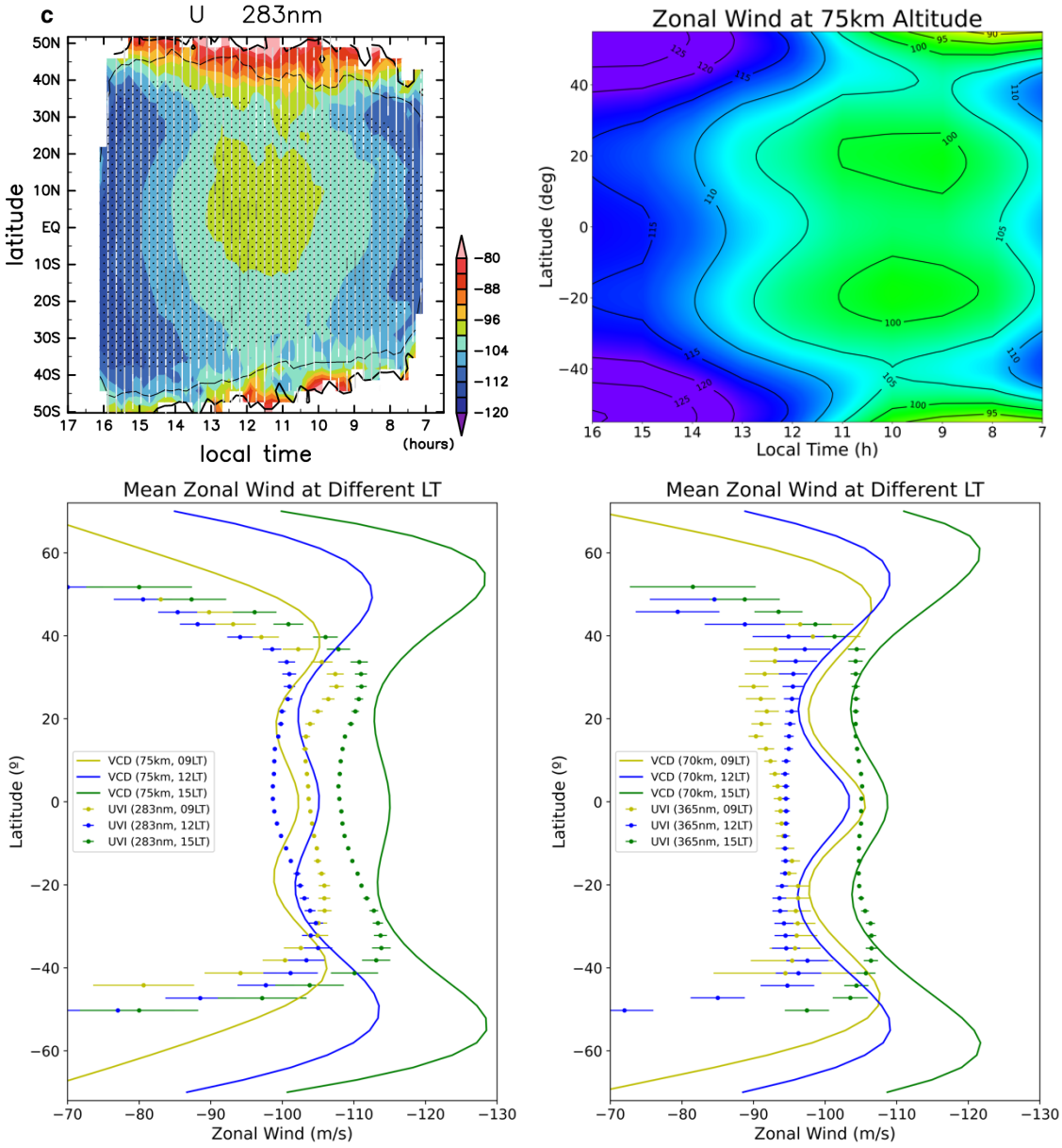

***Figure 14**: mean zonal wind fields and profiles at cloud's top as a function of latitude and local time. Upper row: mean zonal wind fields (units: m/s) measured by Akatsuki UVI at 283 nm (~75km) (left) and VCD zonal winds (units: m/s) at 75km altitude (right). Lower row: Akatsuki UVI at 283 nm (~75km) and VCD data at 75km altitude (left) and Akatsuki UVI at 365 nm (~70km) and VCD data at 70km altitude (right) at 09LT (light green), 12LT (blue), and 15LT (green). All Akatsuki UVI data is from Horinouchi et al., 2018. All VCD altitudes are above Venus's reference sphere of radius 6052km.*

For VCD-Akatsuki comparison of local time dependent zonal wind maps at 70km altitude, the reader is referred to Appendix Fig. 40. In Appendix Figs. 31, 32, and 33 VIRTIS-VCD local time dependance comparison for south hemisphere at the top of the clouds (67-70km altitude) and just below the top of the clouds (57-63km altitude) can be seen. Appendix Fig. 34 shows Akatsuki-VCD local time dependance comparison for nighttime at deep cloud (53-50km).

Regarding dayside meridional winds at the uppermost part of the cloud (see left panel on Fig. 15), VCD poleward tendency matches VIRTIS and Akatsuki observations. However, there are some issues regarding meridional wind speeds at the top of the clouds (67-75km). At latitudes higher than 40°, VCD winds accelerate violently presenting up to 20-22m/s dayside averaged southerly winds as compared to 5-10m/s averaged observational values. These doubled/tripled meridional wind intensities rectify at upper cloud's base (57-63km), showing a good correspondence between VIRTIS and VCD with southward values between 0-5m/s.

VCD dayside poleward meridional wind tendency at the top of the clouds is clearly depicted on Fig. 16. As it was the case with the zonal winds, VCD local time dependance pattern is in good agreement when compared with Akatsuki but, once again, there is a time deviation. Observations show roughly calm meridional winds early in the morning (08-10LT) while VCD winds at 09 LT are already marked and with an evident poleward tendency (especially for 75km altitude). Therefore, meridional winds local time dependance is not completely accurate on VCD as they commence 2-3h in advance (same situation as with zonal winds). This VCD local time mismatch persists along the day with VCD meridional winds reaching its maximum at noon versus the Akatsuki peak at 14LT (see upper panels on Fig. 16).

The reversal of meridional wind direction during the night, as observed in Venus, is properly modelled in the VCD, being very consistent with Akatsuki observational results at deep cloud (see Appendix Figs. 35 and 39).

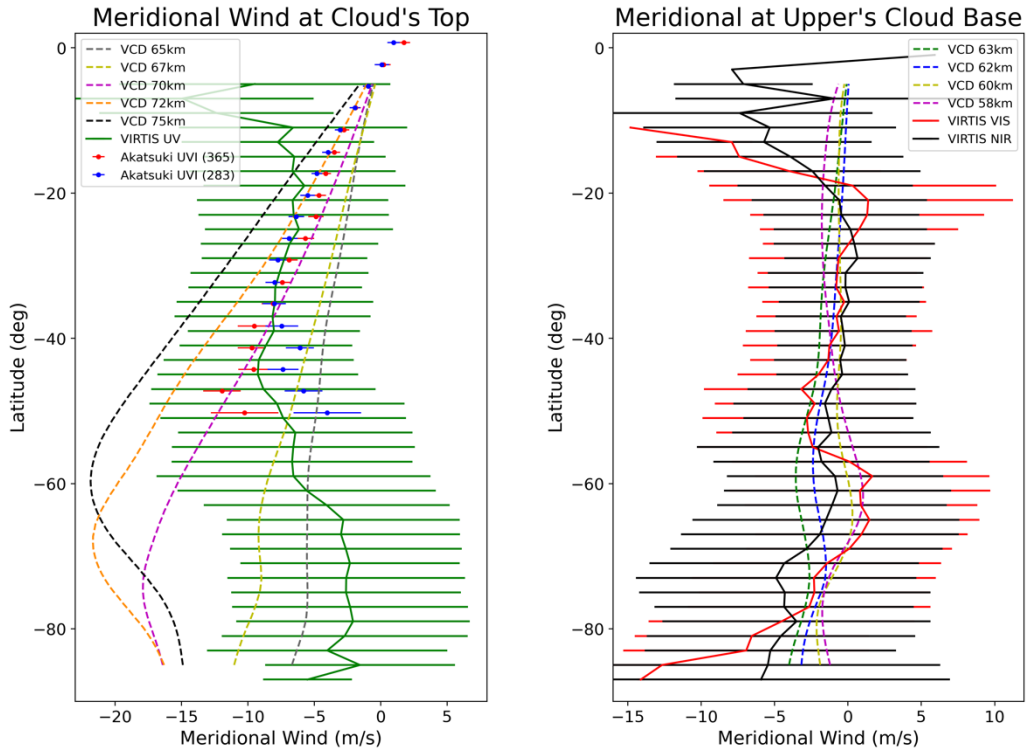

***Figure 15**: meridional wind profiles at different cloud regions as a function of latitude. Several VCD altitudes have been considered in order to find the best fit. Values are taken above Venus's reference sphere of radius 6052km. Left: VEx's VIRTIS UV at 360-400 nm dayside mean meridional winds from Hueso et al., 2014 corresponding to 67-70km altitude (green), and Akatsuki UVI at 365 nm (70km) (dotted red) and 283nm (75km) (dotted blue) meridional winds at noon (12LT) from Horinouchi et al., 2018. VCD meridional winds are dayside mean values between 07LT and 17LT (dashed). Right: VEx's VIRTIS VIS (red) at 570-680 nm and NIR (black) at 900-955 nm from Hueso et al., 2014 corresponding to ~62km and ~58km altitude, respectively, are shown. VCD data is the dayside mean values between 07LT and 17LT (dashed).*

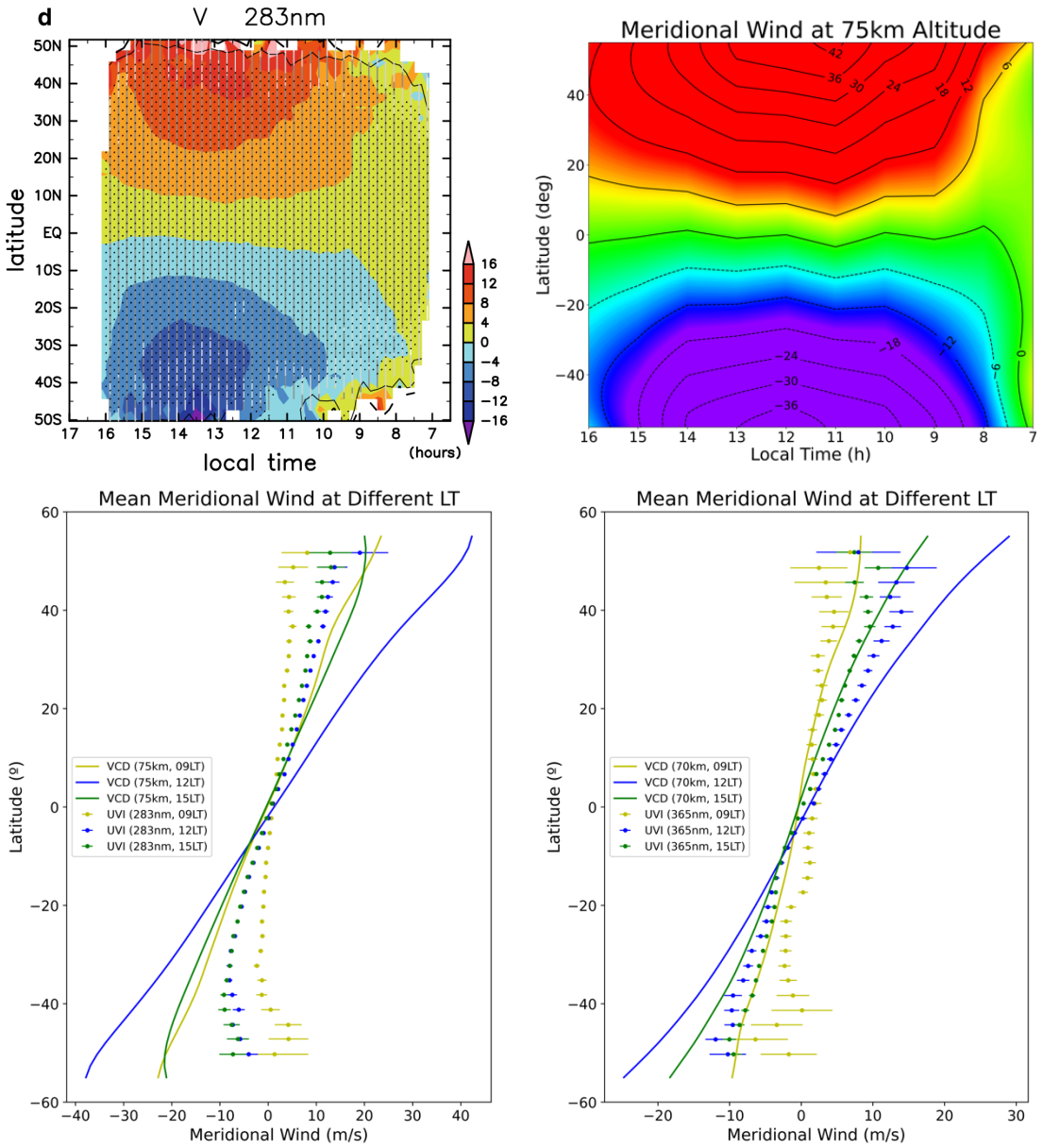

***Figure 16**: mean meridional wind fields and profiles at cloud's top as a function of latitude and local time. Upper row: mean meridional wind fields (units: m/s) measured by Akatsuki UVI at 283 nm (~75km) (left) and VCD meridional winds (units: m/s) at 75km altitude (right). Lower row: Akatsuki UVI at 283 nm (~75km) and VCD data at 75km altitude (left) and Akatsuki UVI at 365 nm (~70km) and VCD data at 70km altitude (right) at 09LT (light green), 12LT (blue), and 15LT (green). All Akatsuki UVI data is from Horinouchi et al., 2018. All VCD altitudes are above Venus's reference sphere of radius 6052km.*

According to Fig. 16 dayside meridional wind intensities are again (as in Fig. 15) too strong, with a noon wind peaking speeds up to 36-40m/s (in comparison to 12-16m/s winds for Akatsuki observations). Repeatedly, as it was the case with zonal winds, the wind strength difference between observations and VCD is more acute locally than when comparing averaged meridional winds. Both upper and lower panels on Fig. 16 show the meridional wind decline in the mid-afternoon (14-16h), somewhat anticipating the later meridional wind direction reversal during nighttime. Appendix Fig. 36, 37 and 38 complement the VCD meridional wind local time dependance validation at different cloud altitudes at dayside as compared with VIRTIS.

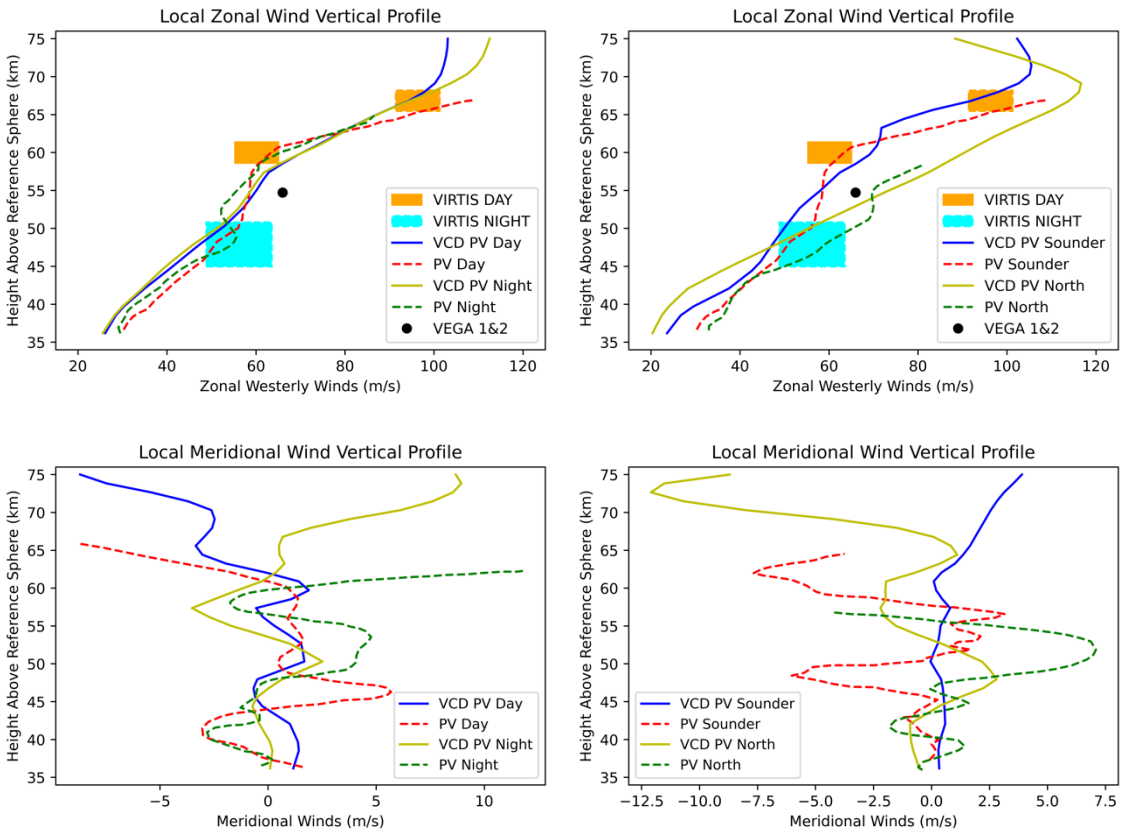

***Figure 17**: vertical profiles of zonal (upper row) and meridional (lower row) winds. Pioneer-Venus Day, Night, North and Sounder measurements (dashed lines) (Colin et al., 1983) compared to VCD Pioneer Venus quick pre-set wind results (solid lines) are shown. Zonal wind results are also compared with mean values from long-term measurements by VEx VIRTIS at daytime (orange rectangle) and nighttime (cyan rectangle) (Sánchez-Lavega et al., 2008; Hueso et al., 2015) and Vega Balloons measurements (Sagdeev et al., 1986). All four panels are an adaptation of figures from Sánchez-Lavega et al., 2017.*

Fig. 17 supposes a good final review of zonal and meridional winds all along the cloud region. The main comparison is made between VCD output and Pioneer Venus (PV) results, being these the only in-situ results included in the validation, so far. Though from a local perspective, this analysis includes the study of north and south hemispheres (at spread out latitudes) and day and night periods, giving the validation a complete and global approach.

Local measurements of zonal winds by PV are combined with long-termed VIRTIS results and clearly show one of the main properties of Venus's atmosphere: its super-rotation at the cloud top, where zonal winds reach values of 100-120 m/s. VCD presents the same trend as Pioneer Venus, with intensifying zonal winds with altitude, with even very similar altitude-related variations. Moreover, VCD zonal wind values are in good agreement with PV and VIRTIS long term measurements, confirming the model super-rotation. Night and Day probes confirm the little zonal wind variation between day and night periods for both PV and VCD.

Meridional wind vertical profiles depict the light and erratic meridional winds observed in both VCD an PV below ~55-60km. VCD and PV Day results clearly confirm the poleward wind tendency at the top of the clouds while VCD and PV Night results show the opposite equatorward one. Nevertheless, VCD meridional winds seem to intensify a bit higher than PV ones. North and Sounder PV results describe some meridional wind peaks not so properly replicated by VCD (especially in the case of VCD Sounder).

3.3 NUMBER DENSITY

Number density is the absolute number of particles within a certain volume. Number density will be validated separately for dayside, nightside and terminators. Al VCD comparison will be made with VeRa instrument, able of acquiring number density data at the cloud region altitudes (40 to 75km) at all local times. VeRa morning (06LT) and evening (18LT) terminators results are extremely similar, both resulting in the same curve in the plots. VCD number density results are obtained by separately retrieving temperature and pressure data from the VCD, for the desired latitude and local time, and then mathematically calculating the values for number density according to the Ideal Gas Law.

Due to the similarity of the number density profiles at nighttime and terminators for a certain latitude band, either the nightside or terminator profile is shown in the main text. Dayside temperature validation at 30-50° latitude band has been also supressed because of its similarity with the 30-50° latitude band. The complete validation is shown in Appendix Figs. 41, 42 and 43.

Fig. 18 shows great consistency between VCD and VeRa for the dayside number density, particularly at low latitudes. With increasing latitude, values are not perfectly coincident, especially for north hemisphere results, but they are reasonably close. Fig. 19 presents very good VCD and VeRa results correlation for both night and terminators.

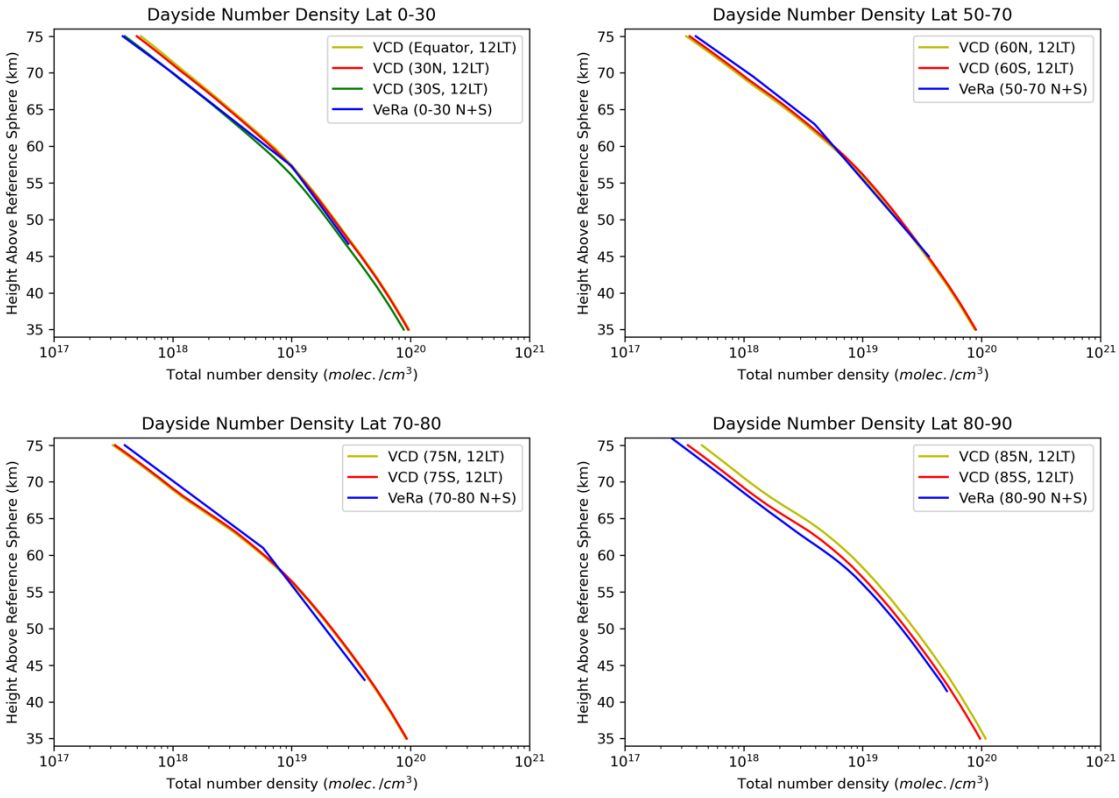

***Figure 18**: vertical profiles of zonally averaged dayside total number density at different latitudes. Blue lines represent VEx's VeRa dayside mean number density between 07:00LT and 17:00LT as presented on Limaye et al., 2017 for the different latitude bands. Red lines (for south hemisphere) and yellow lines (for north hemisphere) represent VCD dayside number density at 12:00LT at latitudes 15°, 60°, 75°, 85° N/S.*

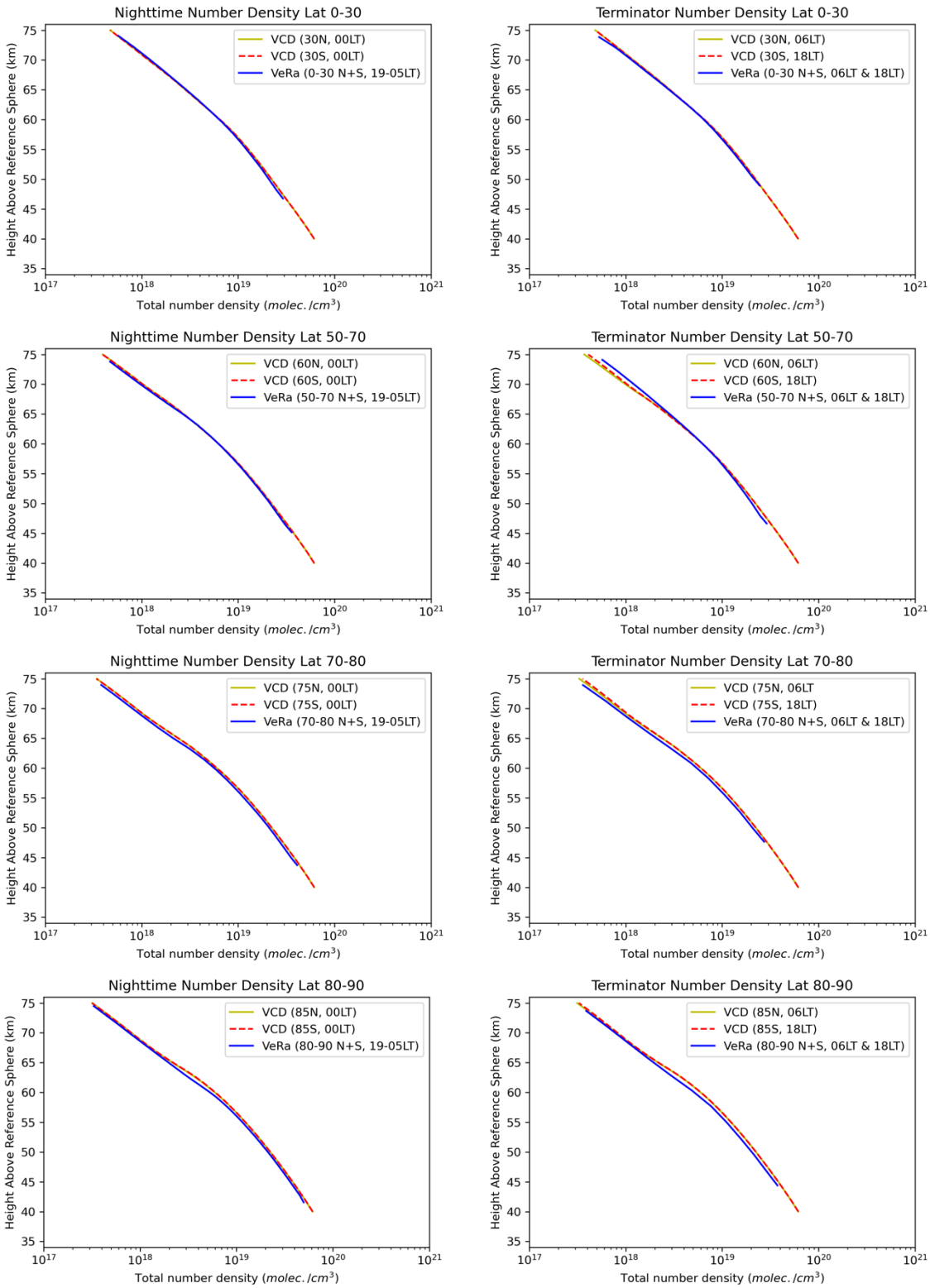

***Figure 19**: vertical profiles of zonally averaged nightside and terminators total number density at different latitudes. Blue lines represent VEx's VeRa nightside mean number density between 19:00LT and 05:00LT (left) and VEx's VeRa number density at both morning (05:00LT – 07:00LT) and evening (17:00LT – 19:00LT) terminators (right) as presented on Limaye et al., 2017 for the different latitude bands. Red dashed lines (for south hemisphere) and yellow lines (for north hemisphere) represent VCD nightside number density at 00:00LT at latitudes 15°, 60°, 75°, 85° N/ S (left) and morning/evening terminator number density at 06:00LT for latitudes 15°, 60°, 75°, 85° N and 18:00LT for latitudes 15°, 45°, 60°, 75°, 85° S (right).*

3.4 COMPOSITION

Composition will be studied according to the five principal minor atmospheric constituents that can be obtained from VCD Web Interface database: oxygen, water vapour, sulphur dioxide, hydrochloric acid, and carbon monoxide. The source of the observational data is very ample and diverse, varying from in-situ measurements, in-orbit remote sensing and ground-based telescopic observations.

Each compound will be studied at four different latitudes (0°, 45°, 60°, 75°) so that VCD latitudinal variation can be analysed. Unfortunately, most of the literature do not detail the latitude value of the observation (very few times slightly different values are given for low-to-mid or high latitudes although that has not been the case for the data used in this validation). For that reason, same observational data will be presented at all four latitudes, omitting any possible latitudinal variation. In addition, great measuring errors are given in altitude and mixing ratio and in some cases the values given by one source differs from others. All these implies that observational data must be very carefully selected, so that validation is reliable.

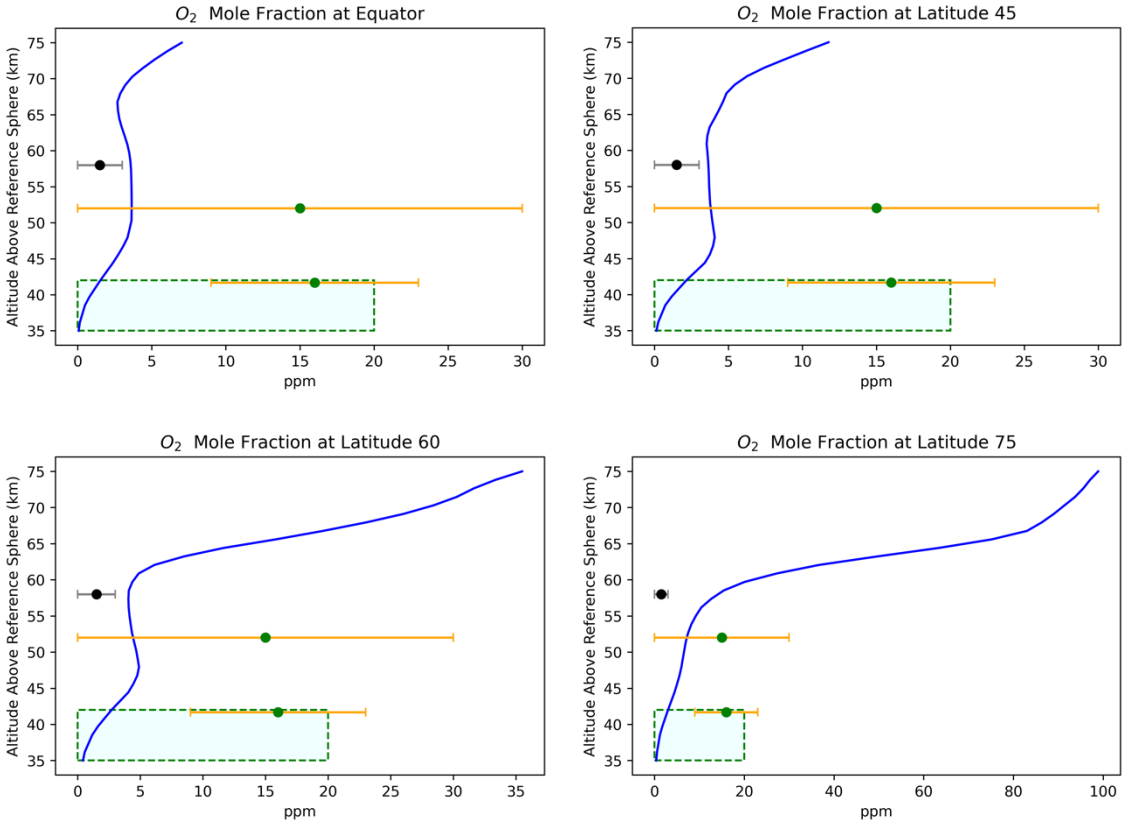

***Figure 20**: oxygen mixing ratio vertical profile in parts per million at different latitudes. Blue lines represent VCD results at each latitude at 00:00LT. Observational data have the same values for all four panels as there is no cited latitudinal dependence/variation in the chosen literature. Green rectangle shows Venera 12 in situ measurements by gas chromatography (Gel'man et al., 1979), black dot represents values measured by Earth Based Telescope Spectrometer (Mills et al., 1999), green dots are results from Pioneer Venus in situ measurements by LGC instrument (Oyama et al., 1980). Rectangles and errorbars show altitude and mixing ratio ranges given by the authors.*

Fig. 20 shows oxygen mixing ratio. Between 35km and 60km altitude VCD values present fairly good results, considering the uncertainties of the different observations. Nonetheless, VCD oxygen mixing ratio presents a significant latitudinal dependence, largely increasing at high latitudes above 60km altitude. Fig. 20 is interesting because no oxygen is initialised on the simulations on which VCD is based, but it seems to be filling the deep atmosphere. In other words, it seems that the model is able to produce oxygen without having to give it a non-zero initial value. This should be further studied so that the VCD simulations can be improved as there is a possibility that oxygen could not be in equilibrium.

Water vapour mixing ratio is depicted on Fig. 21. This is the VCD atmospheric compound that best matches with observational data in this validation and at the same time it is compared with the greatest number of observations. VCD values are quite accurate, even showing an evident drop between 60km and 65km (close to cloud top) also manifest in observations. VCD results do not present appreciable latitudinal dependence for H_2O mixing ratio.

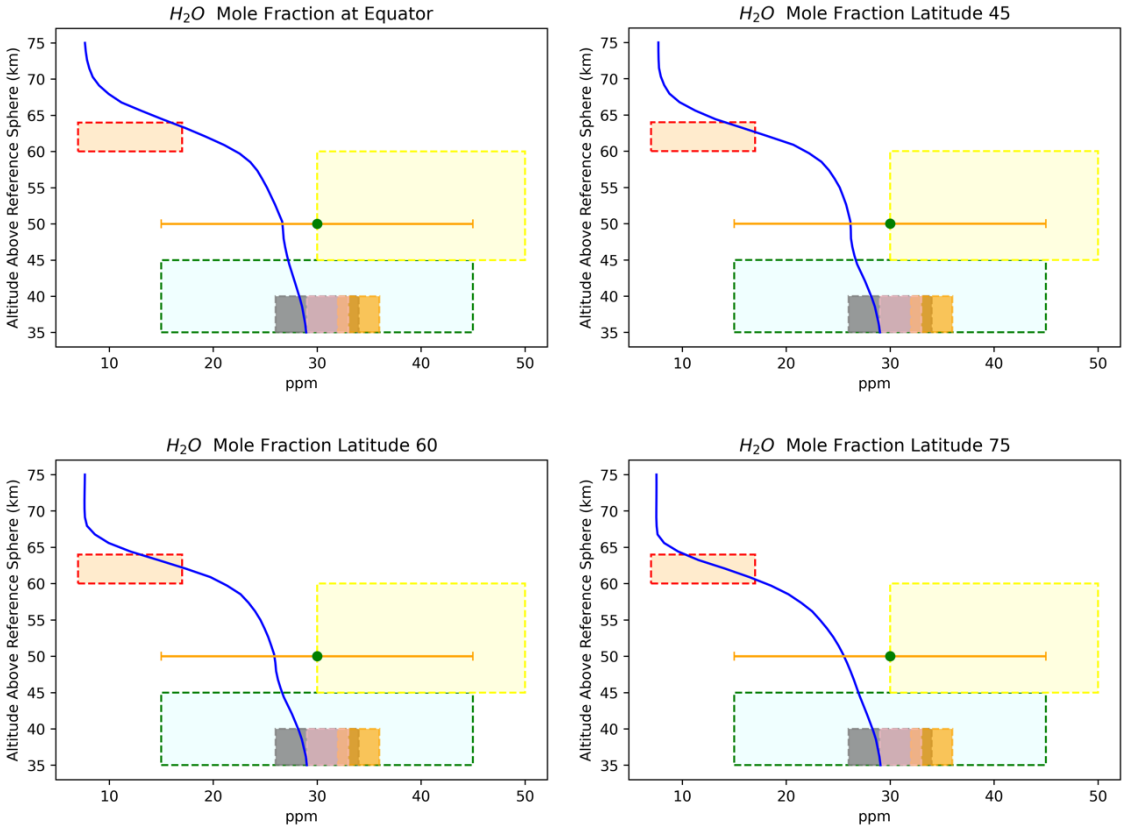

***Figure 21**: water vapour mixing ratio vertical profile in parts per million at different latitudes. Blue lines represent VCD results at each latitude at 00:00LT. Observational data have the same values for all four panels as there is no cited latitudinal dependence/variation in the chosen literature. Red rectangle shows Venera 15 and Pioneer Venus in situ measurements (Kokouli et al., 2005), yellow rectangle shows Venera 11 in situ measurements by gas chromatography (Ignatiev et al., 1997), green rectangle represents values measured by Earth Based Telescope near IR sounding (Taylor et al., 1997), grey rectangle data from VEx/VIRTIS-M (Tsang et al., 2008), pink rectangle data from VEx/VIRTIS-H (Marcq et al., 2008), orange rectangle shows Earth Based Telescope spectrograph results (Arney et al., 2014), green dot results from VEx/VIRTIS (Barstow et al., 2012). Rectangles and errorbars show altitude and mixing ratio ranges given by the authors.*

Sulphur dioxide mixing ratio is presented on Figure 22, being undoubtedly the less consistent VCD result, with a mixing ratio below 10 ppm for the whole altitude range analysed, whereas observations suggest a SO_2 mixing ratio within the cloud region varying between 50-200 ppm. It is well known to VCD developers that SO_2 is problematic to adjust, because it is extremely difficult to stabilize it at the observed levels. If the observed amount is put in the deep atmosphere, it exceeds the observed values above the clouds; and vice versa. No significant latitudinal variation is appreciable in Fig. 22.

Finally, VCD carbon monoxide and hydrochloric acid mixing ratios present a good behaviour when compared with observational results within the studied cloud region (see Appendix Figs. 44 and 45).

The last thing to remark regarding the composition validation is the unavailability of H_2SO_4 mixing ratio in the VCD database, as this is one major characteristic of the Venusian clouds.

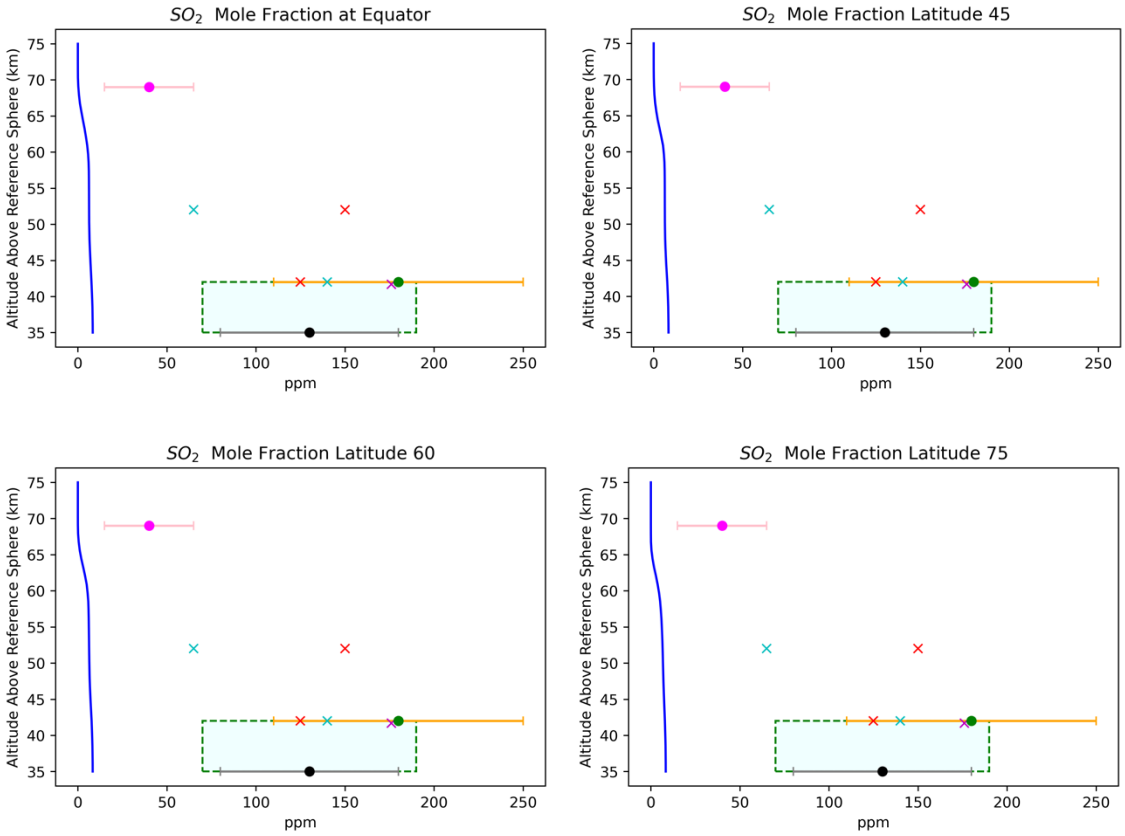

***Figure 22**: sulphur dioxide mixing ratio vertical profile in parts per million at different latitudes. Blue lines represent VCD results at each latitude at 00:00LT. Observational data have the same values for all four panels as there is no cited latitudinal dependence/variation in the chosen literature. Green rectangle shows Venera 12 in situ measurements by gas chromatography (Gel'man et al., 1979), pink dot represents Venera 15 in situ IR measurements (Zasova et al., 1993), green dot is the value measured by Earth Based Telescope Fourier Transform Spectrometer (Pollack et al., 1993), purple cross results from Pioneer Venus in situ measurements by LGC instrument (Oyama et al., 1980), black dot data from VEx/VIRTIS-H (Marcq et al., 2008), red crosses results from VEGA 1 UV Spectrometer and cyan crosses from VEGA 2 UV Spectrometer (Bertaux et al., 1996). Rectangles and errorbars show altitude and mixing ratio ranges given by the authors.*

4. CONCLUSIONS

Venus present unique characteristics among the planets on the Solar System, hiding numerous evolutional and behavioural mysteries. Many of these reside on its very singular atmospheric features and characteristics, representing one main target for scientific research.

The use of *General Circulation Models (GCMs)* is tremendously useful to understand planetary atmospheric general circulation, dynamics, and climate. In the case of Venus, models are also a powerful mean of exploring and understanding the unanswered questions to the most complex puzzles such as Venus's super-rotation or polar vortex dynamics. Moreover, these models have also a direct application when referring to future mission proposals and concepts, allowing for optimised longer-living cost-adjusted spacecraft and instruments designs.

Nonetheless, Venus's very dense and opaque atmosphere, the slow rotation of the planet, and the retrograde super rotation result in modelling challenges to be overcame, mostly related with radiative transfer calculations, albedo, and angular momentum budget. It is therefore essential to assess if the output of a model is satisfactorily representing the long-term system behaviour and characteristics, so that it is possible to benefit from such a powerful tool. This is accomplished by model validation, which mainly consists of directly or indirectly comparing the output of a simulation with measurements acquired from the observations of the various studies that have analysed the involved atmosphere.

In this work, the *Laboratoire de Météorologie Dynamique (LMD)* model in which the Venus Climate Database (VCD) is based has been validated within the Venus's cloud region (~40-75km). The main four variables studied are temperature, winds, number density and composition. Some of the main VCD validation conclusions of this thesis within the cloud region will be presented now. In general terms, both observational and modelled data correlate reasonably good within the cloud region (especially at latitudes below ~45°). The high temperatures and the strong zonal winds (retrograde super-rotation), which are the main dynamical and atmospheric features are correctly replicated. However, some important biases have been also detected, showing room for improvement, and suggesting the need for some corrective actions.

Considering the temperature results, the main principal VCD bias is the latitudinal shift of the cold collar to higher latitudes by 10 to 20 degrees (*see Figs. 8 and 9*). Additionally, this cold collar is slightly displaced to higher altitudes in the VCD as compared with observational data (2 to 4 kilometres). According to *Garate-Lopez and Lebonnois, 2018*, the cold collar appeared for the first time in the model when the decrease of the cloud top altitude from equator to pole and the latitudinal variation of the particles modes were taken into account. Maybe the latitudinal variations considered by the authors were not the most realistic and parameters such as particles' sizes and radiative properties or cloud's height still need to be adjusted in order to reproduce the cold collar perfectly.

Despite those cold collar position deviations, VCD night temperature fields and VCD night cold collar temperature fields are quite consistent with Venus Express observations. VCD temperature values are just slightly warmer than VIRTIS datasets, but at all times this temperature difference is maintained below 10 Kelvin what can be considered as a tolerable model deviation (3-5%). Terminator and dayside temperatures conclusion are the same as for nighttime results.

VCD temperature hemispheric symmetry is also very consistent with observations, being the south hemisphere scarcely warmer than the north hemisphere. According to nighttime temperature fields local time dependence, VCD follows very similar cooling trends than observations. Nevertheless, the VCD night temperature variation pattern is a bit offset as compared to the observed behaviour, with the atmospheric cooling and the cold collar's core prominence occurring with 1 to 2 hours lag (*see Fig. 11*).

In relation with VCD winds output, VCD zonal wind values at cloud's top are very consistent with the observational datasets meaning that the main Venus's atmospheric feature, the retrograde super-rotation, is well simulated. However, the observed strong mid-latitude zonal jet streams are drifted 10 to 20 degrees to higher latitudes in the VCD (*see Figs. 13 and 14*). This is closely related with the cold collar poleward shift. This problem is also present in the VCD base of the upper cloud and in the low to middle cloud where the jet stream appears to be even more pronounced.

Regarding VCD meridional winds, they stick to the observational pattern, describing a clear poleward direction in the dayside and opposite equatorward direction during nighttime. However, VCD meridional dayside winds above mid-latitudes at the top of the clouds are significantly stronger when compared to observations (*see Figs. 15 and 16*). These VCD meridional wind speeds double and even triple Akatsuki's and VIRTIS's results, giving some room for model improvement. At lower altitudes, within the upper cloud's top and the low to middle cloud, VCD meridional wind intensities are more consistent with observations.

Zonal and meridional VCD wind time dependence results adhere correctly to the observed daytime trend: diminishing zonal winds in the morning, to afterwards increase again; and peaking meridional winds during the afternoon, to then decay again in the late evening. Nonetheless, there is a time offset (as it was the case with the temperature variation with local time) as these VCD wind variations occur 1 to 3 hours in advance as compared to observational results (*see Figs. 14 and 16*).

When comparing VCD and Venus Express number density results on the dayside, nighttime and terminators they show great consistency (*Figs. 18 and 19*). This means that the model satisfactorily reproduces the order of magnitude of the number of particles present in the cloud region, at least in general terms, what implies a correct relationship between the modelled mean temperature and pressure.

Finally, the validation of the atmospheric composition has been carried out. It could be concluded that observational results might not be as robust as one would like them to be, because of the large observational uncertainties associated with the measuring methods. For that reason, this part of the validation could be the more open to debate and interpretation, although some clear conclusions can be obtained.

One of these conclusions is that composition validation shows some evident disagreements between the simulations and the observations. This analysis highlights the well-known problem of SO_2 adjustment between VCD and observations (*see Fig.22*). It seems that the balance of this compound is unstable in the Venusian atmosphere and adjusting its abundance to the observed values at one level causes a mismatch at another level. Perhaps initialising oxygen in the simulations, in addition to other compounds such as H_2O and HCl, could help in stabilising O_2 first and SO_2 later at certain levels, and thus at the rest of the atmosphere. On the other hand, the rest of constituents studied in the validation are considerably more consistent.

Now that both ESA and NASA have planned missions to Venus, the modelling of its atmosphere turns especially demanding. For this reason, the LMD model in which the VCD is based is under continuous improvement and refinement. This has been the aim of this work, to help in that VCD fine-tuning and to complement other VCD validations.

Future Venus research and the upgrading of computational technology will contribute to Venus's modelling development too, not only for VCD but for many other existing and new models. These will continue evolving and overcoming the main challenges obtaining better and better results, thus allowing us to better understand Venus's atmospheric dynamics and to make the most out of such a powerful tool planetary models represent.

REFERENCES

Arney, G., Meadows, V., Crisp, D., Schmidt, S. J., Bailey, J., & Robinson, T. (2014). Spatially resolved measurements of H_2O, HCl, CO, OCS, SO_2, cloud opacity, and acid concentration in the Venus near-infrared spectral windows. *Journal of Geophysical Research: Planets*, *119*(8), 1860–1891. https://doi.org/10.1002/2014JE004662

Barstow, J. K., Tsang, C. C. C., Wilson, C. F., Irwin, P. G. J., Taylor, F. W., McGouldrick, K., Drossart, P., Piccioni, G., & Tellmann, S. (2012). Models of the global cloud structure on Venus derived from Venus Express observations. *Icarus*, *217*(2), 542–560. https://doi.org/10.1016/j.icarus.2011.05.018

Basilevsky, A. T., & Head, J. W. (2003). The surface of Venus. *Reports on Progress in Physics*, *66*(10), 1699–1734. https://doi.org/10.1088/0034-4885/66/10/R04

Basilevsky, A. T., Pronin, A. A., Ronca, L. B., Kryuchkov, V. P., Sukhanov, A. L., & Markov, M. S. (1986). Styles of tectonic deformations on Venus: Analysis of Venera 15 and 16 data. *Journal of Geophysical Research: Solid Earth*, *91*(B4), 399–411. https://doi.org/10.1029/JB091iB04p0D399

Bertaux, J.-L., Khatuntsev, I. v., Hauchecorne, A., Markiewicz, W. J., Marcq, E., Lebonnois, S., Patsaeva, M., Turin, A., & Fedorova, A. (2016). Influence of Venus topography on the zonal wind and UV albedo at cloud top level: The role of stationary gravity waves. *Journal of Geophysical Research: Planets*, *121*(6), 1087–1101. https://doi.org/10.1002/2015JE004958

Bertaux, J.-L., Nevejans, D., Korablev, O., Villard, E., Quémerais, E., Neefs, E., Montmessin, F., Leblanc, F., Dubois, J. P., Dimarellis, E., Hauchecorne, A., Lefèvre, F., Rannou, P., Chaufray, J. Y., Cabane, M., Cernogora, G., Souchon, G., Semelin, F., Reberac, A., … Gérard, J. C. (2007). SPICAV on Venus Express: Three spectrometers to study the global structure and composition of the Venus atmosphere. *Planetary and Space Science*, *55*(12), 1673–1700. https://doi.org/10.1016/j.pss.2007.01.016

Bézard, B., & de Bergh, C. (2007). Composition of the atmosphere of Venus below the clouds. *Journal of Geophysical Research*, *112*(E4), E04S07. https://doi.org/10.1029/2006JE002794

Bézard, B., de Bergh, C., Crisp, D., & Maillard, J.-P. (1990). The deep atmosphere of Venus revealed by high-resolution nightside spectra. *Nature*, *345*(6275), 508–511. https://doi.org/10.1038/345508a0

Blamont, J. E., Young, R. E., Seiff, A., Ragent, B., Sagdeev, R., Linkin, V. M., Kerzhanovich, V. v., Ingersoll, A. P., Crisp, D., Elson, L. S., Preston, R. A., Golitsyn, G. S., & Ivanov, V. N. (1986). Implications of the VEGA Balloon Results for Venus Atmospheric Dynamics. *Science*, *231*(4744), 1422–1425. https://doi.org/10.1126/science.231.4744.1422

Bonnet, R.-M., Grinspoon, D., & Rossi, A. P. (2013). History of Venus Observations. In *Towards Understanding the Climate of Venus* (pp. 7–16). Springer New York. https://doi.org/10.1007/978-1-4614-5064-1_2

Bullock, M. A. , et al. (2009). Venus Flagship Mission Study: Report of the Venus Science and Technology Definition Team. *40th Lunar and Planetary Science Conference*.

Colin, L., & Hall, C. F. (1977). The Pioneer Venus Program. *Space Science Reviews*, *20*(3), 283–306. https://doi.org/10.1007/BF02186467

Counselman, C. C., Gourevitch, S. A., King, R. W., Loriot, G. B., & Ginsberg, E. S. (1980). Zonal and meridional circulation of the lower atmosphere of Venus determined by radio interferometry. *Journal of Geophysical Research*, *85*(A13), 8026. https://doi.org/10.1029/JA085iA13p08026

Covey, C., & Schubert, G. (1982). Planetary-Scale Waves in the Venus Atmosphere. *Journal of the Atmospheric Sciences*, *39*(11), 2397–2413. https://doi.org/10.1175/1520-0469(1982)039<2397:PSWITV>2.0.CO;2

Edwards, P. N. (2000). *A Brief History of Atmospheric General Circulation Modeling* (pp. 67–90). https://doi.org/10.1016/S0074-6142(00)80050-9

ESPOSITO, L. W., BERTAUX, J.-L., KRASNOPOLSKY, V., MOROZ, V. I., & ZASOVA, L. v. (2022). CHEMISTRY OF LOWER ATMOSPHERE AND CLOUDS. In *Venus II* (pp. 415–458). University of Arizona Press. https://doi.org/10.2307/j.ctv27tct5m.18

Esposito, L. W., Knollenberg, R. G., Marov, M. Ia., Toon, O. B., & Turco, R. P. (1983). The clouds and hazes of Venus. In *Venus* (pp. 484–564). University of Arizona Press.

Garate-Lopez, I. (2014). *Dynamics of the South Polar Vortex of Venus*.

Garate-Lopez, I., Hueso, R., Sánchez-Lavega, A., Peralta, J., Piccioni, G., & Drossart, P. (2013). A chaotic long-lived vortex at the southern pole of Venus. *Nature Geoscience*, *6*(4), 254–257. https://doi.org/10.1038/ngeo1764

Garate-Lopez, I., & Lebonnois, S. (2018). Latitudinal variation of clouds' structure responsible for Venus' cold collar. *Icarus*, *314*, 1–11. https://doi.org/10.1016/j.icarus.2018.05.011

GIERASCH, P. J., GOODY, R. M., YOUNG, R. E., CRISP, D., EDWARDS, C., KAHN, R., McCLEESE, D., RIDER, D., del GENIO, A., GREELEY, R., HOU, A., LEOVY, C. B., & NEWMAN, M. (2022). THE GENERAL CIRCULATION OF THE VENUS ATMOSPHERE: In *Venus II* (pp. 459–500). University of Arizona Press. https://doi.org/10.2307/j.ctv27tct5m.19

Gierasch, P. J., & Yung, Y. L. (2003). Venus Atmosphere. In *Planetary Atmospheres* (pp. 1755–1760). Elsevier.

Golovin, Yu. M., & E. A. Ustinov. (1982). Subcloud aerosol on Venus. *Cosmic Res., 20, 104–110*.

Grassi, D., Politi, R., Ignatiev, N. I., Plainaki, C., Lebonnois, S., Wolkenberg, P., Montabone, L., Migliorini, A., Piccioni, G., & Drossart, P. (2014). The Venus nighttime atmosphere as observed by the VIRTIS-M instrument. Average fields from the complete infrared data set. *Journal of Geophysical Research: Planets*, *119*(4), 837–849. https://doi.org/10.1002/2013JE004586

Grinspoon, D. (2013). Chasing the Lost Oceans of Venus. In *Alien Seas* (pp. 3–9). Springer New York. https://doi.org/10.1007/978-1-4614-7473-9_2

Haus, R., Kappel, D., & Arnold, G. (2014). Atmospheric thermal structure and cloud features in the southern hemisphere of Venus as retrieved from VIRTIS/VEX radiation measurements. *Icarus*, *232*, 232–248. https://doi.org/10.1016/j.icarus.2014.01.020

Hausler, B. , et al. (2007). VENUS ATMOSPHERIC, IONOSPHERIC, SURFACE AND INTERPLANETARY RADIO- WAVE PROPAGATION STUDIES WITH THE VERA RADIO SCIENCE EXPERIMENT. *ESA Special Publication*.

Häusler, B., Pätzold, M., Tyler, G. L., Simpson, R. A., Bird, M. K., Dehant, V., Barriot, J.-P., Eidel, W., Mattei, R., Remus, S., Selle, J., Tellmann, S., & Imamura, T. (2006). Radio science investigations by VeRa onboard the Venus Express spacecraft. *Planetary and Space Science*, *54*(13–14), 1315–1335. https://doi.org/10.1016/j.pss.2006.04.032

Horinouchi, T., Kouyama, T., Lee, Y. J., Murakami, S., Ogohara, K., Takagi, M., Imamura, T., Nakajima, K., Peralta, J., Yamazaki, A., Yamada, M., & Watanabe, S. (2018). Mean winds at the cloud top of Venus obtained from two-wavelength UV imaging by Akatsuki. *Earth, Planets and Space*, *70*(1), 10. https://doi.org/10.1186/s40623-017-0775-3

Hueso, R., Peralta, J., Garate-Lopez, I., Bandos, T. V., & Sánchez-Lavega, A. (2015). Six years of Venus winds at the upper cloud level from UV, visible and near infrared observations from VIRTIS on Venus Express. *Planetary and Space Science*, *113–114*, 78–99. https://doi.org/10.1016/j.pss.2014.12.010

Hueso, R., Peralta, J., & Sánchez-Lavega, A. (2012). Assessing the long-term variability of Venus winds at cloud level from VIRTIS–Venus Express. *Icarus*, *217*(2), 585–598. https://doi.org/10.1016/j.icarus.2011.04.020

Ignatiev, N. I., Titov, D. v., Piccioni, G., Drossart, P., Markiewicz, W. J., Cottini, V., Roatsch, Th., Almeida, M., & Manoel, N. (2009). Altimetry of the Venus cloud tops from the Venus Express observations. *Journal of Geophysical Research*, *114*, E00B43. https://doi.org/10.1029/2008JE003320

Imamura, T., Higuchi, T., Maejima, Y., Takagi, M., Sugimoto, N., Ikeda, K., & Ando, H. (2014). Inverse insolation dependence of Venus' cloud-level convection. *Icarus*, *228*, 181–188. https://doi.org/10.1016/j.icarus.2013.10.012

Johnson, N. M., & Oliveira, M. R. R. (2019). Venus Atmospheric Composition In Situ Data: A Compilation. *Earth and Space Science*, *6*(7), 1299–1318. https://doi.org/10.1029/2018EA000536

Johnson, W. T. K. (1991). Magellan imaging radar mission to Venus. *Proceedings of the IEEE*, *79*(6), 777–790. https://doi.org/10.1109/5.90157

Kasprzak, W. T. (1990). The Pioneer Venus Orbiter: 11 Years Of Data. *A Laboratory For Atmospheres Seminar Talk*.

Kasting, J. F., & Pollack, J. B. (1983). Loss of water from Venus. I. Hydrodynamic escape of hydrogen. *Icarus*, *53*(3), 479–508. https://doi.org/10.1016/0019-1035(83)90212-9

Knollenberg, R., Travis, L., Tomasko, M., Smith, P., Ragent, B., Esposito, L., McCleese, D., Martonchik, J., & Beer, R. (1980). The clouds of Venus: A synthesis report. *Journal of Geophysical Research*, *85*(A13), 8059. https://doi.org/10.1029/JA085iA13p08059

Krasnopolsky, V. A. (1985). Chemical composition of venus clouds. *Planetary and Space Science*, *33*(1), 109–117. https://doi.org/10.1016/0032-0633(85)90147-3

Lebonnois, S., Lee, C., Yamamoto, M., Dawson, J., Lewis, S. R., Mendonca, J., Read, P., Parish, H. F., Schubert, G., Bengtsson, L., Grinspoon, D., Limaye, S. S., Schmidt, H., Svedhem, H., & Titov, D. v. (2013). Models of Venus Atmosphere. In *Towards Understanding the Climate of Venus* (pp. 129–156). Springer New York. https://doi.org/10.1007/978-1-4614-5064-1_8

Lebonnois, S., Millour, F., Forget, A., Martinez, A., & Pierron, T. (2021a). *Venus Climate Database v1.1 User Manual*.

Lebonnois, S., Millour, F., Forget, F., Martinez, A., & Pierron, T. (2021b). *Venus Climate Database v1.1 Validation Document*.

Lee, Y. J., Titov, D. V., Tellmann, S., Piccialli, A., Ignatiev, N., Pätzold, M., Häusler, B., Piccioni, G., & Drossart, P. (2012). Vertical structure of the Venus cloud top from the VeRa and VIRTIS observations onboard Venus Express. *Icarus*, *217*(2), 599–609. https://doi.org/10.1016/j.icarus.2011.07.001

LELLOUCH, E., CLANCY, T., CRISP, D., KLIORE, A. J., TITOV, D., & BOUGHER, S. W. (2022). MONITORING OF MESOSPHERIC STRUCTURE AND DYNAMICS. In *Venus II* (pp. 295–324). University of Arizona Press. https://doi.org/10.2307/j.ctv27tct5m.14

Lewis, S. R., Dawson, J., Lebonnois, S., & Yamamoto, M. (2013). Modeling Efforts. In *Towards Understanding the Climate of Venus* (pp. 111–127). Springer New York. https://doi.org/10.1007/978-1-4614-5064-1_7

Limaye, S. S., Lebonnois, S., Mahieux, A., Pätzold, M., Bougher, S., Bruinsma, S., Chamberlain, S., Clancy, R. T., Gérard, J.-C., Gilli, G., Grassi, D., Haus, R., Herrmann, M., Imamura, T., Kohler, E., Krause, P., Migliorini, A., Montmessin, F., Pere, C., … Zasova, L. (2017). The thermal structure of the Venus atmosphere: Intercomparison of Venus Express and ground based observations of vertical temperature and density profiles. *Icarus*, *294*, 124–155. https://doi.org/10.1016/j.icarus.2017.04.020

Limaye, S. S., Mogul, R., Smith, D. J., Ansari, A. H., Słowik, G. P., & Vaishampayan, P. (2018). Venus' Spectral Signatures and the Potential for Life in the Clouds. *Astrobiology*, *18*(9), 1181–1198. https://doi.org/10.1089/ast.2017.1783

Lynch, P. (2008). The origins of computer weather prediction and climate modeling. *Journal of Computational Physics*, *227*(7), 3431–3444. https://doi.org/10.1016/j.jcp.2007.02.034

Machado, P., Peralta, J., Silva, J. E., Brasil, F., Gonçalves, R., & Silva, M. (2022). Venus' Cloud-Tracked Winds Using Ground- and Space-Based Observations with TNG/NICS and VEx/VIRTIS. *Atmosphere*, *13*(2), 337. https://doi.org/10.3390/atmos13020337

Marcq, E., Mills, F. P., Parkinson, C. D., & Vandaele, A. C. (2018a). Composition and Chemistry of the Neutral Atmosphere of Venus. *Space Science Reviews*, *214*(1), 10. https://doi.org/10.1007/s11214-017-0438-5

Marcq, E., Mills, F. P., Parkinson, C. D., & Vandaele, A. C. (2018b). Composition and Chemistry of the Neutral Atmosphere of Venus. *Space Science Reviews*, *214*(1), 10. https://doi.org/10.1007/s11214-017-0438-5

Markiewicz, W. J., Titov, D. v., Limaye, S. S., Keller, H. U., Ignatiev, N., Jaumann, R., Thomas, N., Michalik, H., Moissl, R., & Russo, P. (2007). Morphology and dynamics of the upper cloud layer of Venus. *Nature*, *450*(7170), 633–636. https://doi.org/10.1038/nature06320

Marov, M. Ya. (1972). Venus: A perspective at the beginning of planetary exploration. *Icarus*, *16*(3), 415–461. https://doi.org/10.1016/0019-1035(72)90094-2

Mechoso, C. R., & Arakawa, A. (2003). GENERAL CIRCULATION | Models. In *Encyclopedia of Atmospheric Sciences* (pp. 861–869). Elsevier. https://doi.org/10.1016/B0-12-227090-8/00157-3

Mechoso, C. R., & Arakawa, A. (2015). NUMERICAL MODELS | General Circulation Models. In *Encyclopedia of Atmospheric Sciences* (pp. 153–160). Elsevier. https://doi.org/10.1016/B978-0-12-382225-3.00157-2

Mendonça, J. M., & Read, P. L. (2016). Exploring the Venus global super-rotation using a comprehensive general circulation model. *Planetary and Space Science*, *134*, 1–18. https://doi.org/10.1016/j.pss.2016.09.001

Mills, F. P., Esposito, L. W., & Yung, Y. L. (2007). *Atmospheric composition, chemistry, and clouds* (pp. 73–100). https://doi.org/10.1029/176GM06

Molaverdikhani, K., McGouldrick, K., & Esposito, L. W. (2012). The abundance and vertical distribution of the unknown ultraviolet absorber in the venusian atmosphere from analysis of Venus Monitoring Camera images. *Icarus*, *217*(2), 648–660. https://doi.org/10.1016/j.icarus.2011.08.008

Nimmo, F. (2002). Why does Venus lack a magnetic field? *Geology*, *30*(11), 987. https://doi.org/10.1130/0091-7613(2002)030<0987:WDVLAM>2.0.CO;2

Nimmo, F., & McKenzie, D. (1998). VOLCANISM AND TECTONICS ON VENUS. *Annual Review of Earth and Planetary Sciences*, *26*(1), 23–51. https://doi.org/10.1146/annurev.earth.26.1.23

Palmieri, P. (2001). Galileo and the Discovery of the Phases of Venus. *Journal for the History of Astronomy*, *32*(2), 109–129. https://doi.org/10.1177/002182860103200202

Parkinson, C. D., Gao, P., Schulte, R., Bougher, S. W., Yung, Y. L., Bardeen, C. G., Wilquet, V., Vandaele, A. C., Mahieux, A., Tellmann, S., & Pätzold, M. (2015). Distribution of sulphuric acid aerosols in the clouds and upper haze of Venus using Venus Express VAST and VeRa temperature profiles. *Planetary and Space Science*, *113–114*, 205–218. https://doi.org/10.1016/j.pss.2015.01.023

Patsaeva, M. V., Khatuntsev, I. V., Patsaev, D. V., Titov, D. V., Ignatiev, N. I., Markiewicz, W. J., & Rodin, A. V. (2015). The relationship between mesoscale circulation and cloud morphology at the upper cloud level of Venus from VMC/Venus Express. *Planetary and Space Science*, *113–114*, 100–108. https://doi.org/10.1016/j.pss.2015.01.013

Peralta, J., Muto, K., Hueso, R., Horinouchi, T., Sánchez-Lavega, A., Murakami, S., Machado, P., Young, E. F., Lee, Y. J., Kouyama, T., Sagawa, H., McGouldrick, K., Satoh, T., Imamura, T., Limaye, S. S., Sato, T. M., Ogohara, K., Nakamura, M., & Luz, D. (2018). Nightside Winds at the Lower Clouds of Venus with *Akatsuki* /IR2: Longitudinal, Local Time, and Decadal Variations from Comparison with Previous Measurements. *The Astrophysical Journal Supplement Series*, *239*(2), 29. https://doi.org/10.3847/1538-4365/aae844

Piccialli, A., Titov, D. V., Sanchez-Lavega, A., Peralta, J., Shalygina, O., Markiewicz, W. J., & Svedhem, H. (2014). High latitude gravity waves at the Venus cloud tops as observed by the Venus Monitoring Camera on board Venus Express. *Icarus*, *227*, 94–111. https://doi.org/10.1016/j.icarus.2013.09.012

Piccioni, G. , et al. (2007). VIRTIS: THE VISIBLE AND INFRARED THERMAL IMAGING SPECTROMETER. *ESA Special Publication*.

Pollack, J. B., Dalton, J. B., Grinspoon, D., Wattson, R. B., Freedman, R., Crisp, D., Allen, D. A., Bezard, B., DeBergh, C., Giver, L. P., Ma, Q., & Tipping, R. (1993). Near-Infrared Light from Venus' Nightside: A Spectroscopic Analysis. *Icarus*, *103*(1), 1–42. https://doi.org/10.1006/icar.1993.1055

Pollack, J. B., Toon, O. B., Whitten, R. C., Boese, R., Ragent, B., Tomasko, M., Esposito, L., Travis, L., & Wiedman, D. (1980). Distribution and source of the UV absorption in Venus' atmosphere. *Journal of Geophysical Research*, *85*(A13), 8141. https://doi.org/10.1029/JA085iA13p08141

Ragent, B., Esposito, L. W., Tomasko, M. G., Marov, M. Ya., Shari, V. P., & Lebedev, V. N. (1985). Particulate matter in the Venus atmosphere. *Advances in Space Research*, *5*(11), 85–115. https://doi.org/10.1016/0273-1177(85)90199-1

Sánchez-Lavega, A., Lebonnois, S., Imamura, T., Read, P., & Luz, D. (2017). The Atmospheric Dynamics of Venus. *Space Science Reviews*, *212*(3–4), 1541–1616. https://doi.org/10.1007/s11214-017-0389-x

Sato, T. M., Satoh, T., Sagawa, H., Manago, N., Lee, Y. J., Murakami, S., Ogohara, K., Hashimoto, G. L., Kasaba, Y., Yamazaki, A., Yamada, M., Watanabe, S., Imamura, T., & Nakamura, M. (2020). Dayside cloud top structure of Venus retrieved from Akatsuki IR2 observations. *Icarus*, *345*, 113682. https://doi.org/10.1016/j.icarus.2020.113682

Satoh, T., Imamura, T., Hashimoto, G. L., Iwagami, N., Mitsuyama, K., Sorahana, S., Drossart, P., & Piccioni, G. (2009). Cloud structure in Venus middle-to-lower atmosphere as inferred from VEX/VIRTIS 1.74 μ m data. *Journal of Geophysical Research*, *114*, E00B37. https://doi.org/10.1029/2008JE003184

Schubert, G. (1983). *General circulation, and the dynamical state of the Venus atmosphere*.

Schulze-Makuch, D., Grinspoon, D. H., Abbas, O., Irwin, L. N., & Bullock, M. A. (2004). A Sulfur-Based Survival Strategy for Putative Phototrophic Life in the Venusian Atmosphere. *Astrobiology*, *4*(1), 11–18. https://doi.org/10.1089/153110704773600203

Seiff, A., Schofield, J. T., Kliore, A. J., Taylor, F. W., Limaye, S. S., Revercomb, H. E., Sromovsky, L. A., Kerzhanovich, V. V., Moroz, V. I., & Marov, M. Ya. (1985). Models of the structure of the atmosphere of Venus from the surface to 100 kilometers altitude. *Advances in Space Research*, *5*(11), 3–58. https://doi.org/10.1016/0273-1177(85)90197-8

Smith, M. D., Gierasch, P. J., & Schinder, P. J. (1993). Global-Scale Waves in the Venus Atmosphere. *Journal of the Atmospheric Sciences*, *50*(24), 4080–4096. https://doi.org/10.1175/1520-0469(1993)050<4080:GSWITV>2.0.CO;2

Smrekar, S. E., Stofan, E. R., Mueller, N., Treiman, A., Elkins-Tanton, L., Helbert, J., Piccioni, G., & Drossart, P. (2010). Recent Hotspot Volcanism on Venus from VIRTIS Emissivity Data. *Science*, *328*(5978), 605–608. https://doi.org/10.1126/science.1186785

Solomon, S. C., Smrekar, S. E., Bindschadler, D. L., Grimm, R. E., Kaula, W. M., McGill, G. E., Phillips, R. J., Saunders, R. S., Schubert, G., Squyres, S. W., & Stofan, E. R. (1992). Venus tectonics: An overview of Magellan observations. *Journal of Geophysical Research*, *97*(E8), 13199. https://doi.org/10.1029/92JE01418

Sonett, CharlesP. (1963). A summary review of the scientific findings of the Mariner Venus mission. *Space Science Reviews*, *2*(6). https://doi.org/10.1007/BF00208814

Svedhem, H., Titov, D., Taylor, F., & Witasse, O. (2009). Venus Express mission. *Journal of Geophysical Research*, *114*, E00B33. https://doi.org/10.1029/2008JE003290

Taylor, F. W. (2014). *The Scientific Exploration of Venus*. Cambridge University Press. https://doi.org/10.1017/CBO9781139151245

Tellmann, S., Pätzold, M., Häusler, B., Bird, M. K., & Tyler, G. L. (2009). Structure of the Venus neutral atmosphere as observed by the Radio Science experiment VeRa on Venus Express. *Journal of Geophysical Research*, *114*, E00B36. https://doi.org/10.1029/2008JE003204

Titov, D. v., Ignatiev, N. I., McGouldrick, K., Wilquet, V., & Wilson, C. F. (2018). Clouds and Hazes of Venus. *Space Science Reviews*, *214*(8), 126. https://doi.org/10.1007/s11214-018-0552-z

Titov, D. v., Markiewicz, W. J., Ignatiev, N. I., Song, L., Limaye, S. S., Sanchez-Lavega, A., Hesemann, J., Almeida, M., Roatsch, T., Matz, K.-D., Scholten, F., Crisp, D., Esposito, L. W., Hviid, S. F., Jaumann, R., Keller, H. U., & Moissl, R. (2012). Morphology of the cloud tops as observed by the Venus Express Monitoring Camera. *Icarus*, *217*(2), 682–701. https://doi.org/10.1016/j.icarus.2011.06.020

Titov, D. v., Svedhem, H., Taylor, F. W., Barabash, S., Bertaux, J.-L., Drossart, P., Formisano, V., Häusler, B., Korablev, O., Markiewicz, W. J., Nevejans, D., Pätzold, M., Piccioni, G., Sauvaud, J.-A., Zhang, T. L., Witasse, O., Gerard, J.-C., Fedorov, A., Sanchez-Lavega, A., … Hoofs, R. (2009). Venus express: Highlights of the nominal mission. *Solar System Research*, *43*(3), 185–209. https://doi.org/10.1134/S0038094609030010

Vorder Bruegge, R. W., & Head III, J. W. (1991). Processes of formation and evolution of mountain belts on Venus. *Geology*, *19*(9), 885. https://doi.org/10.1130/0091-7613(1991)019<0885:POFAEO>2.3.CO;2

Way, M. J., del Genio, A. D., Kiang, N. Y., Sohl, L. E., Grinspoon, D. H., Aleinov, I., Kelley, M., & Clune, T. (2016). Was Venus the first habitable world of our solar system? *Geophysical Research Letters*, *43*(16), 8376–8383. https://doi.org/10.1002/2016GL069790

Widemann, T., Lellouch, E., & Campargue, A. (2007). New wind measurements in Venus' lower mesosphere from visible spectroscopy. *Planetary and Space Science*, *55*(12), 1741–1756. https://doi.org/10.1016/j.pss.2007.01.005

Zhang, T. L., Delva, M., Baumjohann, W., Volwerk, M., Russell, C. T., Wei, H. Y., Wang, C., Balikhin, M., Barabash, S., Auster, H.-U., & Kudela, K. (2008). Induced magnetosphere and its outer boundary at Venus. *Journal of Geophysical Research*, *113*, E00B20. https://doi.org/10.1029/2008JE003215

Zhang, X., Liang, M. C., Mills, F. P., Belyaev, D. A., & Yung, Y. L. (2012). Sulfur chemistry in the middle atmosphere of Venus. *Icarus*, *217*(2), 714–739. https://doi.org/10.1016/j.icarus.2011.06.016

APPENDIX

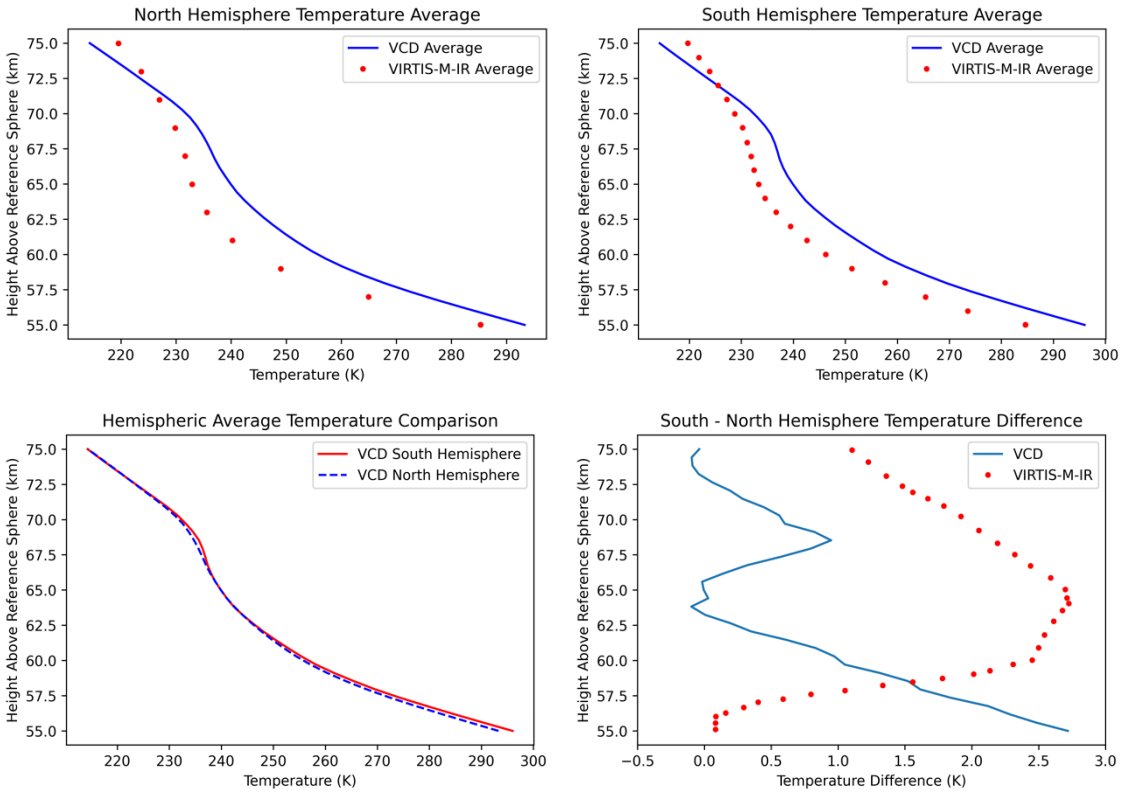

***Figure 23**: vertical profiles of hemispheric average temperature in the night side (19:00LT - 05:00LT). Red marks are for south (upper left) and north (upper right) hemispheres temperatures measured by Haus et al., 2014, from VEx's VIRTIS-M-IR data. Blue lines are for south (upper left) and north (upper right) hemisphere average temperatures as given by VCD. Lower left figure is the comparison between south hemisphere (red) and north hemisphere (blue) temperature vertical profiles. Lower right figure shows the hemispheric difference (south minus north) for the average temperature according to Haus et al., 2014 (red) and VCD (blue).*

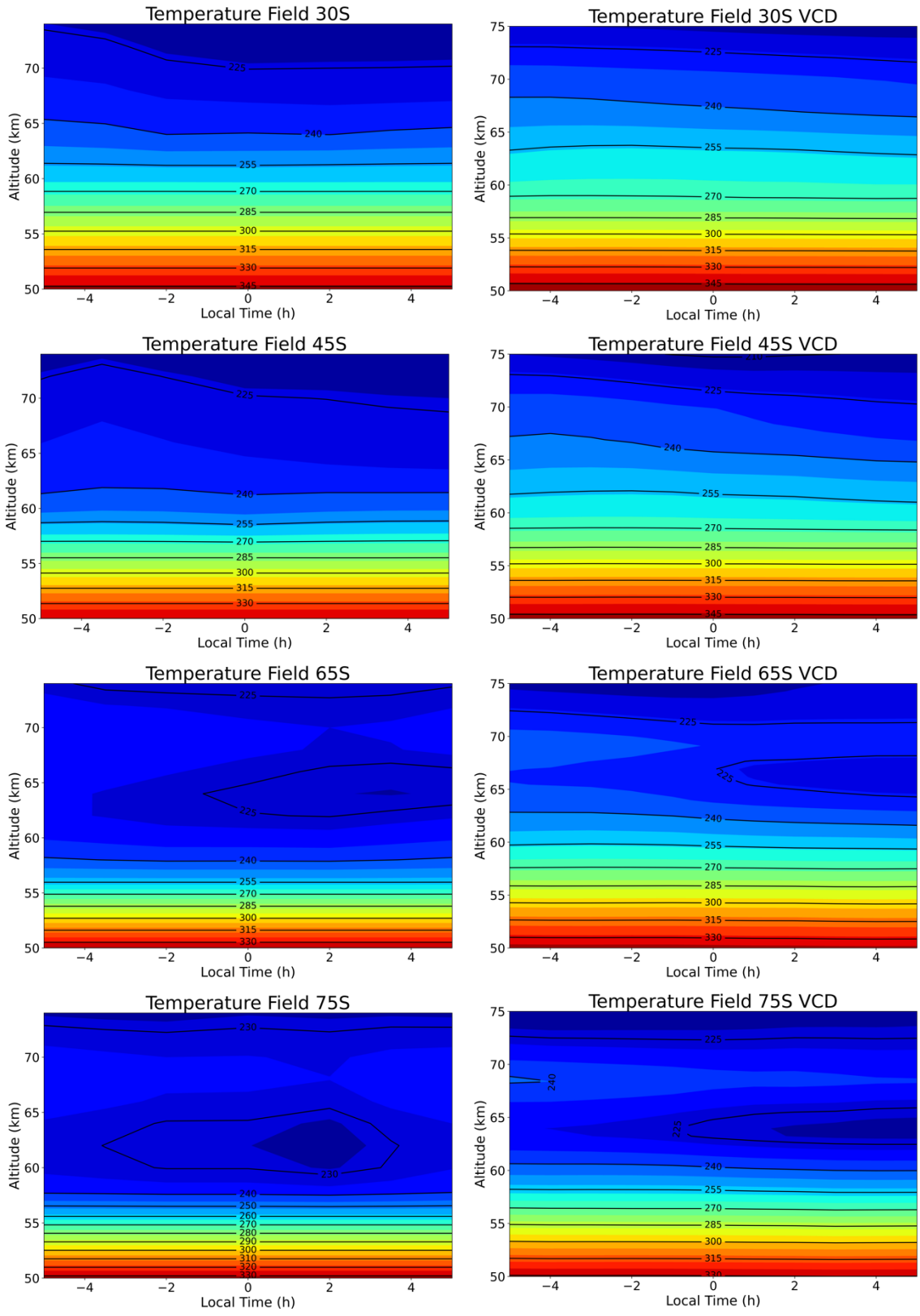

***Figure 24**: mean temperature fields (units: Kelvin) as function of local time (-05:00LT - 05:00LT) and altitude at different latitudes (30°S, 45°S, 65°S and 75°S). On the left, self-crafted contour maps from VIRTIS-M-IR data at the Appendix of Haus et al., 2014. On the right, contour maps from VCD data with altitudes above a reference sphere of radius 6052km.*

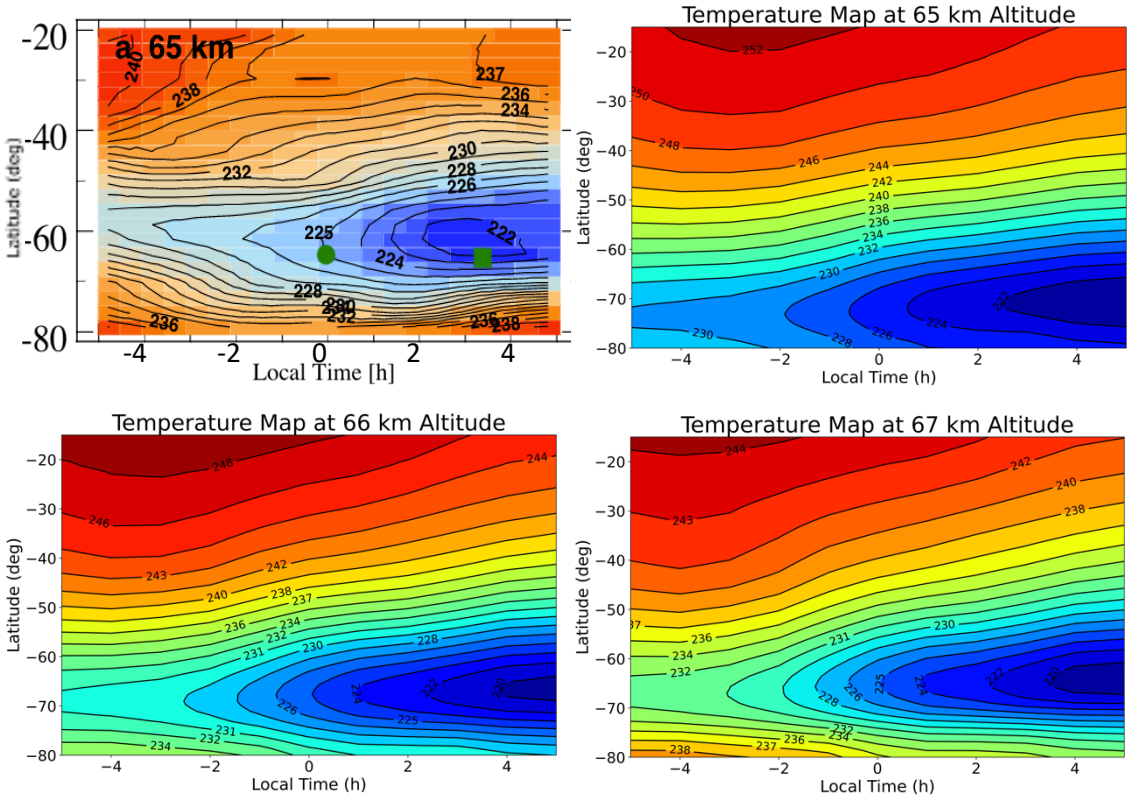

***Figure 25**: mean temperature fields (units: Kelvin) as function of local time (-05:00LT - 05:00LT) and latitude. Upper left contour map from Haus et al., 2014 measured by VEx's VIRTIS-M-IR at 65km altitude. The other three from VCD output at 65km, 66km and 67km altitudes above a reference sphere of radius 6052km.*

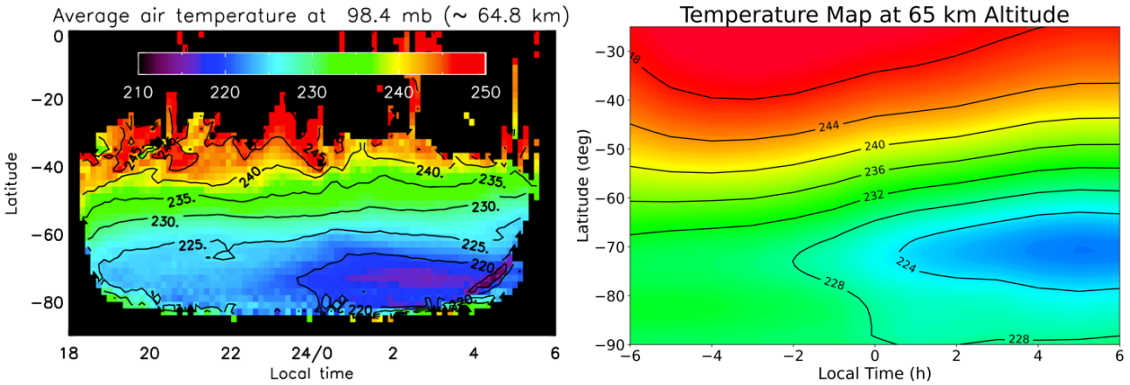

***Figure 26**: mean temperature fields (units: Kelvin) as function of local time (-06:00LT - 06:00LT) and latitude. Left contour map is from Grassi et al., 2014 measured by VEx's VIRTIS-M at ~65km altitude above a reference sphere of radius 6052km. On the right, VCD output at 65km altitude.*

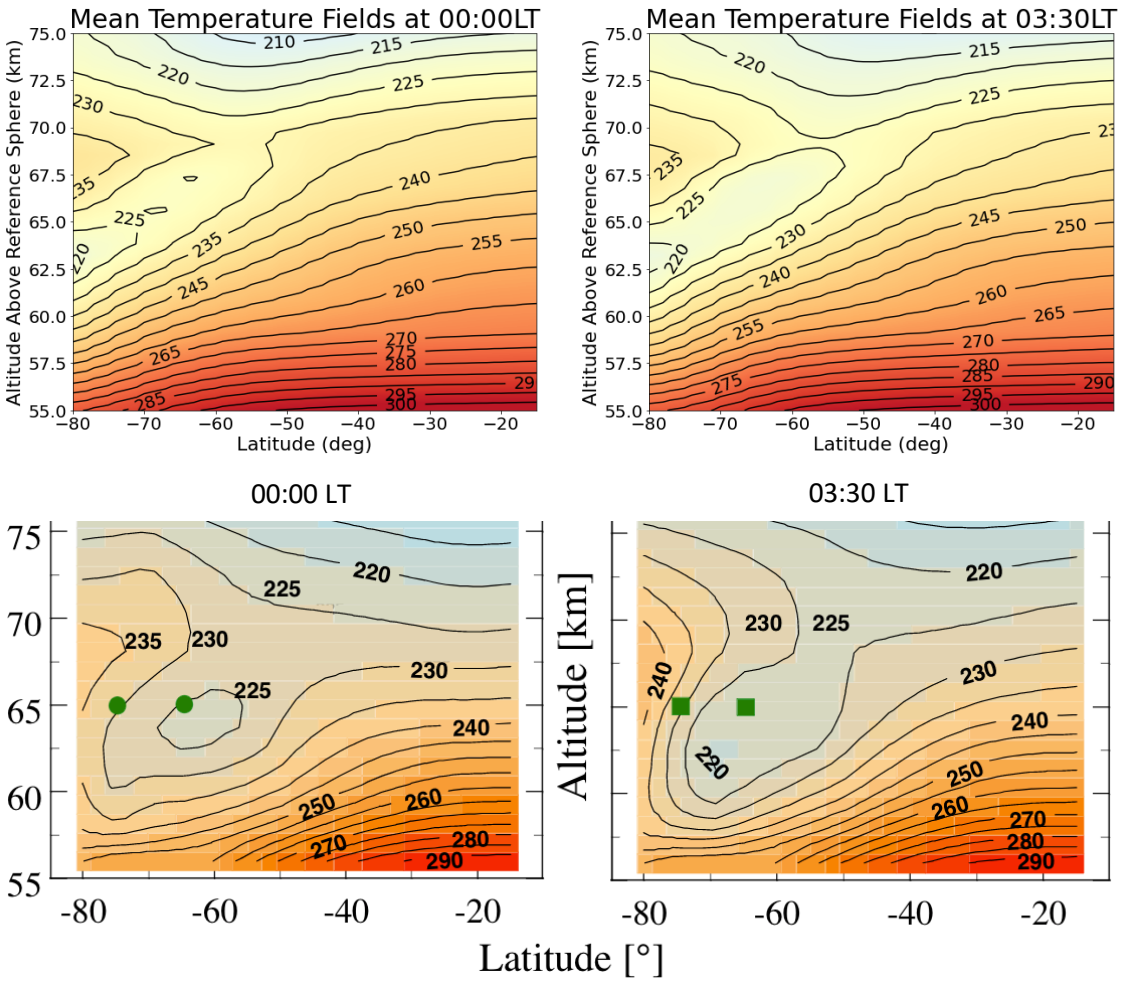

***Figure 27**: mean temperature fields (units: Kelvin) as function of latitude and altitude at 00:00LT (left) and 03:30LT (right). Upper contour maps are from VCD data and lower contour maps are from VEx's VIRTIS-M-IR measurements by Haus et al., 2014.*

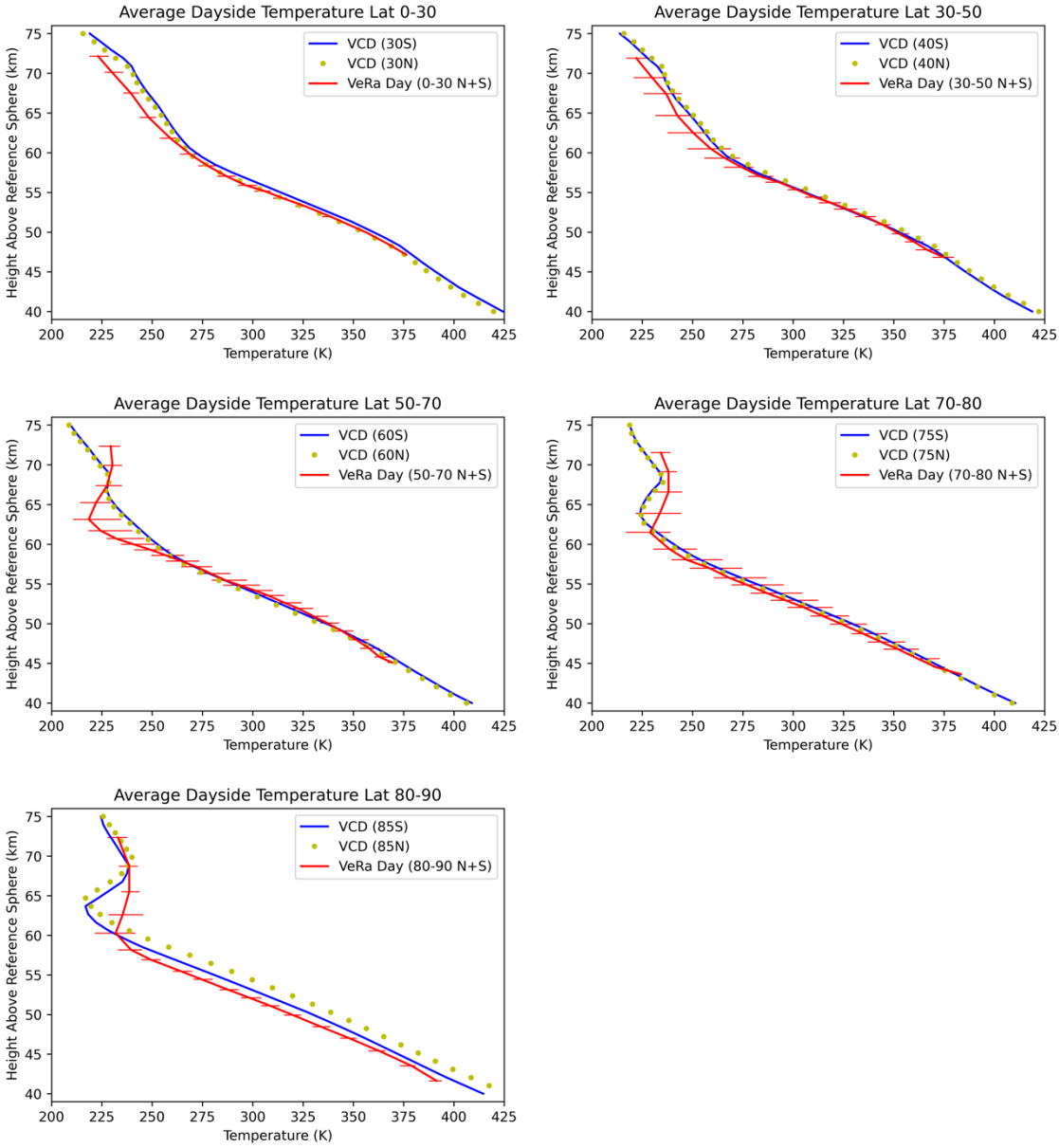

***Figure 28**: vertical profiles of zonally averaged dayside temperature at different latitudes. Red lines represent VEx's VeRa dayside mean temperatures between 07:00LT and 17:00LT as presented on Limaye et al., 2017 for the different latitude bands. Blue lines (for south hemisphere) and yellow marks (for north hemisphere) represent VCD dayside temperature at 12:00LT at latitudes 15° N/S, 45° N/S, 60° N/S, 75° N/S, 85° N/S.*

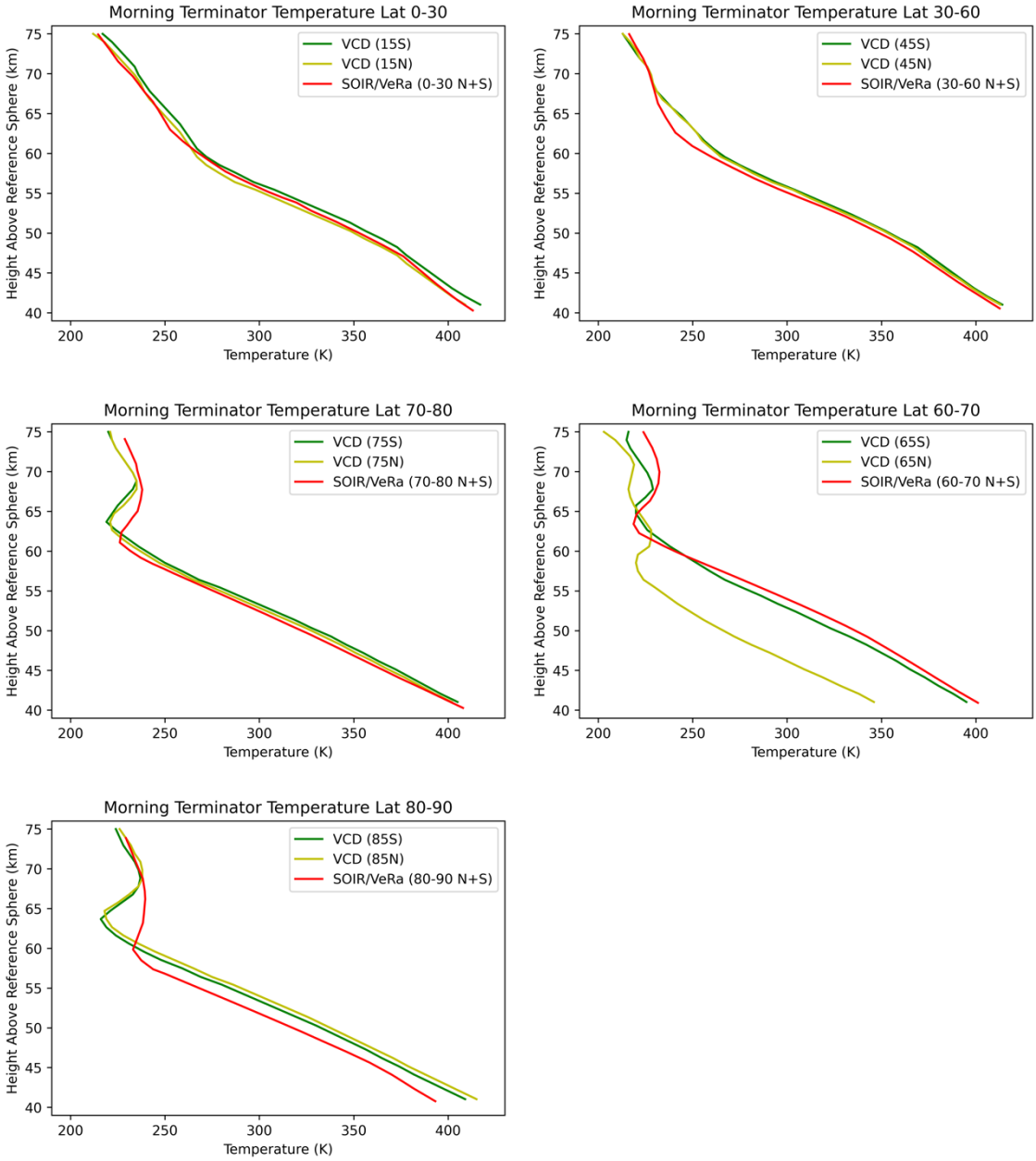

***Figure 29**: vertical profiles of morning terminator temperature at different latitudes. Red lines represent VEx's SOIR/VeRa terminator mean temperatures between 05:00LT and 07:00LT as presented on Parkinson et al., 2015 for the different latitude bands. Green lines (for south hemisphere) and light green lights (for north hemisphere) represent VCD morning terminator temperatures at 06:00LT at latitudes 15°N/S, 45° N/S, 60°N/S, 75°N/S, 85°N/S.*

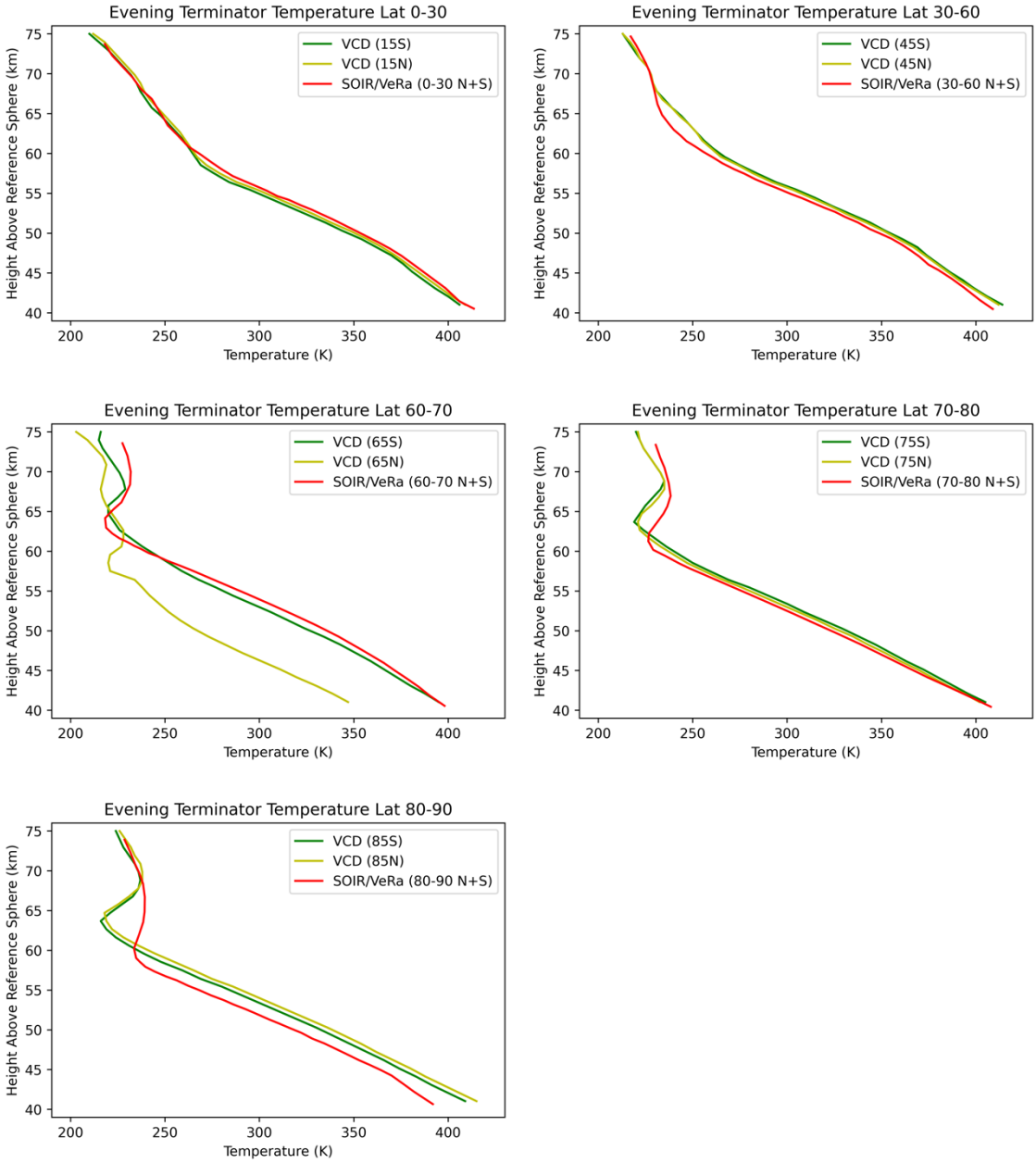

***Figure 30**: vertical profiles of evening terminator temperature at different latitudes. Red lines represent VEx's SOIR/VeRa terminator mean temperatures between 17:00LT and 19:00LT as presented on Parkinson et al., 2015 for the different latitude bands. Green lines (for south hemisphere) and light green lights (for north hemisphere) represent VCD morning terminator temperatures at 18:00LT at latitudes 15°N/S, 45° N/S, 60°N/S, 75°N/S, 85°N/S.*

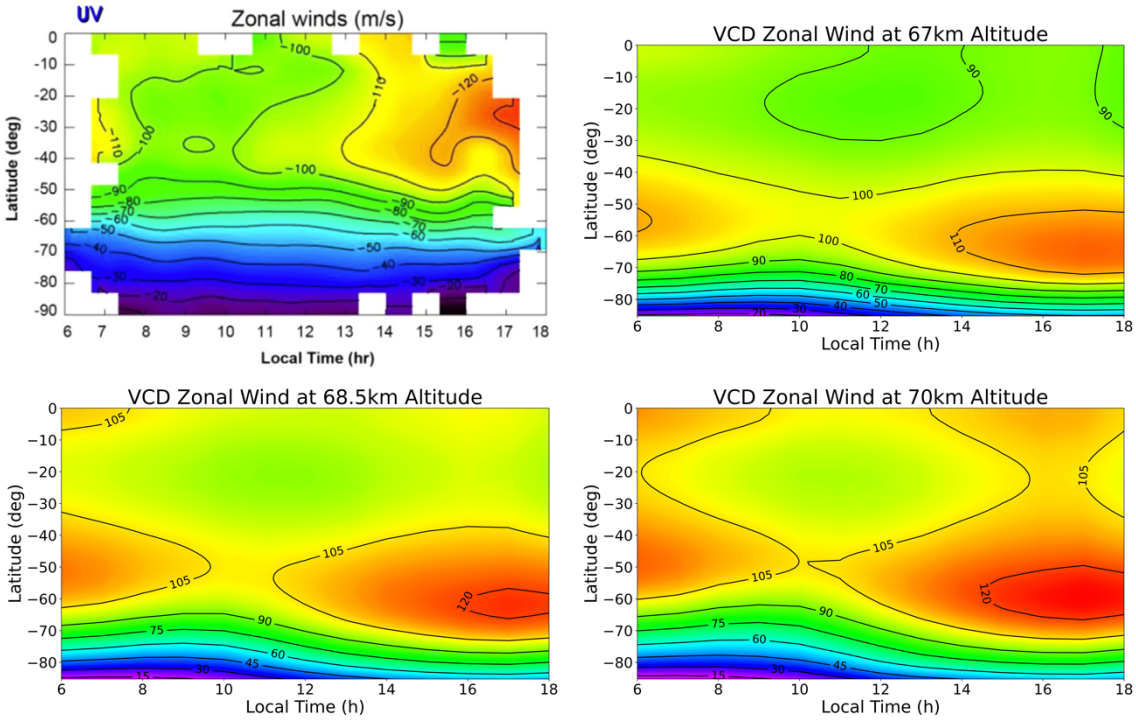

***Figure 31**: mean zonal wind maps (units: m/s) at cloud top as function of local time and latitude. <u>Upper left</u>: VEx's VIRTIS UV winds at 360-400 nm from Hueso et al., 2014 corresponding to 67-70km altitude. <u>Lower left and upper and lower right</u>: VCD zonal winds at three different altitudes. VCD altitudes above Venus's reference sphere of radius 6052km.*

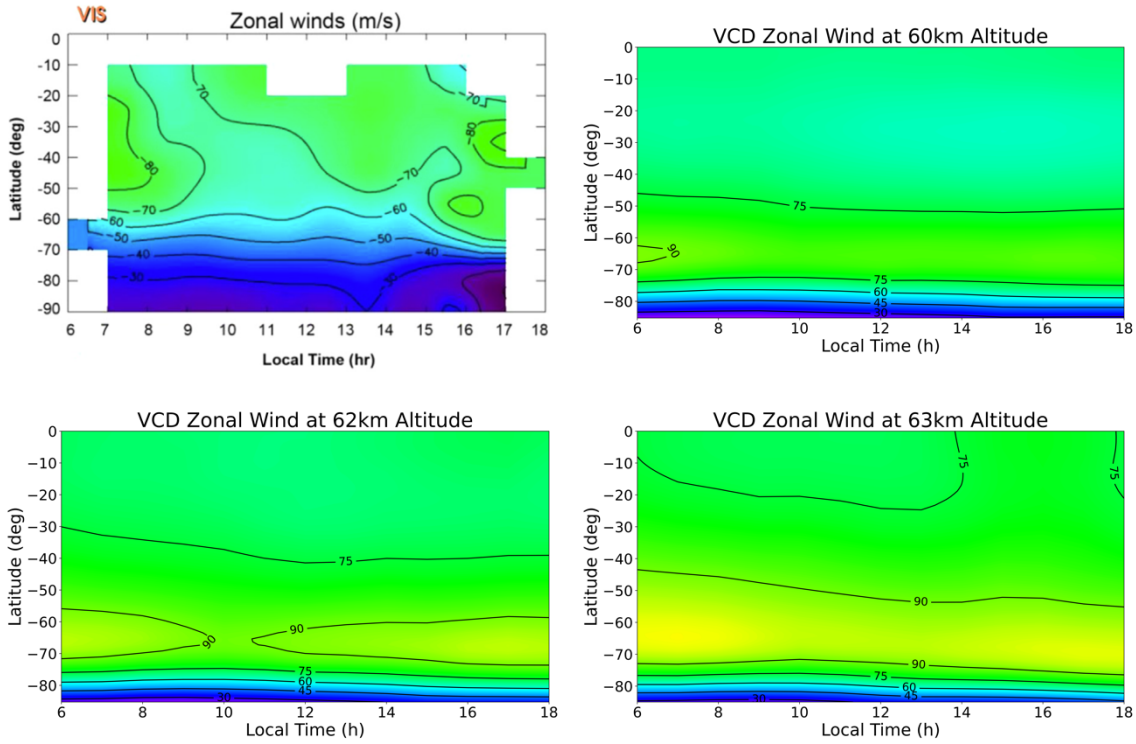

***Figure 32**: same as Figure 31 but for VEx's VIRTIS VIS at 570-680 nm from Hueso et al., 2014 corresponding to ~62km altitude (upper middle cloud).*

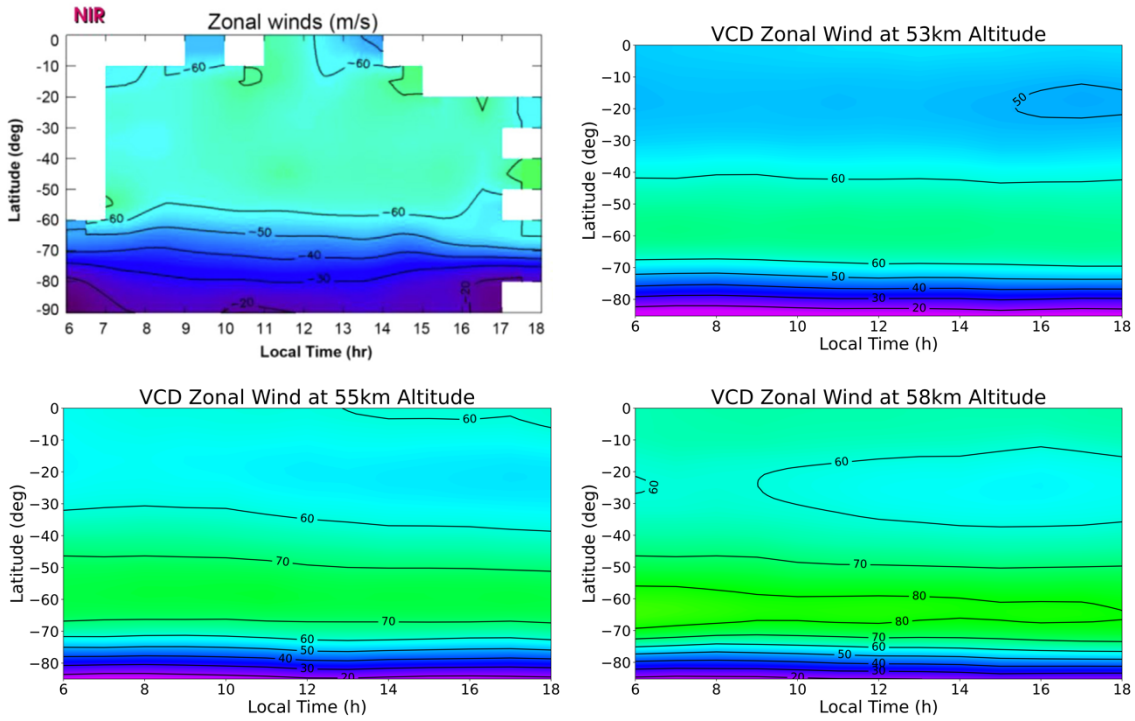

***Figure 33**: same as Figure 31 but for VEx's VIRTIS NIR at 900-955 nm from Hueso et al., 2014 corresponding to ~58km altitude (middle cloud).*

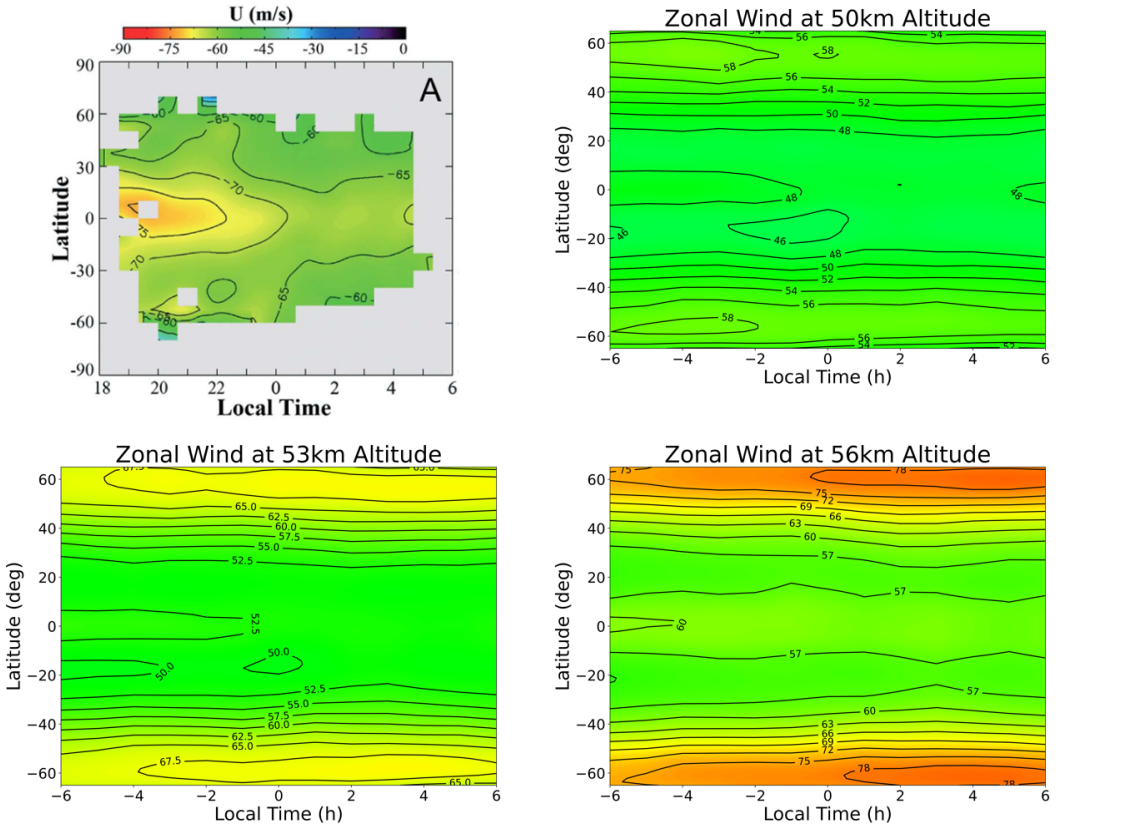

***Figure 34**:mean zonal wind maps (units: m/s) at lower cloud as function of local time and latitude. Upper left: Akatsuki IR2 at 2.26 μm from Peralta et al., 2018 corresponding to 50km altitude. Lower left and upper and lower right: VCD zonal winds at three different altitudes. VCD altitudes above Venus's reference sphere of radius 6052km.*

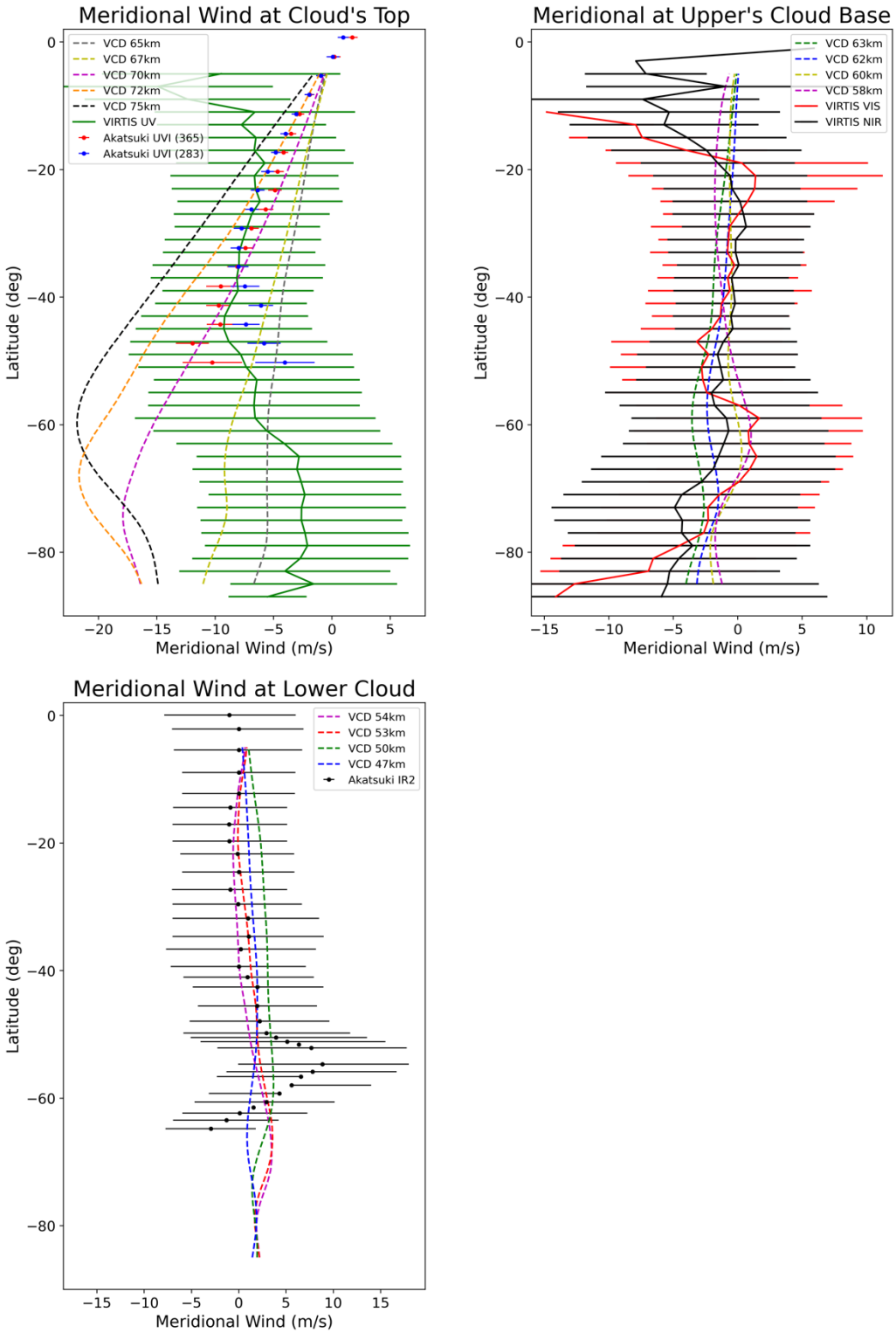

***Figure 35**: meridional wind profiles at different cloud regions as a function of latitude. Several VCD altitudes have been considered in order to find the best fit. Values are taken above Venus's reference sphere of radius 6052km. Upper left: VEx's VIRTIS UV at 360-400 nm dayside mean meridional winds from Hueso et al., 2014 corresponding to 67-70km altitude (green), and Akatsuki UVI at 365 nm (70km) (dotted red) and 283nm (75km) (dotted blue) meridional winds at noon (12LT) from Horinouchi et al., 2018. VCD meridional winds are dayside mean values between 07LT and 17LT. Upper right: VEx VIRTIS VIS (red) at 570-680 nm and NIR (black) at 900-955 nm from Hueso et al., 2014 corresponding to ~62km and ~58km altitude, respectively, are shown. VCD data is the dayside mean values between 07LT and 17LT. Lower left and right: Akatsuki IR2 at 2.26 μm (50km) (black) from Peralta et al., 2018. VCD data is retrieved at 00LT.*

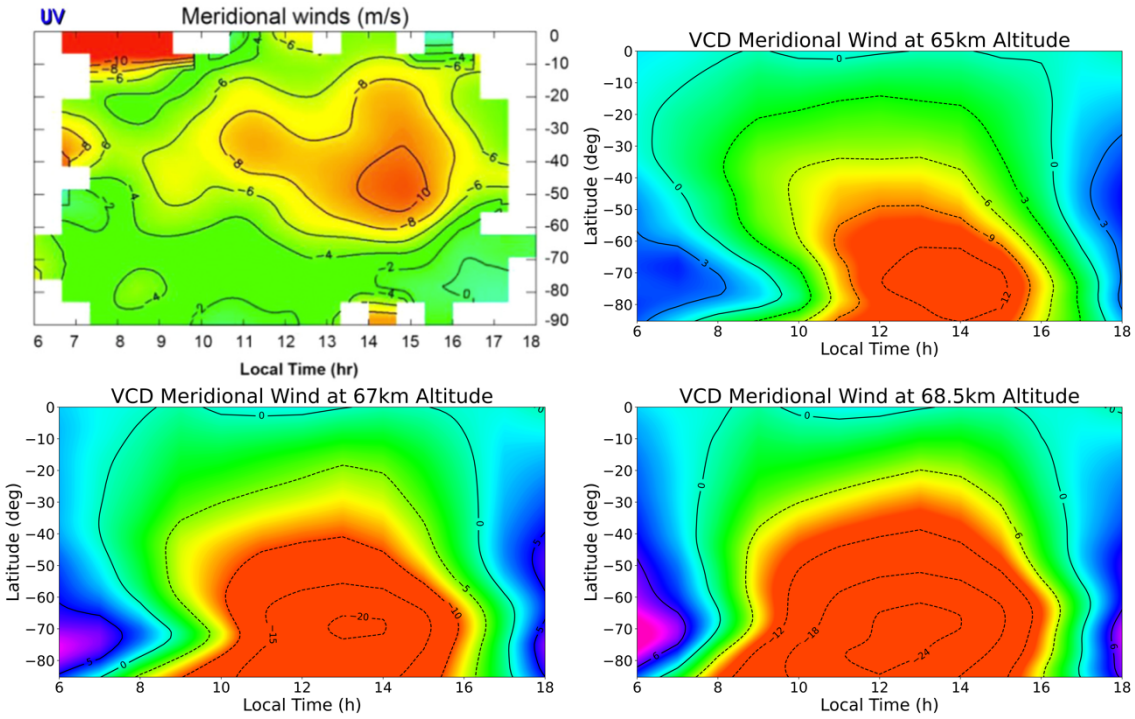

***Figure 36**: mean meridional wind maps (units: m/s) at cloud top as function of local time and latitude. Upper left: VEx's VIRTIS UV winds at 360-400 nm from Hueso et al., 2014 corresponding to 67-70km altitude. Lower left and upper and lower right: VCD meridional winds at three different altitudes. VCD altitudes above Venus's reference sphere of radius 6052km.*

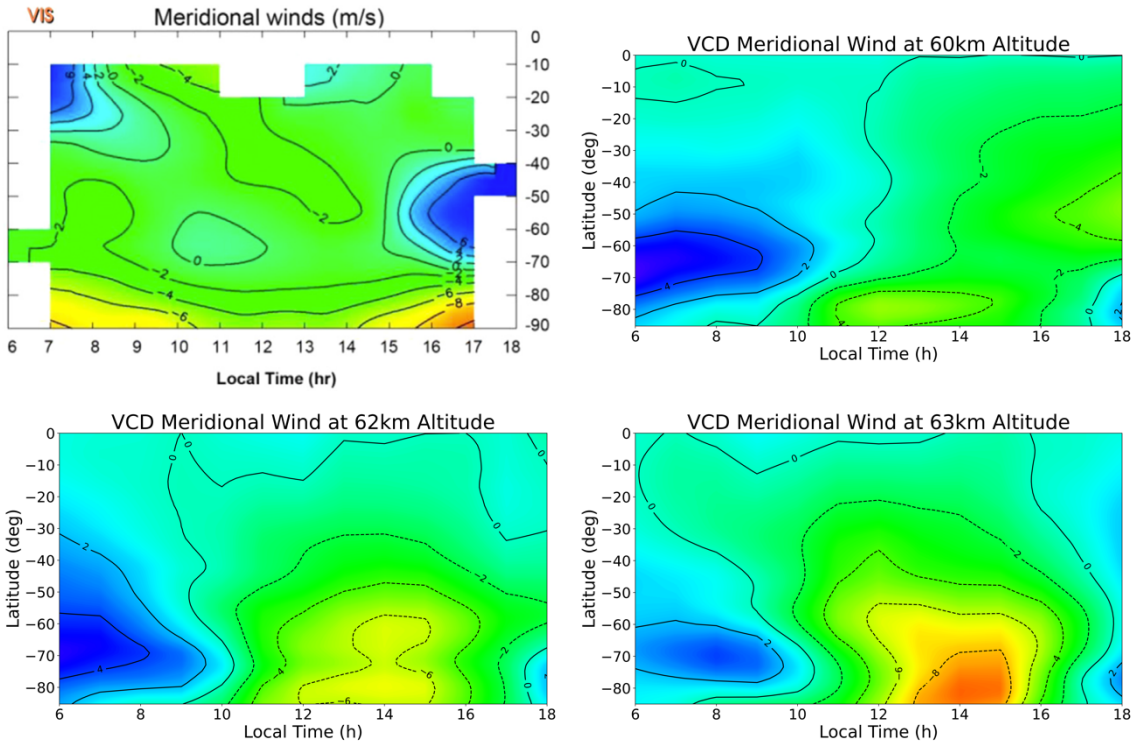

***Figure 37**: same as Figure 36 but for VEx's VIRTIS VIS at 570-680 nm from Hueso et al., 2014 corresponding to ~62km altitude (upper middle cloud).*

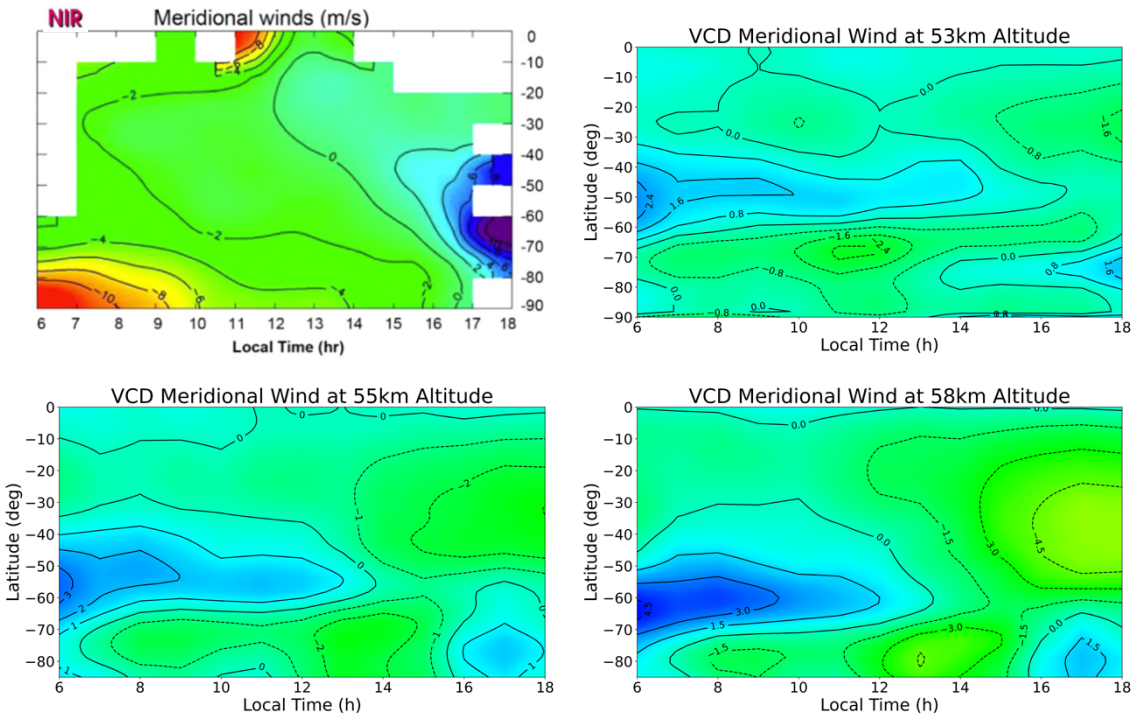

***Figure 38**: same as Figure 36 but for VEx's VIRTIS NIR at 900-955 nm from Hueso et al., 2014 corresponding to ~58km altitude (middle cloud).*

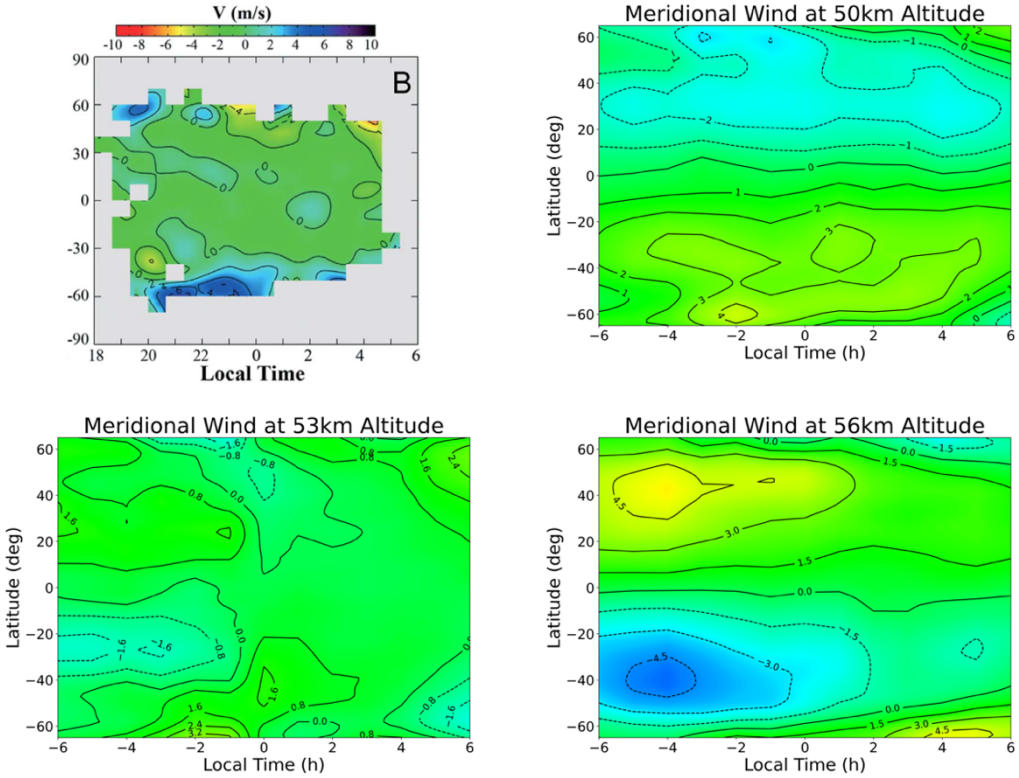

***Figure 39**: mean meridional wind maps (units: m/s) at lower cloud as function of local time and latitude. Upper left: Akatsuki IR2 at 2.26 μm from Peralta et al., 2018 corresponding to 50km altitude. Lower left and upper and lower right: VCD meridional winds at three different altitudes. VCD altitudes above Venus's reference sphere of radius 6052km.*

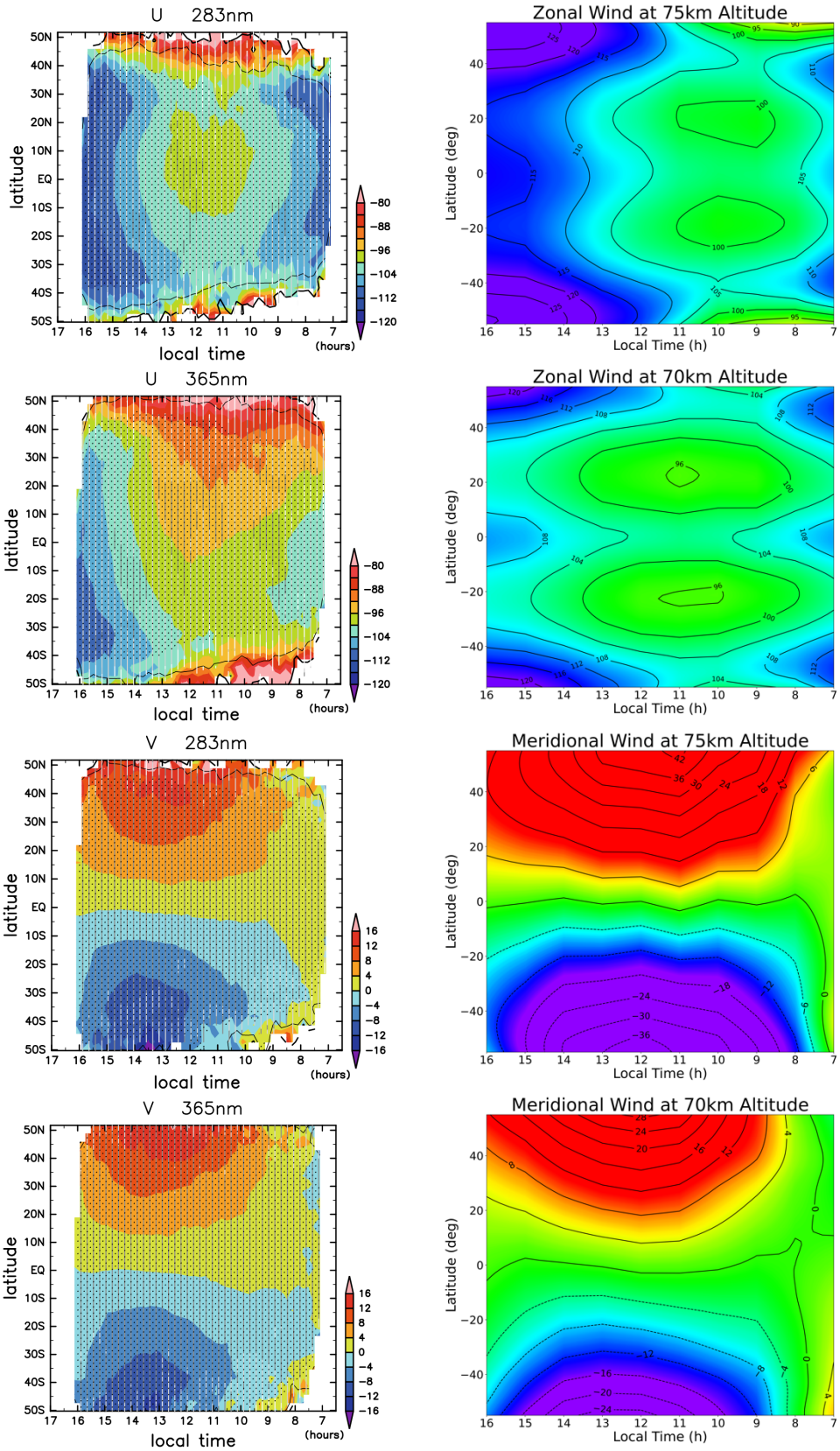

***Figure 40**: mean wind maps as function of local time and latitude. Left: zonal (first and second rows) and meridional winds (third and fourth rows) measured by Akatsuki UVI at 283 nm (~75km) and 365 nm (~70km) from Horinouchi et al., 2018. Right: VCD zonal and meridional winds at 70km and 75km. All VCD altitudes above Venus's reference sphere and winds in m/s.*

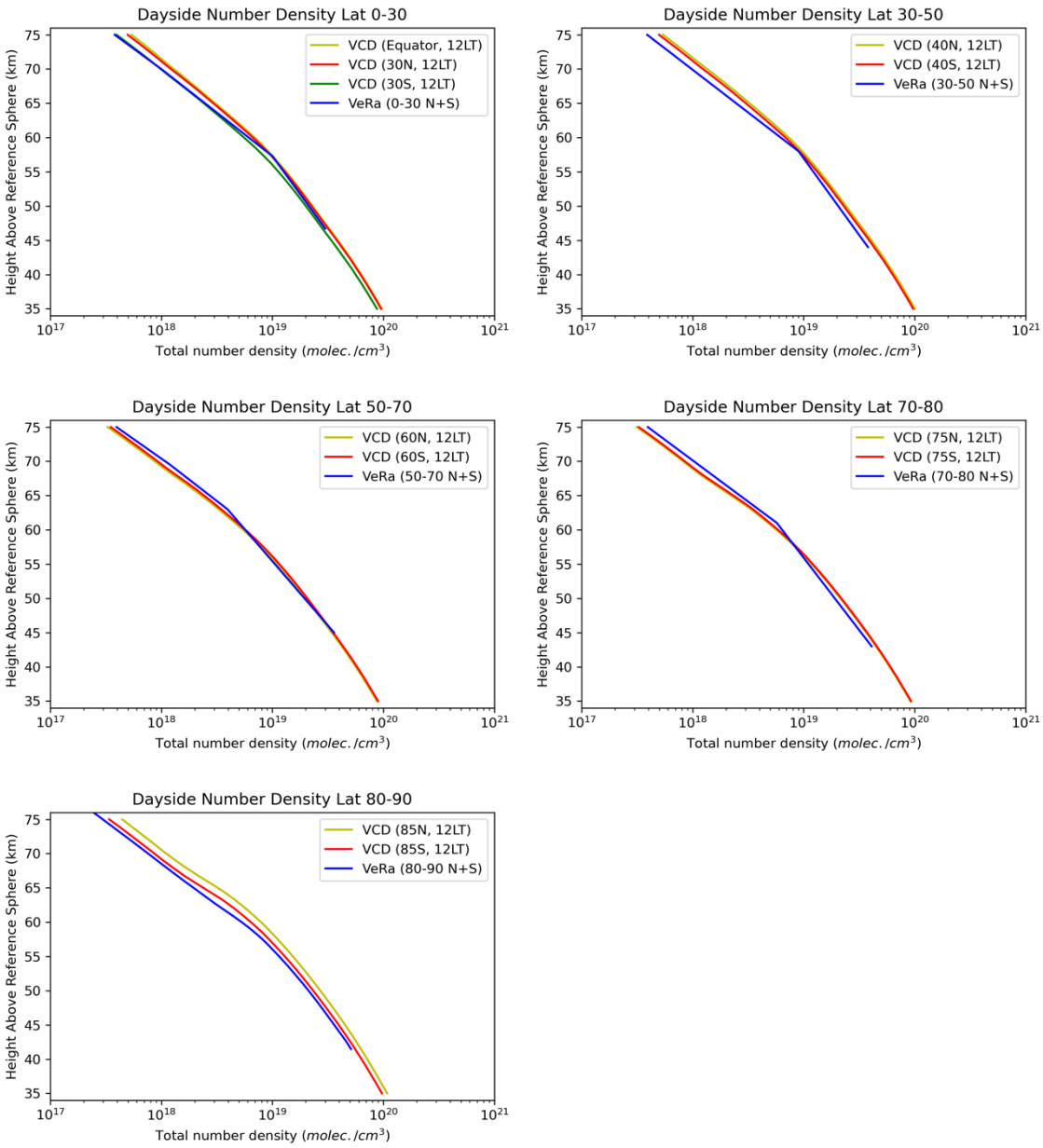

***Figure 41**: vertical profiles of zonally averaged dayside total number density at different latitudes. Blue lines represent VEx's VeRa dayside mean number density between 07:00LT and 17:00LT as presented on Limaye et al., 2017 for the different latitude bands. Red lines (for south hemisphere) and yellow lines (for north hemisphere) represent VCD dayside number density at 12:00LT at latitudes 15° N/S, 45° N/S, 60° N/S, 75° N/S, 85° N/S.*

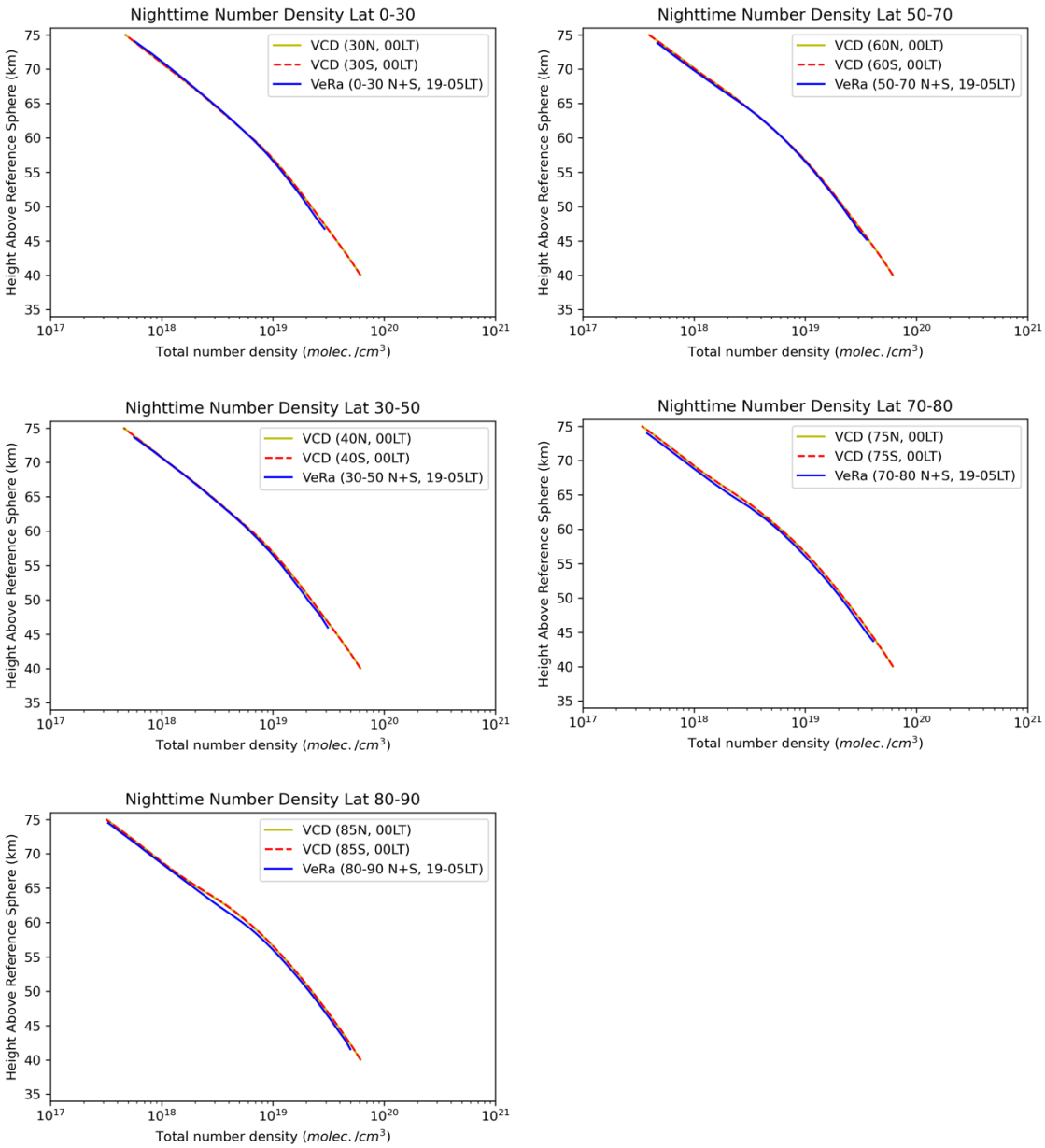

***Figure 42**: vertical profiles of zonally averaged nightside total number density at different latitudes. Blue lines represent VEx's VeRa nightside mean number density between 19:00LT and 05:00LT as presented on Limaye et al., 2017 for the different latitude bands. Red dashed lines (for south hemisphere) and yellow lines (for north hemisphere) represent VCD nightside number density at 00:00LT at latitudes 15°N/S, 45° N/S, 60°N/S, 75°N/S, 85°N/S.*

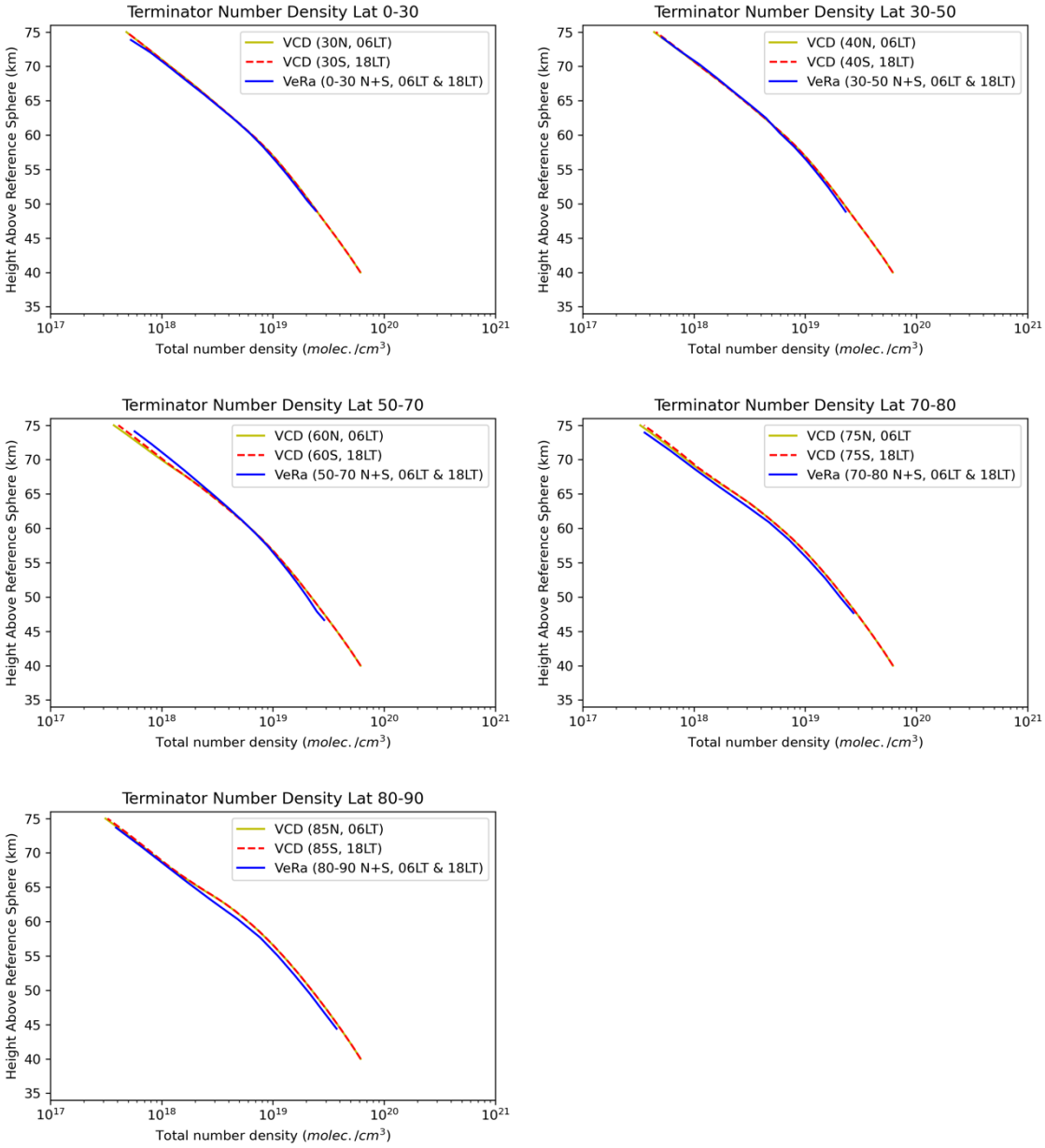

***Figure 43**: vertical profiles of morning and evening terminators total number density at different latitudes. Blue lines represent VEx's VeRa number density at both morning (05:00LT – 07:00LT) and evening (17:00LT – 19:00LT) terminators as presented on Limaye et al., 2017 for the different latitude bands. Yellow solid lines show VCD results at morning terminator (06:00LT) at northern latitudes (15 °N, 45 °N, 60 °N, 75 °N, 85 ° N) and red dashed lines plot VCD output retrieved at evening terminator (18:00LT) at southern latitudes (15 °S, 45 °S, 60 °S, 75 °S, 85 °S).*

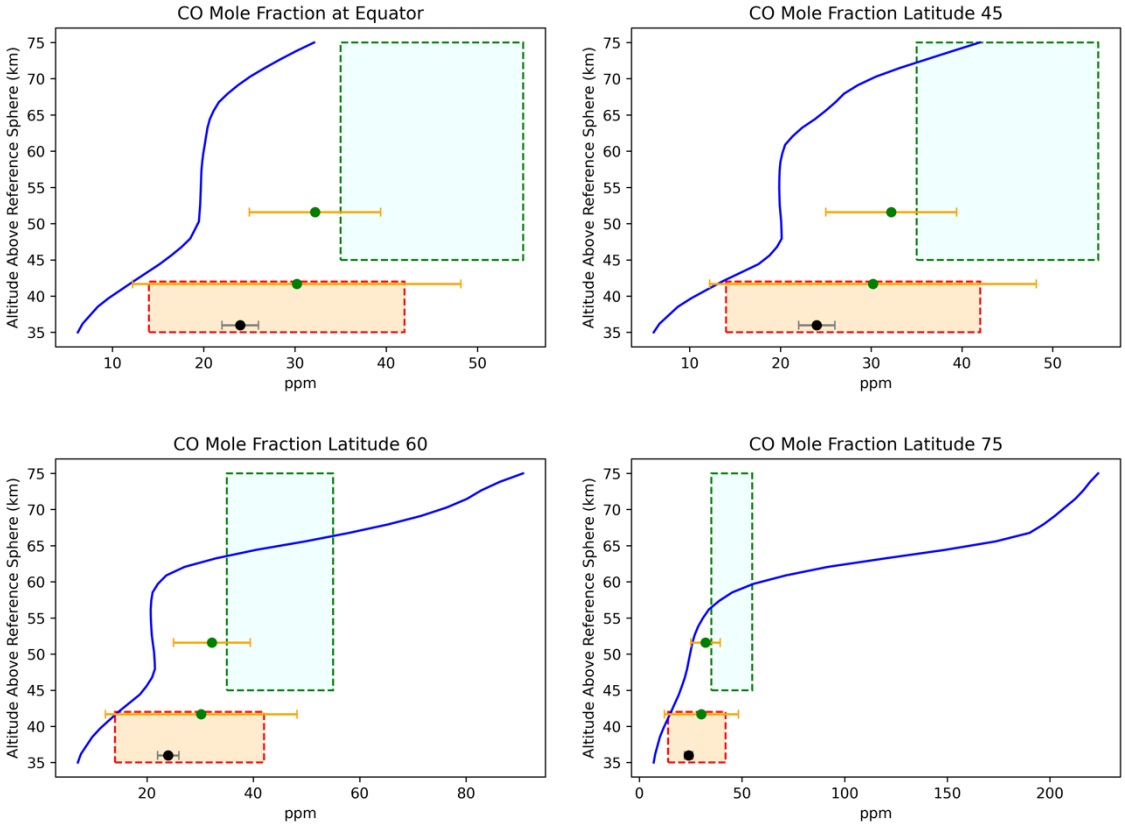

***Figure 44**: carbon monoxide mixing ratio vertical profile in parts per million at different latitudes. Blue lines represent VCD results at each latitude at 00:00LT. Observational data have the same values for all four panels as there is no cited latitudinal dependence/variation in the chosen literature. Red rectangle shows Venera 12 in situ measurements by gas chromatography (Gel'man et al., 1979), green rectangle represents values measured by Earth Based Telescope Interferometer (Connes et al., 1968), green dots are results from Pioneer Venus in situ measurements by LGC instrument (Oyama et al., 1979), black dots are measurements by Earth Based Telescope IR spectroscopy (Marcq et al., 2006). Rectangles and errorbars show altitude and mixing ratio ranges given by the authors.*

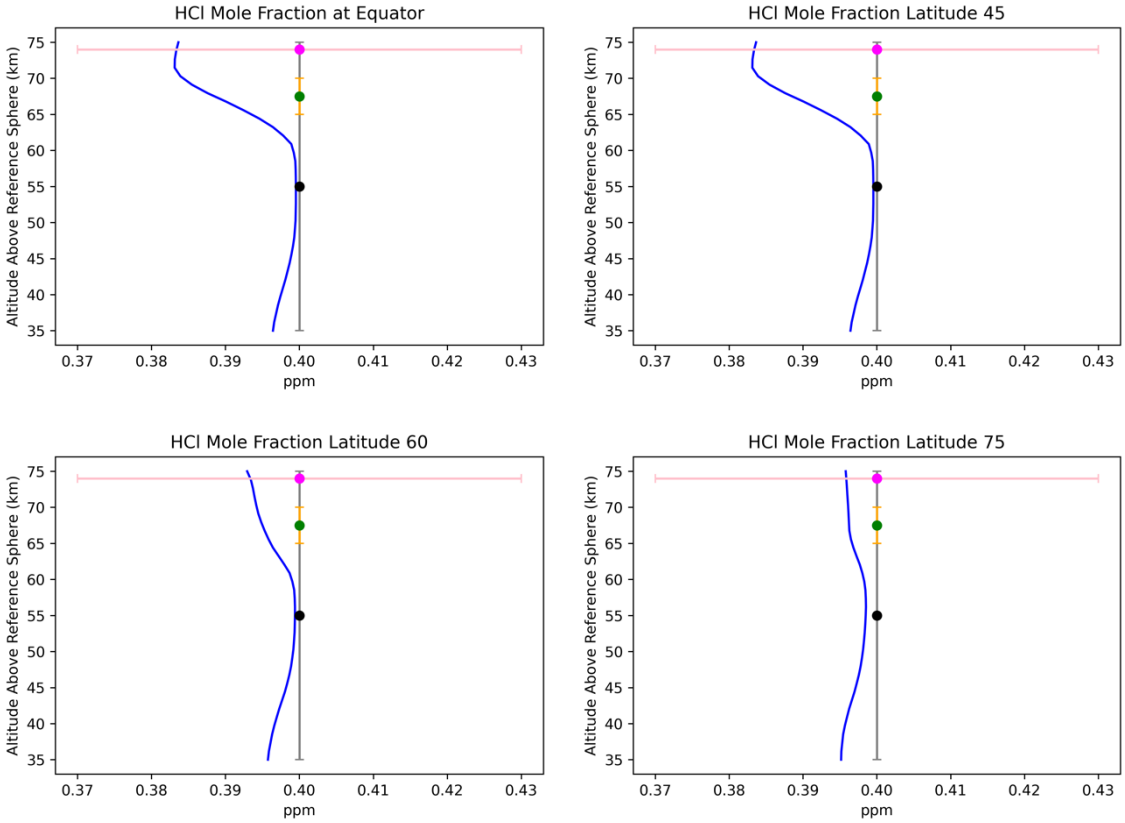

***Figure 45**: hydrochloric acid mixing ratio vertical profile in parts per million at different latitudes. Blue lines represent VCD results at each latitude at 00:00LT. Observational data have the same values for all four panels as there is no cited latitudinal dependence/variation in the chosen literature. Black dot shows Earth Based Telescope near IR sounding (Dalton et al., 2000), green dot represents values measured by Earth Based Telescope Fourier Transform Spectrometer (Bergh et al., 1989), pink dot is the result from Earth Based Telescope near IR sounding (Krasnopolsky et al., 2010). Vertical errorbars show the measurement uncertainty on the altitude.*